Investigation of novel therapeutic strategies for epithelial ovarian cancer

Nobuhisa Yoshikawa

Faculty of health science

This thesis is presented for the degree of Doctor of Philosophy of

The UNIVERSITY OF ADELAIDE

SCHOOL OF MEDICINE

DISCIPLINE OF MEDICINE

AUGUST 2015

Table of Contents

Table of Figures

Abstract

Objective: PRIMA-1MET is a small molecule compound that restores wild-type p53 to mutant p53, and is recently confirmed to be safe at therapeutic plasma levels. The aims of this study were to identify the anti-tumour activity of PRIMA-1MET on epithelial ovarian cancer (EOC) cells and elucidate the underlying mechanism in vitro.

Methods: We used nine EOC cell lines and their chronic cisplatin/paclitaxel-resistant cells and performed cell viability assay and cell apoptosis assay to evaluate the efficacy of PRIMA-1MET. Moreover, we assessed the functional role of reactive oxygen species (ROS) and their scavenger in the EOC cells.

Results: We examined the viability of the total 13 EOC cells after 48 h treatment with PRIMA-1MET. Measuring the half maximal inhibitory concentration (IC_{50}) of EOC cells revealed that the sensitivity was heterogeneous, and did not correlate with *TP53* status. PRIMA-1MET induced apoptosis, PARP cleavage, and intracellular ROS accumulation in a p53-independent manner. The anti-tumour effects of PRIMA-1MET were completely rescued by a ROS scavenger, N-acetyl cysteine. Furthermore, PRIMA-1MET reduced the expression of antioxidant enzymes, PRX3 and GPX1, in a dose-dependent manner.

Conclusion: We demonstrated that PRIMA-1MET had an anti-tumour effect on EOC cells regardless of *TP53* status and chemo-resistance. PRIMA-1MET is a promising therapeutic agent for chemo-resistant EOC patients and may contribute to a better prognosis in the future.

Declaration

I certify that this thesis contains no material which has been accepted for the award of any other degree or diploma in my name in any university or other tertiary institution except Nagoya University. To the best of my knowledge and belief, it contains no material that has previously been published by any other person except where due reference is made. In addition, I certify that no part of this work will, in the future, be used in a submission in my name for any other degree or diploma in any other university of other tertiary institution without the prior approval of the University of Adelaide and where applicable, any partner institution responsible for the joint award of this degree.

I give consent to this copy of my thesis, when deposited in the library of the University of Adelaide to be available for loan and photocopying.

I also give permission for the digital version of my thesis to be made available on the web, via the University's digital research repository, the Library Search and also through web search by the University to restrict access for a period of time.

Nobuhisa Yoshikawa

July 2015

Acknowledgments

I would like to thank my principal supervisor, David Callen, for his support to my submission of this thesis and providing me a chance to work in his group at the Breast Cancer Genetics group. I also thank to Fumitaka Kikkawa, my co-supervisor, for his advice on my project. Thanks to Daniel Worthley, my co-supervisor, for his expertise of molecular biology. Thanks to Kathleen Pishas, my co-supervisor, for her support and cooperation in all experiments. I also thank to Hiroaki Kajiyama, Kiyosumi Shibata, and Takeshi Senga for their assistance and encouragement in my project. I am grateful to the University of Adelaide for giving me a chance to work with my colleagues at Callen's Laboratory, and Nagoya University for providing me the Next Generation of Medical Reserchers Scholarship to have a valuable experience at the University of Adelaide.

I am grateful to all of the members of the Breast Cancer Genetics group at IMVS. Especially, I largely appreciate the friendship of Eric, Alka, Reshma, Vicky, Miao, Laura, and Yu Feng.

Abbreviations

µg	microgram
µL	microLitre
µM	microMolar
bp	base pairs
cDNA	complimentaly DNA
DMEM	Dubecco's Modified Eagle Medium
DMSO	Dimethyl sulfoxide
DNA	Deoxyribonucleic acid
dNTP	Dinucleotide triphosphate
DSB	double strand brake
ECM	extracellular matrix
EMT	Epithelial-to-mesenchymal transition
EOC	epithelial ovarian cancer
FACS	Fluorescence activated cell sorting
FBS	fetal bovine serum
GFP	Green Fluorescent Protein
gRNA	guide RNA
HDR	homology directed repair
HGSOC	high-grade serous ovarian cancer
HPMCs	Human peritoneal mesothelial cells
IGF	Insuline like Growth Factor
M	Molar

mg	milligram
mL	millilitre
MQ	methylene quinuclidinone
mRNA	messenger ribonucleic acid
NaCl	sodium chloride
NHEJ	non-homologous end joining
PARP	Poly ADP-ribose Polymerase
RPMI	Roswell Park Memorial Institute medium
RT-PCR	Reverse transcription real time polymerase chain reaction
shRNA	short hairpin RNA
TGF	Transforming Growth Factor
VEGF	Vascular Endothelial Growth Factor

Conference Presentations

Nobuhisa Yoshikawa, Kathleen Pishas, Daniel Worthley, and David Callen.

Gene correction by CRISPR-Cas system in ovarian cancer. Faculty of Health Sciences 2014 Postgraduate Research Conference, National Wine Centre of Australia, University of Adelaide, Poster presentat

Chapter 1

Identifying gain-of-function of TP53 and anti-tumour activity of PRIMA-1^{MET} in epithelial ovarian cancer cells

Introduction

Epithelial Ovarian Cancer

Each year, more than 100,000 women die of ovarian cancer worldwide [1]. Epithelial ovarian cancer (EOC) accounts for majority of all ovarian malignancies and is one of the most lethal among gynaecologic malignancies in women. In many cases, the diagnosis is delayed due to its asymptomatic nature, and as a consequence 75% of patients are diagnosed at an advanced stage. The prognosis of ovarian cancer is closely related to the stage at diagnosis [2, 3].

Most ovarian cancer patients are managed with surgical resection, followed by systemic chemotherapies. Despite of recent advances in therapeutic agents, such as platinum-taxane combination chemotherapy, the 5-year survival rate is still less than 40% [4]. EOC shows an unfavourable oncologic outcome, based on its asymptomatic feature at an earlier clinical stage, numerous intraperitoneal and/or distant metastases. Despite the relatively high susceptibility of EOC to paclitaxel plus platinum compounds which is a first-line chemotherapeutic agent of EOC, the intrinsic or acquired resistance of the tumour cells to these chemotherapies makes treatment of EOC difficult. In order to overcome the chemo-resistance, various additional molecular-targeting therapies combined with conventional anti-neoplastic agents have been elucidated.

High-grade serous ovarian cancer (HGSOC) which is observed much more frequently at an advanced stage, occupies around 60% of all histological subtypes of EOC. Recent studies have revealed that most of HGSOC carry *TP53* mutations in contrast to other types of EOC which have a much lower incidence of *TP53* mutations [5-7]. Furthermore, a recent study using high-throughput sequencing technology

revealed that *TP53* mutations occurred 96% of 316 HGSOC samples [8]. According to this report, missense mutations accounted for 62%, whereas frame-shift and splice mutations were 14% and 12% respectively. Moreover, *TP53* mutations and mutant p53 protein accumulation have been found in serous tubal intraepithelial carcinoma (STIC), which is a precursor lesion of HGSOC [9]. This suggests that *TP53* mutation occurs at an early stage in the progression of HGSOC and inactivation of p53 function is an essential event in HGSOC tumour development.

Tumour suppressor gene TP53

The *TP53* is located on chromosome 17p and encodes the p53 protein. Wild-type p53 functions predominately as a transcriptional factor, with a potent tumour suppressive function. In the absence of cellular stress, p53 is sustained at a low level. Many types of cellular stress and DNA damage, such as ultraviolet irradiation, exposure to geno-toxic substances, and hypoxia, can activate p53, which result in downstream cellular effect including cell apoptosis and/or cell cycle arrest [10]. In addition, whereas deletion of both p53 copies from the mouse germ line had no significance effect on embryo development, mice lacking both p53 alleles had a significantly short life span because of lymphomas and sarcomas [11]. These results suggested that p53 was likely to be specialized to prevent the emergence of abnormal cells. Considering this important role of p53 in preventing and suppressing carcinogenesis, p53 is inactivated during carcinogenesis in the majority of cancers. In fact, p53 is abrogated by point mutation in about 50% of all cancers (http://www.iarc.fr/p53).

TP53 mutation

The majority of *TP53* mutations found in various cancers suppress the sequence specific DNA-binding activity of wild-type p53 as a transcription factor. To date, a number of tumour-associated p53 alleles have been sequenced, and 74% of them have been found to carry missense mutations (Figure 1) (http://www.iarc.fr/p53).

Figure 1

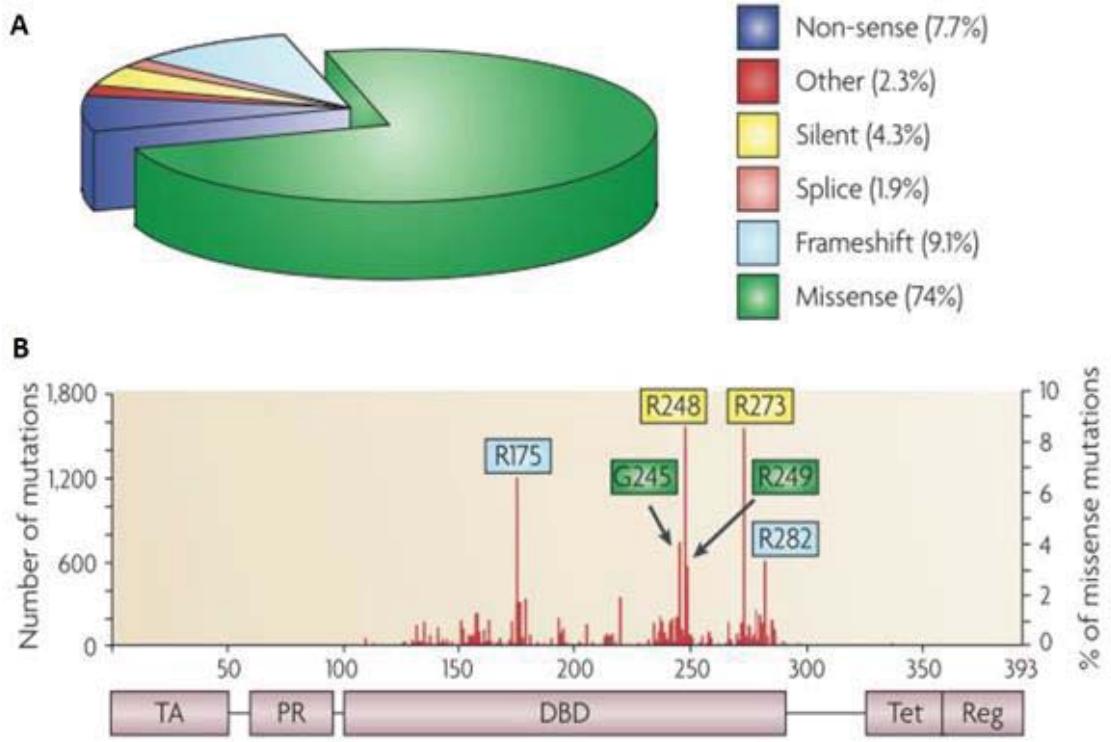

Figure 1 Distribution of *TP53* somatic mutations are shown based on the IARC *TP53* Mutation Database.

A: Distribution of different tumour-derived mutation types reported in the IARC *TP53* Mutation Database. B: Reported missense mutations. The domain architecture of p53 is aligned below. DBD, DNA-binding domain; PR, proline-rich domain; Reg, carboxy-terminal regulatory domain; TA, transactivation domain; Tet, tetramerization domain. (adapted from [12])

Indeed, with respect to HGSOC, TCGA study using large scale sequencing revealed that two thirds of *TP53* mutations were missense, and furthermore truncating mutations of *TP53* led to markedly lower mRNA levels, independent of copy-number status.

Ninety-five percent of such missense mutations are located in DNA binding domain, which affects sequence-specific binding activities. Missense mutations not only lose the function of wild-type p53 protein, but also provide mutant p53 protein in a dominant-negative manner. In addition, p53 protein normally exists in the cell as a homotetramer to function as a transcriptional factor [13]. This tetrameric state suggests that mutant p53 can interfere with functions of wild-type p53. *TP53* mutations can be classified into the two groups based on their effect on p53 protein stability[14]; 'DNA contact' mutations and 'conformational' mutations. The first group contains mutations in those amino acids directly involved in DNA binding, such as R248Q, R273H, R248W, R273C, and R282W. The second group includes mutations which contribute local (such as R249S and G245S) and global (R175H) protein structural change. In addition, *TP53* mutations in cancers are usually followed by loss of heterozygosity (LOH) of the remaining wild-type p53 allele resulting in complete loss of wild type p53 function.

Whereas wild-type p53 protein is sustained at very low levels under unstressed conditions, by regulation of MDM2 E3 ubiquitin ligase generating a negative feed-back, mutant p53 protein is stable and even accumulates in tumour cells [15, 16]. It has been hypothesised that the retention of mutant p53 protein in the cancer cell may confer a tumour promoting potential, compared with cells that lose a wild-type p53 protein [17].

Gain-of-function of mutant p53

Recent studies have shown that missense *TP53* mutations not only eliminate their own tumour suppressive function, but also gain oncogenic properties that promote tumour growth, termed gain-of-function (GOF). This means that mutant p53 proteins gain novel activities to contribute to tumour progression. GOF of mutant p53 is stratified into five groups according to its types of function; genomic instability, cell migration and invasion, anti-apoptosis, cell proliferation, and metabolism.

Genomic instability is defined as an increase of DNA alterations compared to normal cells, and has been proposed to be a mechanism by which cells may require invasive and metastatic properties. So far, several studies have shown that GOF of mutant p53 is implicated in promoting genomic instability. Gualberto et al. showed that by using fibroblasts derived from Li-Fraumeni syndrome with heterozygous missense mutant p53,mutant p53, including the mutant R175H, can disrupt spindle checkpoint control of aneuploidy cells, resulting in increasing number of cells with polyploid genomes [18]. Moreover, in p53-null mouse mammary cells ectopic expression of mutant p53 R172H, which is equivalent to human mutant p53 R175H resulted in abnormal centrosome amplification and increased chromosome number though binding to the centrosome [19, 20]. Additional studies using the mouse model carrying mutant p53 R172H revealed expression of mutant p53 resulted in a significantly higher frequency of genomic instability [21]. These studies indicated that mutant p53 contributes to genomic instability.

Promotion of cancer cell migration and invasion by mutant p53 has been shown by several studies. Using human lung cancer cells in mouse zenografts, Adorno

et al. reported that R175H mutant p53 protein activates TGF-induced metastasis through interacting p63 [22]. In addition, Nielsen et al. described that mutant p53 can drive invasion in breast cancer in a miRNA-mediated manner [23]. Furthermore, Muller et al. reported that mutant p53 regulates Dicer, resulting in the promotion an invasive phenotype via p63-dependent and –independent mechanism [24]. Recent studies concerning the association between p53 mutational status in sporadic cancers and their clinical properties have shown that p53 mutations are likely to be associated with poor survival or chemo-resistance [8, 12, 25]. Though this aspect of mutant p53 function is limited in a few types of cancer, such as breast cancer and lung cancer, it could be a hot spot of mutant p53 research, considering the association between mutant p53 and clinical implications, especially in HGSOC [26].

One of the most distinctive features of mutant p53 is to confer chemo-resistance to tumour cells. Overexpression of mutant p53 can make tumour cells more resistant to a number of anticancer agents, such as etoposide and cisplatin [27, 28]. Moreover, according to a recent report about HGSOC, GOF of mutant p53 was associated with poor patient prognosis and chemo-resistance [8]. In diffuse large B-cell lymphoma, mutations and/or deletion of p53 was associated with a negative impact on survival rates [29]. On the other hand, this anti-apoptotic nature of mutant p53 does not always mean that cancers with mutant p53 are more resistant to anticancer therapy compared with those with wild-type p53 [30]. Furthermore, it has been shown that cells with mutant p53 increase the sensitivity to DNA damaging drugs through upregulation of the expression of MAP4, which leads to microtubules disruption [31]. Overall the literature regarding chemoresistance of mutant p53 is inconsistent, thus further studies

are necessary to evaluate what mutant p53 contributes to chemoresistance and how it functions to confer chemoresistace in cancer tissues.

According to a recent report, mutant p53 can activate tumour metabolic change by mediating lipid metabolism. Freed-Pastor et al. reported that mutant p53s, such as R175H and R273H, activates a number of genes in the mevalonate pathway which is necessary to maintain the malignant state of breast cancer through upregulation of SREBPs, a transcription factor which activates key enzymes in the fatty acid and sterol biosynthetic pathways [32]. The activation of the mevalonate pathway has been shown to be associated with tumorigenesis by promoting proliferation, invasion, and metastasis [33, 34]. Furthermore, a recent study showed that mutant p53 activates glycolysis and the Warburg effect through the induction of the RhoA/Rock signalling pathway [26]. Goel et al. reported that mutant p53 activates the enzyme hexokinase II, which also results in promoting glycolysis [35]. These findings indicate that mutant p53 is likely to play an essential role in tumorigenesis through changing the metabolic status of tumour cells.

Wild-type p53 functions together with the oncogenic activities of mutant p53 protein, have been extensively investigated for over 30 years since p53 was first reported in 1979 [36]. However the molecular mechanism and clinical implications of GOF of mutant p53 is still controversial. There is little information relating to mutant p53 protein function in EOC, because other than several limited studies, EOC has not been used as model system in basic and clinical research. Therefore, many questions about mutant p53 still remain, especially in EOC.

p53 targeting therapy

Considering the critical role of wild-type p53 protein, p53 is one of the most appealing targets for cancer therapy. Three distinct approaches to target p53 function have been reported so far; 1) activation of wild-type p53, 2) reactivation of mutant p53, and 3) elimination of mutant p53. (Figure 2)

Activation of wild-type p53

There have been a variety of approached to activate wild-type p53, such as chemotherapy/radiation, gene therapy to introduce wild-type p53 and small molecules activating endogenous wild-type p53 function. Chemotherapy/radiation activates endogenous wild-type p53 via the DNA damage response [37, 38]. In general, tumour cells with wild-type p53 are more sensitive to chemotherapy/radiation than those with mutant p53 [39]. With respect to EOC, several reports showed that mutant p53 is related to chemo-resistance [8, 40]. An alternative approach is the use of small molecules, such as Nutlin3a and RITA that disrupt the wild-type p53-MDM2 interaction resulting in stabilisation of wild-type p53 and induction of high levels of apoptosis in several types of cancer [41]. It is expected that restoration of wild-type p53 would be a promising strategy because loss of wild-type p53 function is common in many cancers.

Figure 2

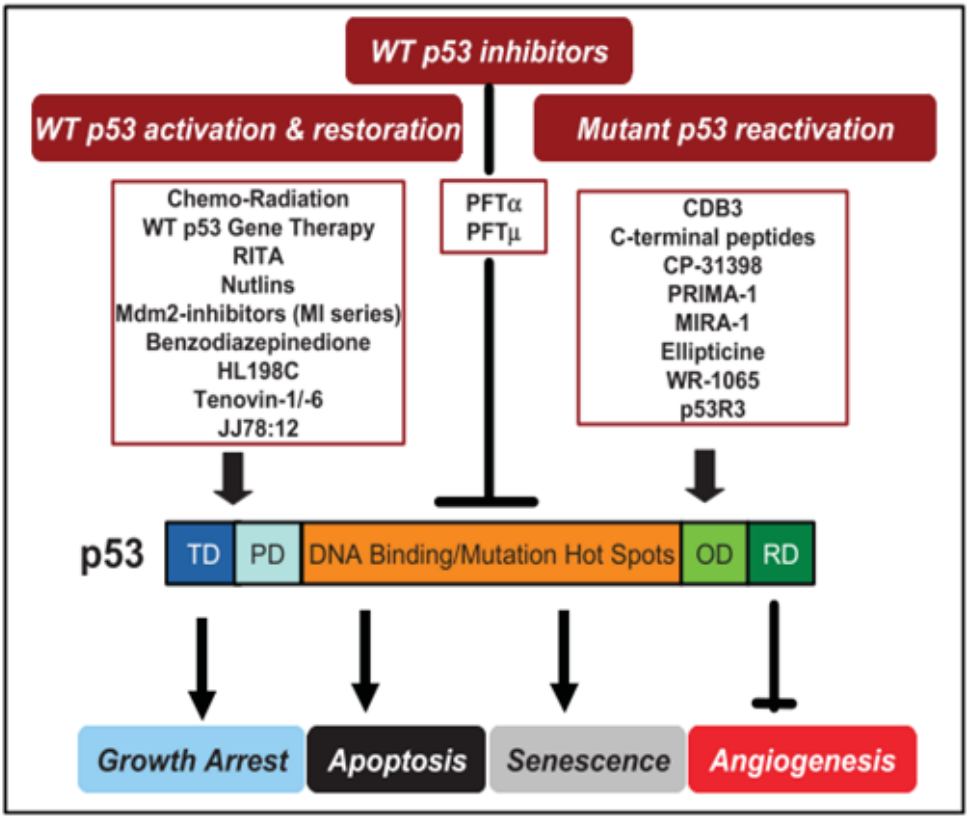

Figure 2 p53 targeting therapies are developing.

p53 consists of 393 amino acids with five domains; transactivation domain (TD), proline-rich domain (PD), DNA binding domain (DBD), oligomelization domain (OD), and regulatory domain (RD). There are three types of p53 targeting compounds. The first is the compound that activates wild-type p53 function. The second is the compound to reactivate mutant p53 in mutant p53 cancers. The third compound inactivates wild-type p53 function during chemotherapy and radiation to block p53 activation in normal cells. (adapted from [42])

Reactivation of mutant p53

Reactivation of wild-type p53 function of mutant p53 would be expected to be an effective cancer therapy, because *TP53* mutations occur in almost all HGSOC patients [5, 43]. The strategies to rescue mutant p53 differ depending on the type of mutation. CDB3, a short synthetic peptide, has been reported to restore some wild-type function to the R175H and R273H p53 mutants as assessed by the activation of MDM2 and CDKN1A, which are target genes of wild-type p53 [44]. Small molecules, such as CP-31398 and PRIMA-1, have been shown to change mutant p53 conformation into a wild-type p53-like conformation, restoring wild-type p53 function and so resulting in induction of cell growth arrest and apoptosis [45-48]. Furthermore, it has been shown that PRIMA-1 sensitized chemo-resistant ovarian cancer cells with mutant p53 to cisplatin through Akt down-regulation [49]. It has also been reported the small molecule, p53R3, which can induce expression of wild-type p53 target genes through the recruitment of both wild-type and mutant p53 [50].

Elimination of cancer cells with mutant p53

It is well established that p53 is tightly regulated in normal cells resulting in low expression levels because following synthesis the p53 protein is rapidly degraded following synthesis by MDM2 [51]. In many cancers with mutant p53, mutant protein accumulates in cancer cells. Elimination of mutant p53 expressing cells is an appealing strategy to achieve a highly specific cancer cell treatment. Some glycoside drugs, such as digoxin, have been identified to reduce the expression of mutant p53 protein through

the Src/MAPK pathway, and may provide a possible therapeutic strategy to eliminate mutant p53 cancer cells [52].

Other therapeutic strategies

Another therapeutic strategy targeting p53 in cancer cells is to induce degradation of mutant p53 protein. Mutant p53 protein is also targeted for proteasomal degradation by MDM2 [53]. Another ubiquitin ligase, CHIP, has also been demonstrated to degrade mutant p53 [54]. Histone deacetylase (HDAC) inhibitors have been shown to destabilize mutant p53 protein by inhibiting the interaction with HDACs [55]. These molecules are potential therapeutics to inhibit mutant p53 function.

Reduction of mutant p53 expression level by siRNA also can be an attractive strategy in cancers with mutant p53. Several publications show that p53 siRNA therapy reduces cancer cell proliferation and induces apoptosis in vitro [56, 57].

Gene correction of mutant p53 into wild-type p53

Theoretically, gene correction of mutant p53 into wild-type p53 in cancer cells can be an appealing therapeutic strategy and also a powerful tool for exploring p53 functions. According to the TCGA database, 74% of HGSOCs have a heterozygous deletion (hetloss) of the wild-type *TP53* allele [5]. This means that in the majority of cancer cells with mutant p53, the p53 locus is found to have undergone a loss of heterozygosity (LOH) event. To investigate wild-type and mutant p53 functions in the same genetic background, a novel approach is to convert mutant p53 into wild-type p53.

In addition, high-efficient conversion of mutant p53 into wild-type p53 may be a therapeutic strategy to restore wild-type p53 function in cancer cells with mutant p53.

Recently, a novel gene editing technology, the CRISPR-Cas system has been reported to efficient for genome editing in mammalian cells [58, 59]. Several reports have shown that the CRISPR-Cas system can be used to modify specific sequence in cell lines and in zygotes by introducing Cas9 nuclease, guide RNAs (gRNA), and repair templates [60-62]. The CRISPR-Cas system is an attractive technology not only for identifying gene functions but also in the study of genetic diseases including cancer.

Utilization of CRISPR-Cas system for gene correction of mutant p53

Clustered, regularly interspaced, short palindromic repeats (CRISPR) and Cas9 nuclease was first reported in the adaptive immune mechanism of bacteria [63]. In bacteria invaded by viruses or plasmids, type II CRISPR system works as an immune system, which recognizes foreign nucleic acids by hybridization of CRISPR RNAs (crRNAs) and transactivating CRISPR RNAs (tracrRNAs). Recently, several groups have reported that the CRISPR-Cas system can be utilized for genome engineering in various species including mammalian cells [58, 59, 64, 65]. Compared to other genome editing methods, such as zinc finger nucleases (ZFNs) and transcription activator-like effector nucleases (TALENs), the CRISPR-Cas system is highly efficient and has a target design, which enables the easy manipulation of genomic sequence. In the CRISPR-Cas system, we need to introduce only two components into cells for genome editing; one is Cas9 nuclease and the other is a gRNA composed of the fusion of crRNA

and tracrRNA. Using these two components, the CRISPR-Cas system enables targeted genome editing.

The gRNA consists of 20 nucleotides with a protospacer adjacent motif sequence (PAM sequence) coding NGG sequence at 3' end of the target sequence, and the scaffold. The gRNA orients the Cas9 nuclease enabling the cleavage of the specific complementary target DNA sites in a gRNA-dependent manner, resulting in a DNA double strand break (DSB). With this system, Cas9 nuclease can be directed to any DNA sequence of the form of N20-NGG by adjusting the gRNA corresponding to the target sequence.

The DSB can be repaired by one of two pathways that work in living cells; one is non-homologous end-joining (NHEJ), the other is homology-directed repair (HDR) (Figure 3). NHEJ can introduce various sizes of insertion/deletion mutations (indels), which can result in disruption of the reading frame of the coding sequence. HDR can be utilized to modify the specific sequence into another sequence, or to insert a desired sequence, mediated by recombination at the DSB site using donor templates. Because of the simplicity and high efficiency of the CRISPR-Cas system, this technology has many applications and potential in biological and biomedical research. The CRISPR-Cas system is theoretically able to modify any genomic DNA sequences into a desired sequence by introducing donor templates at the same time. In addition, to identifying the biological function of a target gene, complete knockout of genes by the CRISPR-Cas system has advantage compared with knock-down effect by RNA interference.

Figure 3

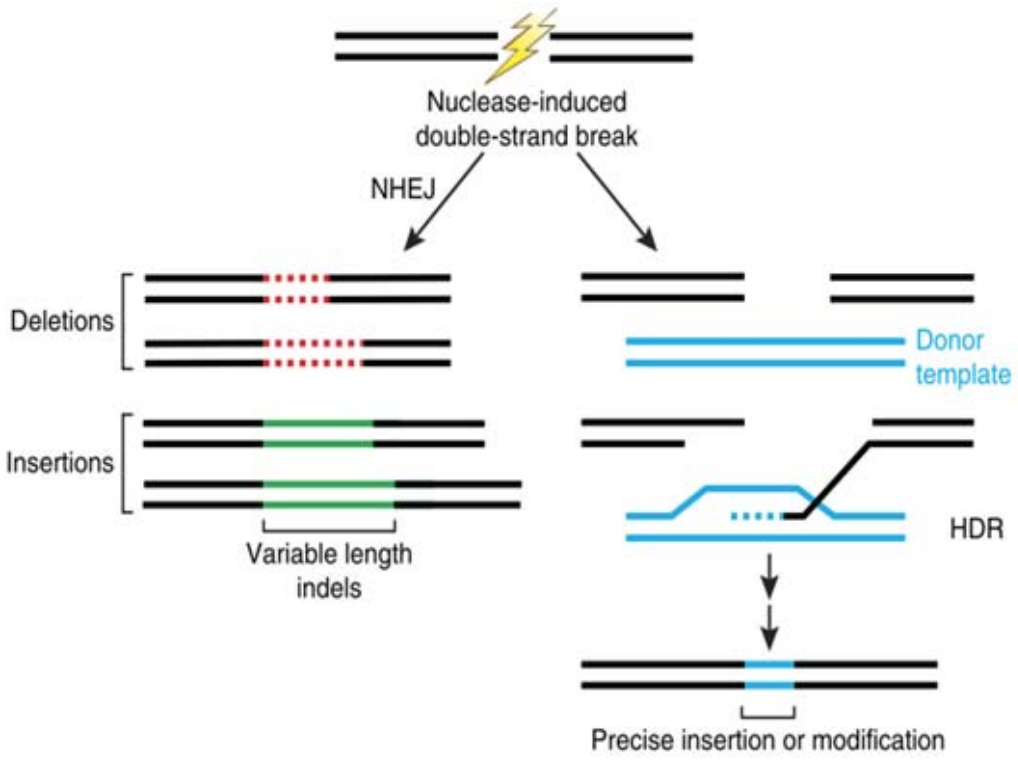

Figure 3 Cas9 induces genome editing.

Cas9 nuclease can induce double strand break (DSB) at the site targeted by gRNA. DSB induced by Cas9 is repaired by intrinsic machinery mechanism of either non-homologous end joining (NHEJ) or homology directed repair (HDR). NHEJ can lead to insertion and/or deletion mutations at DSB site, resulting in variable length indels and premature stop codons. HDR can introduce precise sequences or insertion in the presence of repair templates (adapted from [66]).

Gene correction of mutant p53 by CRISPR-Cas system in EOC

Gene editing by CRISPR-Cas system has been applied to repair disease-causing mutations in human cell lines and mouse zygotes in 2013 [60, 61]. In addition, Yin et al. recently demonstrated gene correction of a Fah mutation in hepatocytes in a mouse model of the hereditary tyrosinemia by tail vein injection of plasmid expressing Cas9 nuclease and sgRNA, with repair template[62].

It is still unclear whether CRISPR-Cas system functions in cancer cells because the repair steps critically depend on intact DNA repair mechanism, which is conferred by a number of genes, such as *BRCA1*, XRCC2 and 53BP1 [67]. . Defective DNA repair by homologous repair is believed to contribute to tumorigenesis in cancers with BRCA1 mutations. In ovarian cancer, *BRCA1* is often mutated or epigenetically silenced, therefore it is unclear whether a fully functional DSB is present and whether the CRISPR-Cas system can be used in such cells [68]. There have been no reports utilising the CRISPR-Cas system for the gene correction of cancer cells. This will be evaluated in this thesis.

Objective

Elucidating mutant p53 function of EOC

In clinical situations, although a significant proportion of HGSOC patients attain complete response, most of them subsequently develop recurrence within 18 months after standard platinum-taxane chemotherapy [69]. Although HGSOC is characterized with initial chemo-sensitivity, the acquisition of chemo-resistance seems inevitable. In the approximately 20 years since platinum-based treatment was introduced, despite the investigation of various approaches to improve systemic chemotherapy, there has been little change in survival rates post-diagnosis of patients with EOC (Figure 4) [70]. Therefore, one of the most critical problems in improving patient survival is to elucidate and overcome the mechanisms of chemo-resistance.

Despite the fact that EOC has one of the highest frequencies of *TP53* mutations, it is controversial whether the presence of *TP53* mutations is significantly associated with prognosis (such as survival and drug sensitivity) [71-75]. Table 1 summarises 14 reports concerning the association between mutation status of EOC and clinical outcome. None of these reports concluded what specific mutation of p53 was associated with clinical outcome. Because *TP53* mutations include a wide variety of types, such as DNA contact mutations, conformational mutation, frame-shift, or null, it is difficult to conclude which *TP53* mutations might be associated with clinical outcome.

Figure 4

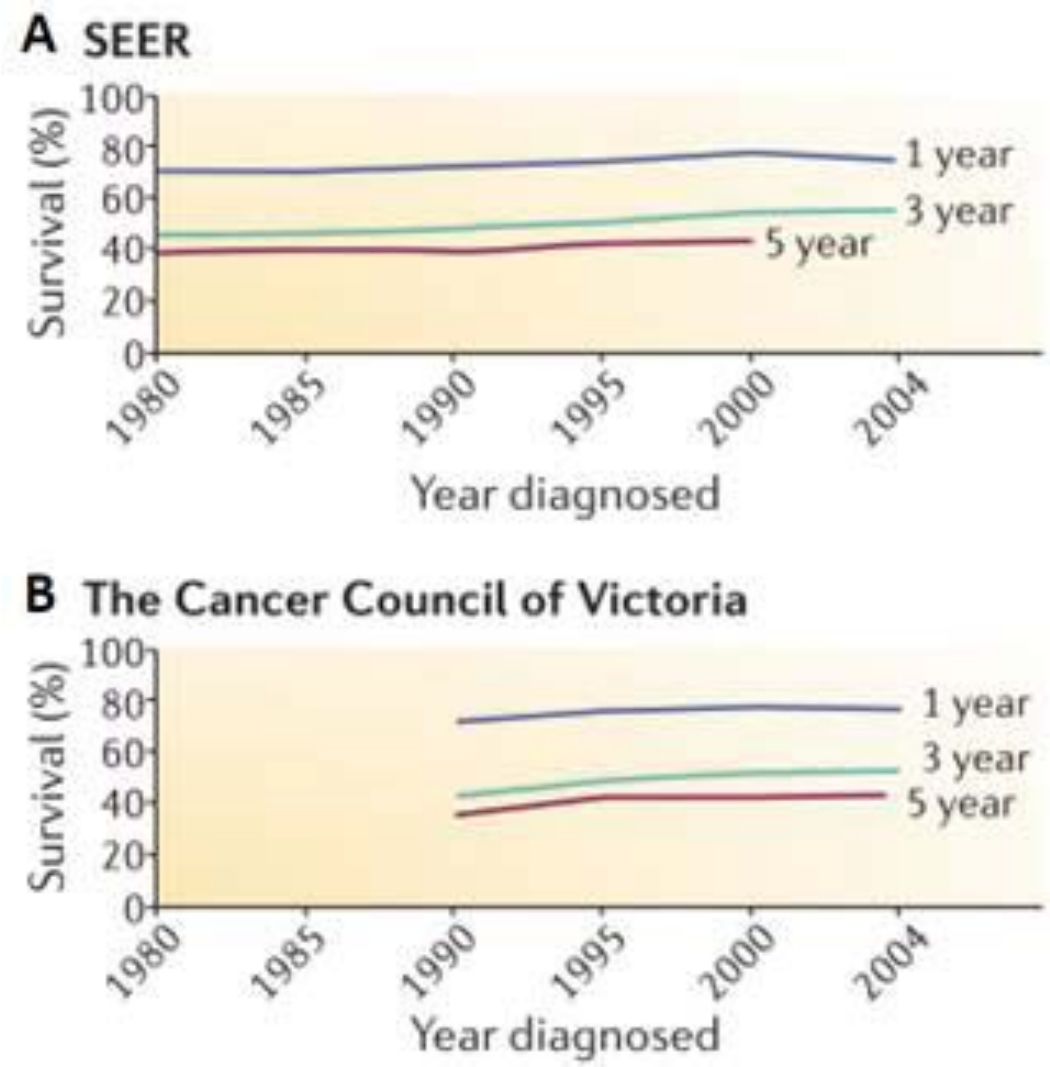

Figure 4 There has been little changes of survival in ovarian cancer over 20 years.

Data from the United States (A) and from Cancer Council of Victoria in Australia (B) show that there has been little change in survival rates of post-diagnosis (1, 3, 5-year overall survival) of patients of ovarian cancer over the past 20 years. Data in part A are from the Surveillance, Epidemiology and End Results (SEER) database obtained between 1980 and 2004. Data in part B are obtained between 1990 and 2004. (adapted from [70])

PMID	p53 mutations associated with	sample (n)	p53 mutation (%)	missense (%)	Serous type (%)	methods
16183105	bad outcome	124	28	85	65	direct sequencing
16322298	bad outcome	122	66	80	37	direct sequencing
15099937	bad outcome	73	34	50	29	direct sequencing
15221786	bad outcome	109	72	66	83	direct sequencing
14519637	bad outcome	125	66	76	52	direct sequencing
11595686	bad outcome	178	56	72	62	SSCP and direct sequencing
11064359	bad outcome	171	58	70	43	SSCP
18172257	bad outcome	107	39	67	58	direct sequencing
16969087	bad outcome	79	63	54	N/A	SSCP
14760384	No association	178	40	75	43	direct sequencing
11720475	No association	102	39	69	50	direct sequencing
17171684	No association	188	55	73	67	direct sequencing
14551300	good outcome	125	77	69	67	direct sequencing
16459017	good outcome	100	43	72	64	direct sequencing

Table 1 The correlation between mutation status of p53 and clinical outcome is inconsistent among studies.

We reviewed 14 independent studies which examined the association between EOC patients prognosis, and p53 mutations and expression level. While 9 out of 14 studies concluded that p53 mutations were related to a bad outcome of EOC patients, the other 5 studies could not find the association between p53 mutations and poor patients prognosis. These studies consist of variable percentage of serous histological types, and used different methods to identify TP53 mutation.

However, based on a recent analysis of 316 HGSOC patients from the TCGA database where reliable and complete *TP53* sequencing is available, 31 GOF p53 mutants, including S127Y, P151S, R156P, Y163N, Y163C, V173L, R175H, C176Y, H179R, H179Q, L194R, Y205C, H214R, Y220C, Y234C, M237I, S241F, G245C, G245S, G245V, G245D, R248W, R248G,R248Q, R273C, R273L, R273H, R273P, C275Y, D281G, and R282W, were associated with a patients' poor status in terms of platinum-sensitivity and distant metastatic properties [8]. Given these reports, it may be worth to re-evaluating the clinical and biological significance of mutant p53 in EOC.

The molecular mechanism underlying GOF of mutant p53 protein has been explored in human cancers, however, there are only a couple of studies in EOC [76-78]. Some of mutant p53, including R175H and R273H, have GOF properties through interacting with NF-Y [79]. It has also been reported that EOC cells expressing mutant p53 activate proliferation and suppress migratory activities in the presence of TGFβ [76]. Furthermore, Sonego et al. reported in ovarian cancer, stathmin, a p53 target gene which is associated with increasing metastatic potential and drug resistance, is necessary for the stability and transcriptional activity of mutant p53 by upregulating DNA-PK which can bind to and phosphorylate mutant p53 [77]. Considering that nearly all HGSOC patients carry p53 mutations, it is meaningful to elucidate the function of other p53 mutations in EOC. In addition, *TP53* mutations have two different aspects in terms of tumour promoting effects; one is loss-of-function of wild-type p53, and the other is gain-of-function of mutant p53. To overcome both aspects at the same time, gene correction of mutant p53 into wild-type p53 is an appealing strategy. The CRISPR-Cas

system provides a helpful tool to understand how wild-type/mutant p53 functions under the same genetic background.

Despite aggressive treatments, EOC is one of the most deadly cancers in women with high mortality rates and high recurrence rates partially due to its chemo-resistance. Based on the TCGA database, the majority of HGSOC have mutations of *TP53* and approximately 60% of HGSOC were missense mutations [5] (Figure 5). This suggests that mutant p53 may contribute to the aggressive phenotypes of HGSOC. Previous studies have shown that mutant p53 can confer genomic instability, increased cell migration and invasion, anti-apoptosis, increased cell proliferation, and altered metabolism in cancer cells through upregulating specific target genes and interaction with several transcription factors [22, 79]. To elucidate the functions of mutant p53 in EOC may provide an understanding of the underlying mechanism of chemo-resistance in EOC. The CRISRP-Cas system provides a unique approach to investigate the functions of wild-type/mutant p53 in the same genetic background.

Figure 5

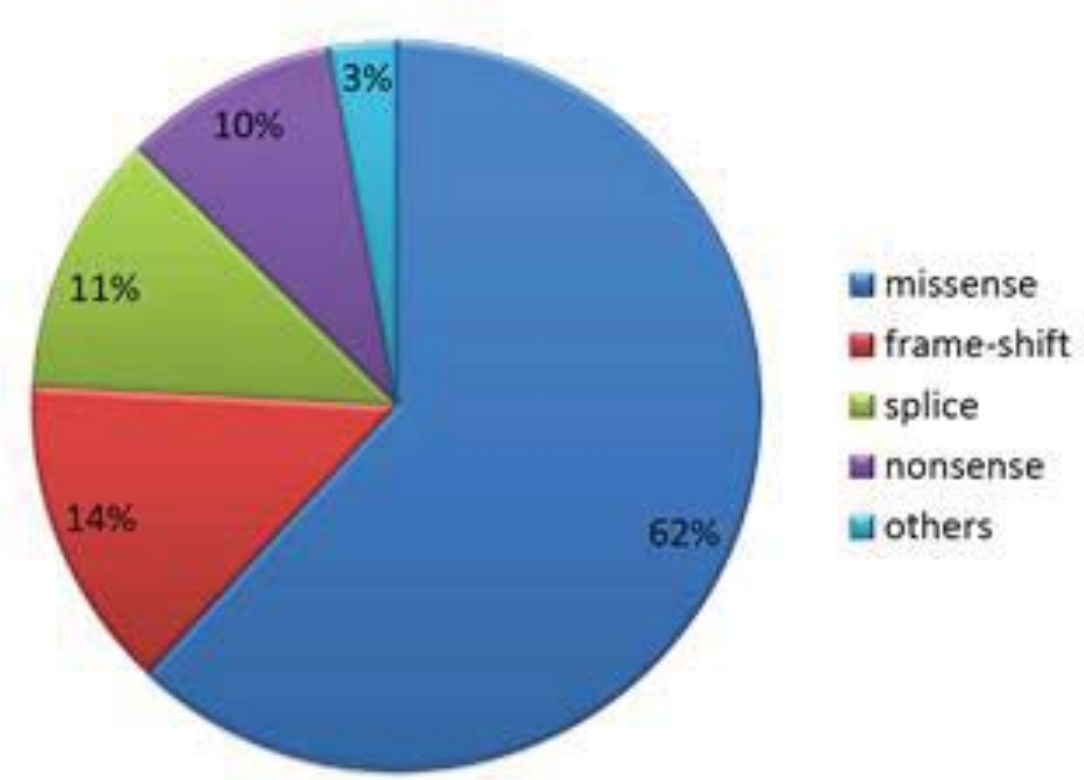

Figure 5 Majority of *TP53* mutations in HGSOC were distributed to missense mutations.

We retrospectively analysed the TCGA database recruiting 316 HGSOC patients. The TCGA study extensively evaluated messenger RNA expression, microRNA expression, promoter methylation and DNA copy number. According to our analysis, 302 of 311 HGSOC were mutated in *TP53*. Furthermore, missense mutation accounted for 62% of all mutations of *TP53* in HGSOC [5].

Identifying the anti-tumour activity of PRIMA-1^{MET} in ovarian cancer cells

Over the last 15 years, a number of mutant p53-targeting compounds have been identified and tested by various strategies. PRIMA-1 (p53-dependent reactivation of massive apoptosis) and its methylated form, PRIMA-1^{MET}/APR-246, are small molecular weight compounds that can restore wild-type p53 functions to mutant p53 through the recovery of transcriptional transactivation by covalent binding to the core domain of the mutant p53 protein [48]. The efficacy and safety of PRIMA-1^{MET} has already been confirmed in a Phase I/II clinical trial in 22 patients with haematological malignancies or hormone-refractory prostate cancer [80].

TP53 mutations frequently occurred in approximately 50% of all cancers, and are associated with poor prognosis and chemo-resistance. Therefore, novel treatment options targeting mutant p53 would have wide applicability in a variety of cancers. In our current study, we investigated whether the small molecule PRIMA-1^{MET} could induce cell death in EOC cell lines with or without *TP53* mutations. We also determined the efficacy of PRIMA-1^{MET} against chemo-resistant EOC cells.

Methods

Cell culture

Human EOC lines A2780, OVCAR-3, ES-2, SKOV-3, CAOV-3, TOV21G, and OV-90 were obtained from ATCC. NOS2 and NOS3 derived from serous EOC were previously established in our Institute [81]. The NOS2CR and NOS2TR cells with chronic resistance to cisplatin and paclitaxel were previously established in our institute [82]. Furthermore, we recently established another two chronic cisplatin/paclitaxel-resistant lines from the parental NOS3 cells: NOS3CR (cisplatin) and NOS3TR (paclitaxel). All EOC cell lines were maintained at 37℃ with 5% CO2 in RPMI-1640 medium (Sigma) supplemented with 10% FBS, streptomycin (100μg/mL), and penicillin (100U/mL). PRIMA-1^{MET} was purchased from Santa Cruz Biotechnology, Inc. PRIMA-1^{MET} was diluted in dimethyl sulfoxide (DMSO) to create a 50mmol/L stock solution and stored at -20℃. Antibodies to p53 (610184) was purchased from BD Pharmingen.

Fluorescent in situ hybridization (FISH)

EOC cell lines were grown in T25 flasks. Cultured cells were fixed with cold methanol. The XL P53 probe was obtained from Metasystems and used to detect deletions in 17p13 which involve the *TP53* locus. The specific probe is labeled orange, while a green labeled probe which hybridizes to the centromere of chromosome 17 is used as a reference probe. After over-night co-hybridization of the probes, the slides were washed and DNA counterstained with DAPI. Each slide was examined by

fluorescence microscopy using the appropriate filter combination. About 100 nuclei were examined for each cell line.

Generation of stable cell lines

SKOV-3 cells that constitutively express the full-length mutant p53 ORF were established by retroviral infection. Full-length mutant p53 R248Q and R248W were amplified from a pCMV-myc encoding mutant p53 ORF, then cloned into pQCXIP retrovirus vector (Clontech, Mountain View, CA) with an N-terminal GFP tag. The pQCXIP vector that encodes each cDNA was transfected into 293T cells in combination with packaging plasmids. The culture supernatant was collected 48 hr later and applied to SKOV3 with 2μg/ml of polybrene. Cells were cultured for 24 h, and then 1 μg/ml of puromycin was added to select for infected cells.

Soft agar assay

Cells (1×10^4) were mixed with 0.36% agar in RPMI supplemented with 10% FCS and overlaid onto a 0.72% agarose layer in 6-well plates. After 2 weeks of incubation, colonies in randomly selected fields were counted.

RNA extraction

RNA extraction from the cells was undertaken by using the Qiagen RNeasy Mini Kit according to the manufacturer's protocols. The cells were lysed in 250μL of buffer RLT and filtered through the filtration spin column. The samples were applied to

RNeasy Mini spin column. Total RNA bound to the membrane and contaminants were removed by washing consecutively with buffers RW1 and buffer RPE consequently. RNA was eluted in RNase free water. Extracted RNA was immediately stored at -80℃. RNA concentration was determined by use of a NanoDrop 1000 Spectrophotometer.

Reverse Transcription

To obtain complementary DNA (cDNA), 1µg of RNA and 0.2µg of random primer (Promega, Madison, USA) was used. After incubation at 72℃ for 4 minutes the mixture of RNA and random primer was placed on ice for 4 minutes. M-MLV RT 1x Reaction Buffer, M-MLV Reverse Transcriptase RNase Minus, and 10mM dNTP (Promega, Madison, USA) was added to the mixture and then incubated at 42℃ for 90 minutes followed by 70℃ for 15 minutes. cDNA was stored at -20℃.

Quantitative Real Time PCR (qRT-PCR)

Quantitative RT-PCR (qRT-PCR) was performed on a MyiQ instrument using the SYBR Green detection system (Bio-Rad). Cycler conditions consisted of a 3 minutes hot start at 95℃, followed by 40 cycles of denaturation at 95℃ for 10 seconds, annealing at 58-60℃ for 10 seconds, and extension at 72℃ for 10 seconds, then a final inactivation at 95℃ for 10 seconds. Dissociation curve analyses were done at the end of cycling to confirm one specific product is measured in each reaction. Relative expression was performed by using ΔΔCT method [83]. Expression normalization was

done by expression of GAPDH, a housekeeping gene shown to have stable expression in cancer cell lines[84]. All experiments were performed in triplicate.

Protein Extraction and Western Blot Analysis

Cultured ovarian cancer cells were washed with PBS and lysed in RIPA buffer (Millipore). The cells were scraped into lysis buffer, centrifuged at 12,000 x g at 4℃ for 15 minutes, and then diluted in 2x sample buffer (125 mM Tris-HCl [pH6.8], 4% SDS, 10% glycerol, 0.01% bromophenol blue, and 10% 2-mercaptoethanol). Equal amounts of proteins (10ug) were mixed with the 2x sample buffer and were boiled at 95℃ for 5 minutes. The samples were loaded and separated by 7.5-15% SDS-polyacrylamide gel electrophoresis (PAGE) with running buffer. The separated proteins were transferred to polyvinylidene difluoride (PVDF) membranes. The membranes were blocked with 1% skim milk, incubated with each primary antibody over night at 4℃, washed with TBS-T buffer (10 mM Tris-HCl pH 7.4, 150 mM NaCl, 0.05% Tween20) and incubated with secondary antibodies. The proteins were visualized using enhanced chemiluminescence (GE Healthcare BioSciences, Uppsala, Sweden).

Direct sequencing of TP53 mutations

Genomic DNA was extracted from cultured cells and the exons of *TP53* were amplified by polymerase chain reaction (PCR). The exons and flanking introns of TP53 were amplified by polymerase chain reaction (PCR). The primers we used are shown in Table 2. The resulting PCR products were sequenced and mutation types were confirmed.

primer			sequence	bp
p53	exon 2-4	Forward	GTGTCTCATGCTGGATCCCCACT	23
		Reverse	GGATACGGCCAGGCATTGAAGT	22
	exon 5-6	Forward	TGCAGGAGGTGCTTACGCATGT	22
		Reverse	CCTTAACCCCTCCTCCCAGAGAC	23
	exon 7-9	Forward	ACAGGTCTCCCCAAGGCGCACT	22
		Reverse	TTGAGGCATCACTGCCCCCTGAT	23
	exon 10	Forward	GTCAGCTGTATAGGTACTTGAAGTGCAG	28
		Reverse	GCTCTGGGCTGGGAGTTGCG	20
	exon 11	Forward	CCTTAGGCCCTTCAAAGCATTGGTCA	26
		Reverse	GTGCTTCTGACGCACACCTATTGCAAG	27

Table 2 The specific primers used for direct sequencing of the TP53 gene.

The exons and flanking introns of TP53 were amplified these primers specific for the genomic sequence. Prior to sequence analysis, 5 μL of PCR products were purified with QIAquick PCR Purification Kit (QIAGEN). Sequencing reaction was performed with BigDye Terminator according to the following protocol.

Mix	amount (μL)	weight
gDNA	x	50 μg
Primer-F (10uM)	0.6	
Primer-R (10uM)	0.6	
10xBuffer(green)	2	
10mM dNTP	0.4	
Fast Start Taq (5 U/uL)	0.2	
DD water	up to 20	
Total	20	

Reaction 1-3			Reaction 4-5		
95℃	2 min		95℃	2 min	
95℃	48 sec		95℃	48 sec	
61℃	48 sec	10 cycle	59℃	48 sec	10 cycle
72℃	48 sec		72℃	48 sec	
95℃	48 sec		95℃	48 sec	
59℃	48 sec	25 cycle	57℃	48 sec	25 cycle
72℃	48 sec		72℃	48 sec	
72℃	10 min		72℃	10 min	
4℃	hold		4℃	hold	

Sequencing was performed by IMVS sequencing service.

Cell viability Assay

Cell proliferative properties and the effect of PRIMA-1^{MET} on the viability of human EOC cell lines were evaluated by use of the CellTiter-Glo Luminescent Cell Viability Assay (Promega, Madison, WI, USA), which quantifies living cells by ATP signal intensity. Luminescent signal was determined by a Luminometer. To evaluate cell proliferation, $3x10^3$ cells of cultured cells were plated to 96-well plate, and then a volume of CellTiter-Glo Reagent equal to the volume of cell culture medium present in each well was added after appropriate hours. To investigate cytotoxic effects on EOC cellsCells were seeded in triplicate n 96-well plates at a density of 2000 cells/well. After 24 h of culture, cells were treated with various concentrations of PRIMA-1^{MET}, and then incubated for 24-72 h. Control cells were treated with the same concentration of DMSO as that of the PRIMA-1^{MET} treated cells.

Detection of apoptosis by staining with Annexin V-FITC and propidium iodide

Cells ($2x10^5$) were cultured in 6-well plate for 24 h before treatment with DMSO (control) or appropriate concentration of PRIMA-1^{MET} for 24 h. Cells were trypsinized ,washed once with PBS, and then stained with Annexin V-FITC and propidium iodide (PI) to determine the early/late apoptotic cell population (MBL).

Results

Elucidating mutant p53 function of ovarian cancer

TP53 status and p53 protein expression in EOC cells

Direct sequencing DNA of *TP53* in ovarian cancer cell lines confirmed the presence of the p53 S215R mutation in OV-90 cells, p53 R248Q mutations in OVCAR-3 cells, *TP53* wild-type status in OVCAR-5 cells, and *TP53* null in SKOV-3. Representative electropherogram of exon 7 in OVCAR-3 and OVCAR-5 are shown (Figure 6a). A summary of the mutations in the four EOC cell lines is shown in Figure 6b. Western blot analysis was performed to detect p53 protein in the four EOC cells and showed that OV-90 and OVCAR-3 with mutant p53 expressed higher levels of expression of p53 than OVCAR-5 with wild-type p53 (Figure 6c). Information about the genotype of the EOC cells is imperious to apply CRISPR-Cas sytem for gene editing.

TP53 gene copy-number alterations in ovarian cancer cell lines

Double-color FISH analysis using a probe for chromosome 17 centromere (green signal) and locus specific for *TP53* (red signal) was performed to identify copy number of *TP53* locus (work under taken by Dr. Mario). Representative fluorescence microscopic images of the four EOC cell lines are shown in Figure 7a. Copy number of the four EOC cell lines in 100 nuclei was counted manually (Figure 7b). The mean copy number of *TP53* was two in OVCAR-3, OVCAR-5, and SKOV-3, but three in OV-90. The results of TP53 status and copy number indicats that the mutations occur in the homozygous state, with no remaining wildtype p53 in the ovarian cancer cells, except

for OVCAR-5. The copy number of p53 is important when assessing the results from the CRISPR-Cas system.

Figure 6

A

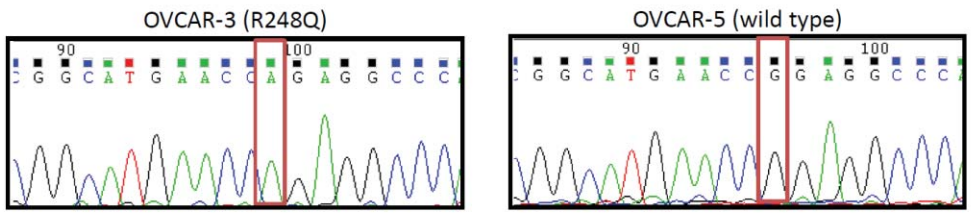

B

Cell line	TP53 status	Mutation sites	Mutation type
OV-90	Mutated	Exon 6, codon 216	Ser → Arg
OVCAR-3	Mutated	Exon 7, codon 248	Arg → Gln
OVCAR-5	Wild-type	-	-
SKOV-3	null	Exon 4, Codon 86	Stop codon

C

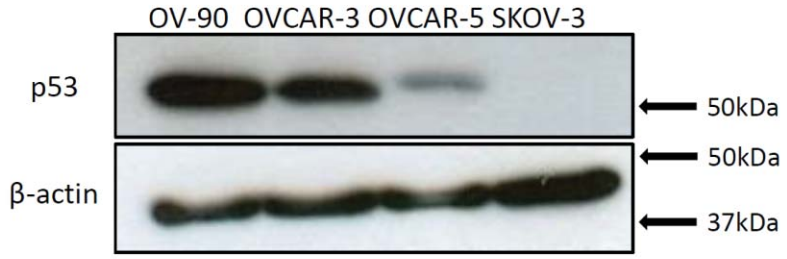

Figure 6 *TP53* status and p53 protein expression in ovarian cancer cell lines.

The exons and flanking introns of TP53 were amplified these primers specific for the genomic sequence. Prior sequence analysis, 5 μL of PCR products were purified with QIAquick PCR Purification Kit (QIAGEN). Sequencing reaction was performed with BigDye Terminator, followed by sequencing. A: Electropherogram shows the exon 7 in OVCAR-3 and OVCAR-5. The red square indicates a missense mutation in exon7 of TP53 of OVCAR-3 in comparison with that of OVCAR-5. B: *TP53* status of the four ovarian cancer cell lines is described. C: Expression levels of p53 protein are shown in the four ovarian cancer cell lines.

Figure 7

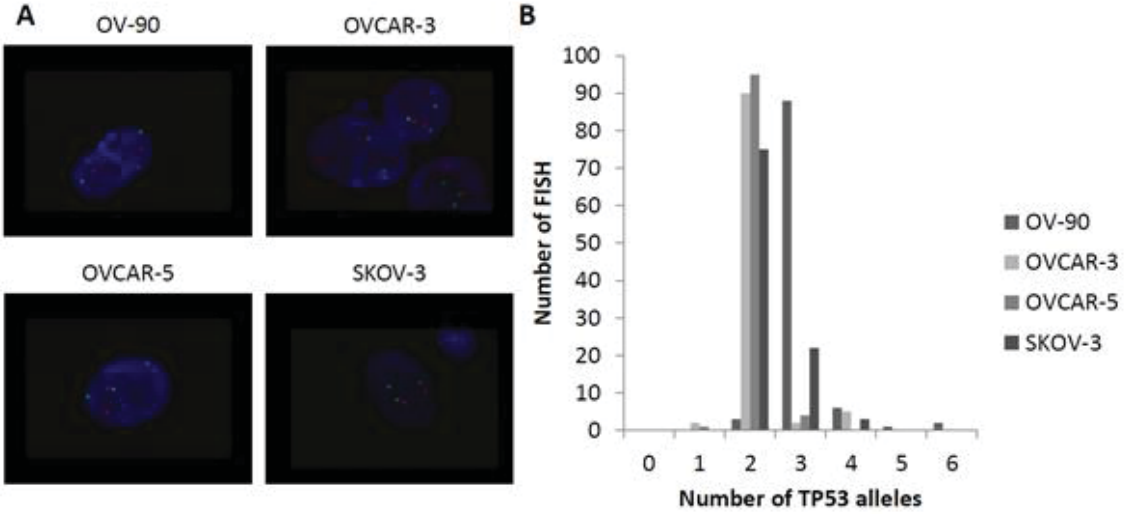

Figure 7 FISH analysis reveals *TP53* gene copy-number alterations in ovarian cancer cell lines.

A: Representative fluorescence microscopic images are shown in OV-90, OVCAR-3, OVCAR-5, and SKOV-3. B: Number of *TP53* alleles of the four cell lines are described, which were counted in total 100 nuclei under fluorescence microscopy.

Establishment of a SKOV-3 mutant p53 cell lines

To identify tumour-promoting roles of mutant p53 in EOC, we established mutant p53 stable expressing cell lines in the p53-null SKOV-3 ovarian cell line. Plasmids encoding either the p53 point mutation R248Q or R248W were generated by inserting a PCR fragment of the open reading frame of *TP53* with point mutation R248Q or R248W into the pQCXIP-GFP plasmid vector (Clontech). The backbone vector map of the pQCXIP-GFP plasmid vector is shown (Figure 8).

Retroviral transfection generated three different SKOV-3 stable cell lines, GFP (empty) and full-length ORF mutant p53-R248Q and p53-R248W. No apparent cellular morphological changes were found in mutant p53 stable expressing cells compared to mock cells, although mutant p53 localized to the nucleus (Figure 9). The exogenous expression of mutant p53 was confirmed by western blot analysis. These results suggest that overexpression of mutant p53 (R248Q and R248W) in SKOV-3 cells does not induce any significant observable cell morphological changes.

Figure 8

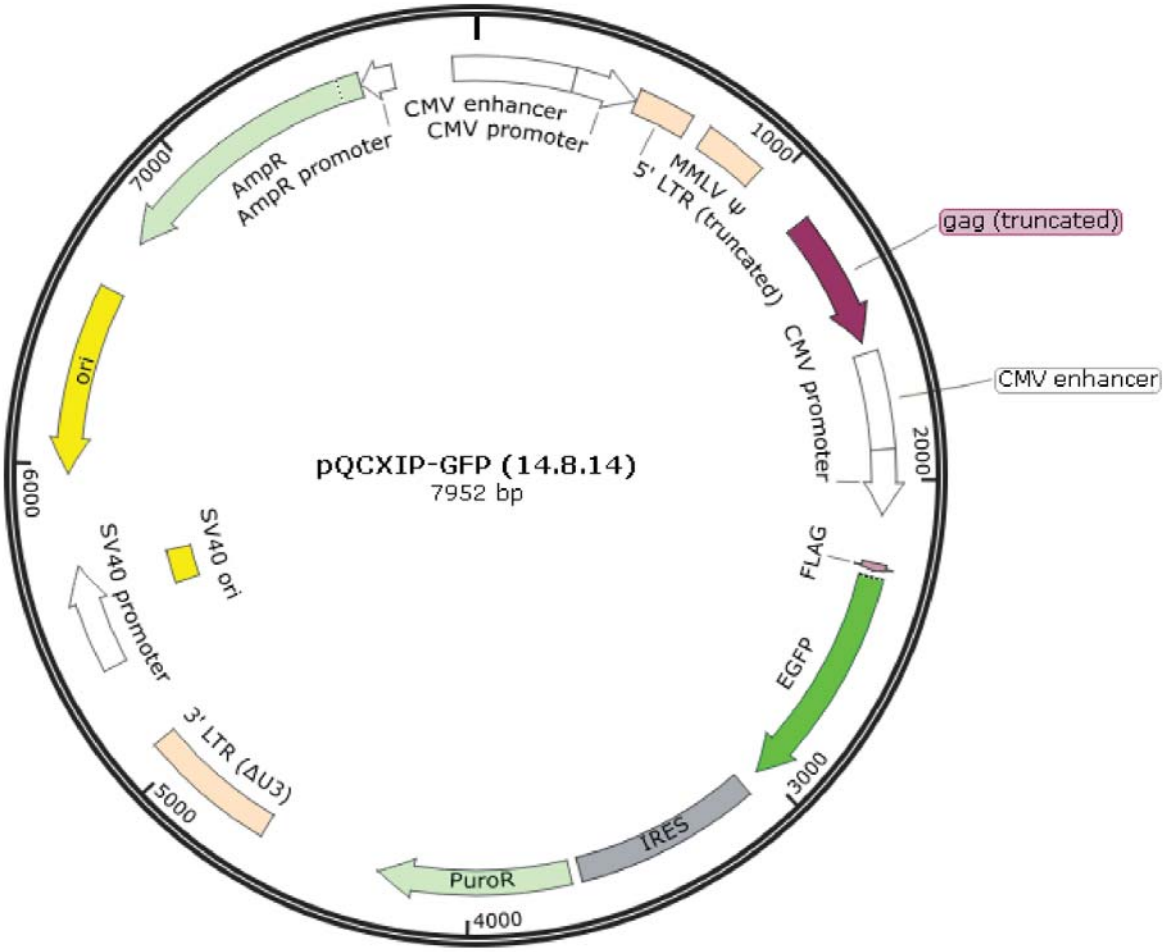

Figure 8 The vector map of the pQCXIP-GFP plasmid vector

This vector was used for establishing stable p53 ORF expressing cells followed by retroviral infection.

Figure 9

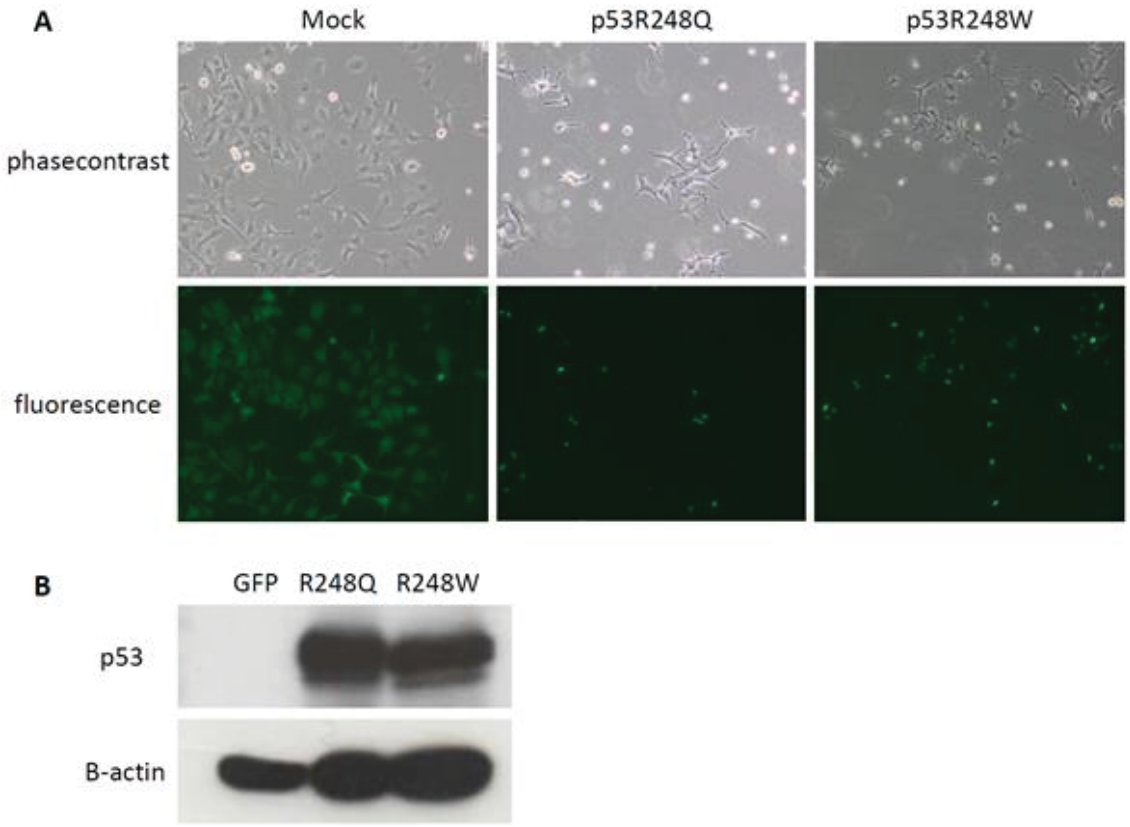

Figure 9 Exogenous expression of mutant p53 in SKOV-3 induces no apparent morphological changes.

A: The pictures are representative images showing the cellular morphology of the indicated cell lines. We established stable cell lines expressing GFP (Mock), p53R248Q-GFP, or p53R248W-GFP by retroviral infection. Briefly, 293T cells were cultured in 12-well plates, and transfected with pQCXIP-GFP plasmid that encodes each cDNA in combination with packaging plasmids. The culture supernatant was collected 48 hr later and applied to SKOV-3 with 2μg/ml of polybrene. SKOV-3 cells were cultured for 24 h, and then 1 μg/ml of puromycin was added to select for infected cells. GFP was observed under a fluorescence microscope. In mock cells, GFP was observed in cytoplasm diffusely, while GFP was observed in nuclei in p53R248Q or p53R248W expressing cells. B: Exogenous expression of mutant p53 in SKOV-3 was confirmed by western blot analysis. Established stable cell lines were cultured in 6-well plates, and then lysed with lysis buffer 48 h later. β-actin was used as a loading control.

Exogenous expression of mutant p53 protein did not confer malignant phenotype nor platinum resistance to SKOV-3

We next determined whether the exogenous expression of mutant p53 protein; R248Q and R248W, confers a malignant phenotype to SKOV-3 cells. To examine whether mutant p53 affected the proliferative activity of SKOV-3 cells, we first investigated the cell viability assay using CellTiter-Glo Luminescent Cell Viability Assay. There was no significant difference in the proliferative activities among the mock cells, R248Q, and R248W stable expressing cells (Figure 10a). We next evaluated the cisplatin resistance to examine whether mutant p53 conferred chemo-resistance to SKOV-3 cells. We found no significant differences among mock cells, R248Q, and R248W stable expressing cells (Figure 10b). We further performed soft agar colony formation assay to assess anchorage-independent cell growth in mutant p53 stable expressing cells. As shown in Figure 10c, exogenous mutant p53 did not affect colony formation in soft agar. These results suggests that exogenous mutant p53 expression does not exert any observable tumour-promoting effects in SKOV-3 cells.

Figure 10

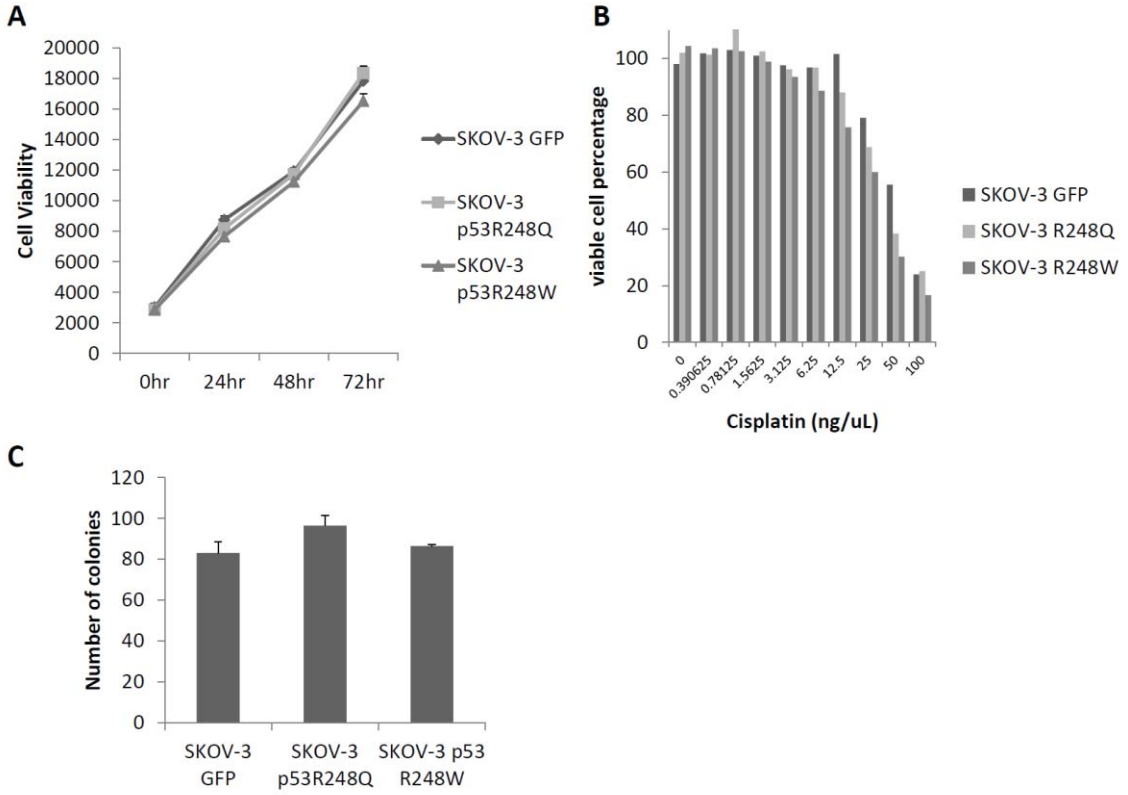

Figure 10 Exogenous expression of mutant p53 was not related to malignant phenotypes in SKOV-3.

A, B: The proliferative properties and platinum-resistance of each cell line were evaluated using an CellTiterGlo assay Kit. In the cell viability assay (A), $3x10^3$ cells in 100 μL of cultured cells were plated to 96-well plate, and then a volume of CellTiter-Glo Reagent equal to the volume of cell culture medium present in each well was added after appropriate hours, followed by measurement with chemiluminescent detection. To evaluate chemo-resistance to cisplatin of stable cell lines, cultured cells in 96-well plates were treated with appropriate concentrations of Cisplatin, and added a volume of CellTiter-Glo Reagent 48 h later. Exogenous mutant p53 induced no significant effects on cell proliferation and cisplatin-resistance. C: Each cell line was subjected to a soft agar colony formation assay to evaluate anchorage-independent cell growth. No significant change was found in and soft agar colony formation assay.

Strategy for the establishment of isogenic mutant p53 cell lines

CRISPR design

To evaluate tumour-promoting functions of mutant p53 in EOC cells, we decided to knockout mutant p53 in OV-90 cells (S215R) using the CRISPR-Cas system [58, 59]. We first designed two sgRNAs against exon 2 of p53, which includes the translation start site (Figure 11). The target sites were selected from a bioinformatics database of target sequences in the human exome (http://crispr.mit.edu/). We determined exon 2 of p53 as a putative target site, as frameshifts mediated by non-homologous end joining around this region could latently result in an early stop codon and thus prevent translation of mutant p53 protein.

CRISPR cloning

We first obtained 25-mer oligos for each target site, and each pair were annealed and phosphorylated. Annealed oligos were directly inserted into a plasmid digested with BbsI containing Cas9, the gRNA scaffold, and also GFP (pSpCas9(BB)-2A-GFP) (Figure 12). To validate the sequence of obtained plasmids, Sanger sequencing was performed by using the U6-Fwd primer.

Figure 11

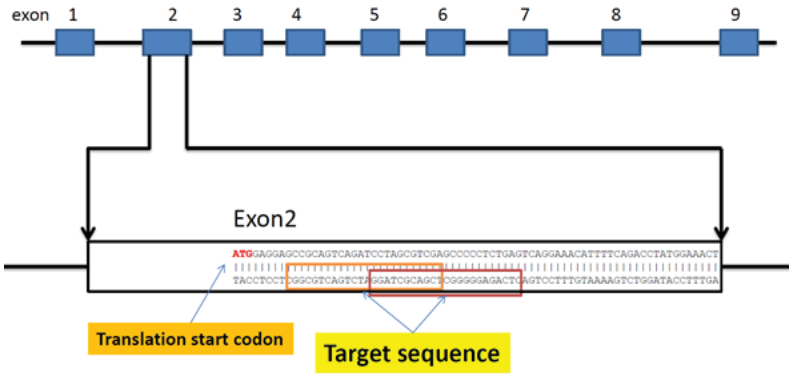

Figure 11 Designing target sites of guide RNA in exon 2 of *TP53* gene.

Exon 2 of *TP53* was selected for guide RNA design. We chose two separated targets to knockout *TP53* gene by using online web tool (http://crispr.mit.edu/).

Figure 12

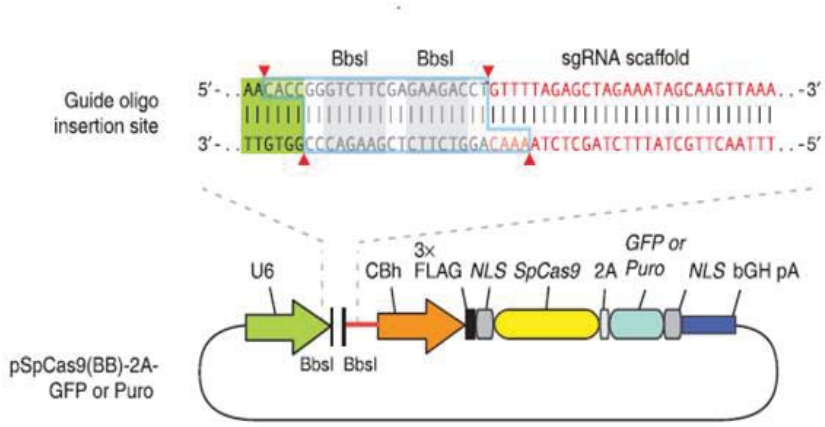

Figure 12 Schematic for cloning of guide sequence oligos into pSpCas9(BB)-2A-GFP.

Schematic of U6 gRNA-CBh Cas9-GFP expressing plasmid vector (pSpCas9(BB)-2A-GFP) was used to introduce gRNA and Cas9 nuclease. Digestion of pSpCas9(BB)-2A-GFP with BbsI restriction enzyme enables the replacement of restriction enzyme sites with direct insertion of annealed oligos which were designed to generate gRNA.

Functional validation of gRNAs

To confirm whether the plasmid whose gRNA targets exon 2 of p53 (pSpCas9(BB)-2A-GFP-p53-exon 2) effectively represses p53 expression, transfections were performed. Briefly, 1 x 10^5 cells of OV-90 were plated onto 24-well plates in RPMI1640 medium without antibiotics 24 h before transfection. On the day of transfection, cells were transfected with 500 ng of the pSpCas9(BB)-2A-GFP-p53-empty or pSpCas9(BB)-2A-GFP-p53-exon 2 with Lipofectamine 2000. We evaluated the efficiency of transfection on the next day of transfection by using a fluorescence microscopy, and about 40-50% of cells were GFP-positive. 48 h after transfection, we extracted protein and performed western blot analysis. As expected, pSpCas9(BB)-2A-GFP-p53-exon 2 effectively suppressed p53 expression compared to pSpCas9(BB)-2A-GFP-p53-empy.

Isolation of clonal cell lines by FACS

To establish isogenic mutant p53 knockout cells, it is necessary to isolate clonal cell populations from the cells transfected with pSpCas9(BB)-2A-GFP-p53-exon 2. Twenty-four h after transfection of pSpCas9(BB)-2A-GFP-p53-exon 2, fluorescence-activated cell sorting analysis (FACS) was used to obtain single GFP-positive cells sorted into a 96-well plate (Figure 14). These were subsequently grown for further analysis.

Figure 13

Figure 13 Suppression effect of pSpCas9(BB)-2A-GFP-p53-exon 2 was confirmed by immunoblot.

To confirm whether the plasmid whose gRNA targets exon 2 of p53 (pSpCas9(BB)-2A-GFP-p53-exon 2) effectively represses p53 expression, transfections were performed. $1x10^5$ cells of OV-90 were plated onto 24-well plates in RPMI1640 medium without antibiotics 24 h before transfection. On the day of transfection, cells were transfected with 500 ng of the pSpCas9(BB)-2A-GFP-empty or pSpCas9(BB)-2A-GFP-p53-exon 2 with Lipofectamine 2000. 48 h after transfection, we extracted protein and performed western blot analysis. As expected, pSpCas9(BB)-2A-GFP-p53-exon 2 effectively suppressed p53 expression compared to empty control vector.

Figure 14

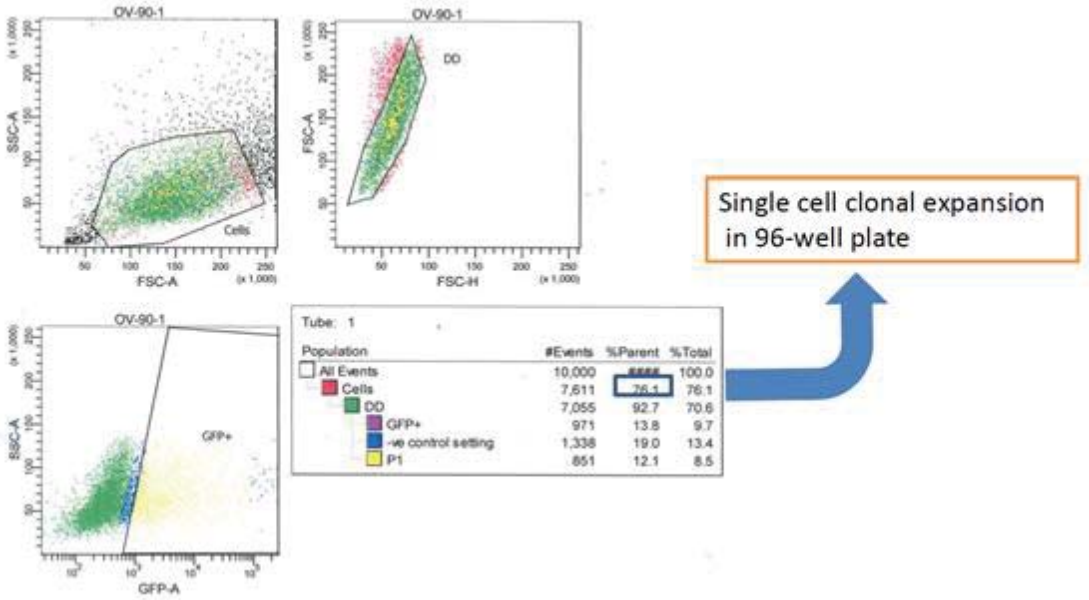

Figure 14 Representative image of FACS for isolating single cell clones after transfection of pSpCas9(BB)-2A-GFP-p53-exon 2.

24 h after transfection of pSpCas9(BB)-2A-GFP-p53-exon 2, fluorescence-activated cell sorting analysis (FACS) was performed to acquire single cell clones. GFP-positive cells were sorted into 96-well plates, then a couple of weeks later the sequences were evaluated.

Assessment of Cas9 cleavage efficiency by Sanger sequencing

Genomic amplicons of the target region (exon 2 of *TP53*) from the isolated clones was directly sequenced by Sanger sequencing to assess Cas9 cleavage efficiency. We obtained 7 and 5 clones from pSpCas9(BB)-2A-GFP-p53-exon2 targeting 1 and 2 regions respectively. The exon 2 sequences of the *TP53* gene in the isolated clones from OV-90 cells are presented in Figure 15. According to the DNA sequencing analysis, we identified total 7 out of 12 (58%) clones carrying genetic modifications of the target region (Figure 15).

To confirm whether Cas9-induced gene modification effectively eliminates mutant p53 protein expression, western blot analysis was performed. As expected, we did not identify protein expression of p53 in clone 3 and 4 where induced CRISPR-Cas changes in both alleles resulted in frameshift mutations. Clone 2 had both an intact unmodified mutant p53 allele and a modified allele predicted to generate a frameshift, thus its p53 expression level was considerable reduced compared with the parental cells (Figure 16). These results suggest that the CRISPR-Cas system is highly efficient and can be used to establish isogenic knockout cells even in the presence of two gene copies at very high frequencies.

Figure 15

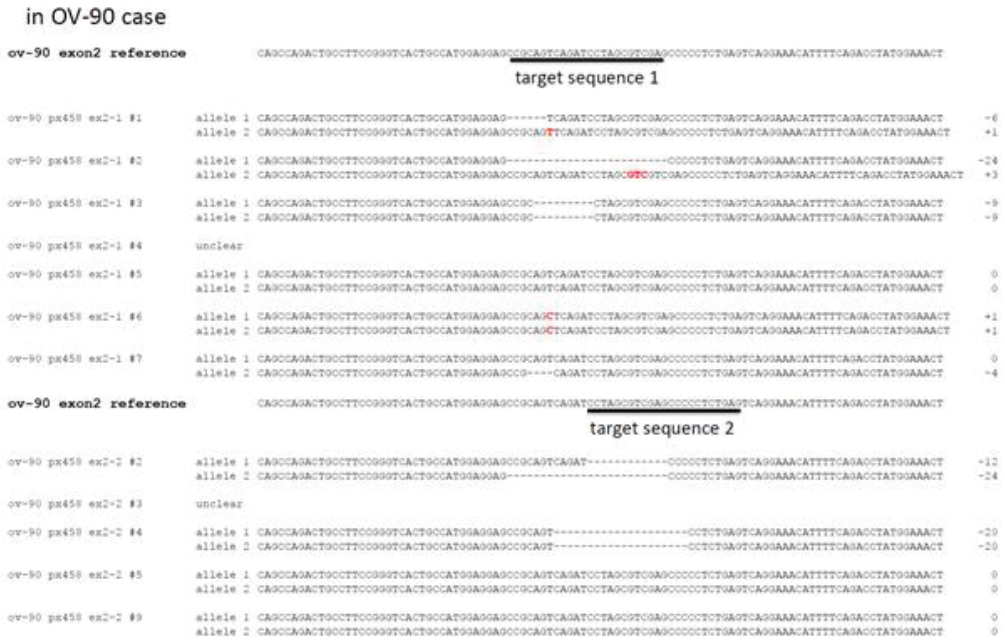

Figure 15 Sufficient genetic modifications by transfection of pSpCas9(BB)-2A-GFP-p53-exon 2.

Genomic amplicons of the target region (exon 2 of p53) from transfected cell clones can be directly sequenced by Sanger sequencing to assess Cas9 cleavage efficiency. According to the DNA sequencing analysis, we identified 7 out of 12 (58%) clones carrying genetic modifications of the target region.

Figure 16

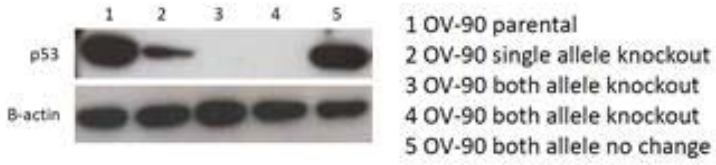

Figure 16 CRISPR-Cas9 induced modifications enables to knockout *TP53* protein expression.

To confirm the knockdown effect of Cas9-induced gene modification at protein level, western blot analysis was performed. As expected, we did not identify the protein expression of p53 in the clone 3 and 4 whose both alleles were frameshift. The clone 2 had both an intact allele and a modified allele, thus its p53 expression level was much less than the parental cells.

Discussion

Based on prior reports, overexpression of mutant p53 (R248Q and R248W) induced a malignant phenotype in SaOS-2 and H1299 cells, although they are not derived from ovarian cancer cells [85, 86]. Some prior reports revealed mutant p53 in ovarian cancer was associated with poor prognosis [71-75]. However, in our current investigation using the p53 null ovarian cancer SKOV-3 cells, we did not observe any observable changes in proliferative activity, cisplatin resistance, and anchorage-dependent cell growth when either p53-R248Q or p53-R248W was stably expressed by retroviral transduction. Liu et al. reported the significant role of mutant p53 GOF in SKOV-3 by transient transfection of R248W vector. We speculate that the lack of any phenotype from expressing mutant p53 in a p53 null background may be due to the particular genetic background of this cancer cell line. To further investigate these findings we utilised the CRISPR-Cas system to change the mutant p53 status of ovarian cancer cell lines. The present study was successful in achieving a high frequency of CRISPR-Cas based mutations of p53 which successfully eliminated p53 protein expression by simultaneously inducing frame-shift mutations in both p53 alleles. This verified that the CRISPR-Cas system can be successfully used in EOC cells and opens up avenues for future research. In our current study, we established isogenic mutant p53 knockout lines from mutant p53 lines, which enables to identify the functional role of mutant p53, such as drug resistance or other malignant phenotypes. Unfortunately there was no sufficient time to complete the full analysis of the mutant p53 knockouts in the ovarian cell line. These cell lines provide a pair of cell lines with genetically identical backgrounds that will provide useful reagents for future studies.

Identifying anti-tumour activity of PRIMA-1^{MET} in ovarian cancer cells

PRIMA-1^{MET}/APR-246 is a methylated form of PRIMA-1 (p53-dependent reactivation of massive apoptosis), which was identified as a compound that restores wild-type p53 functions to tumour cells expressing mutant p53. PRIMA-1 and PRIMA-1^{MET} are prodrugs converted to MQ with potential to bind to cysteine residues and change the conformation of the core domain of mutant p53[48]. PRIMA-1 and PRIMA-1^{MET} have been reported to induce apoptosis in several types of cancers [87-91]. The structures of these compounds are shown in Figure 17. Earlier studies have investigated how PRIMA-1/PRIMA-1^{MET} restores wild-type p53 function to mutant p53 [48, 92, 93]. However, to our knowledge, the efficacy of PRIMA-1^{MET} against EOC has never been investigated systematically.

The purpose of this study is to evaluate the efficacy of PRIMA-1^{MET} against EOC and identify an underlying mechanism how PRIMA-1^{MET} affects EOC cells.

Figure 17

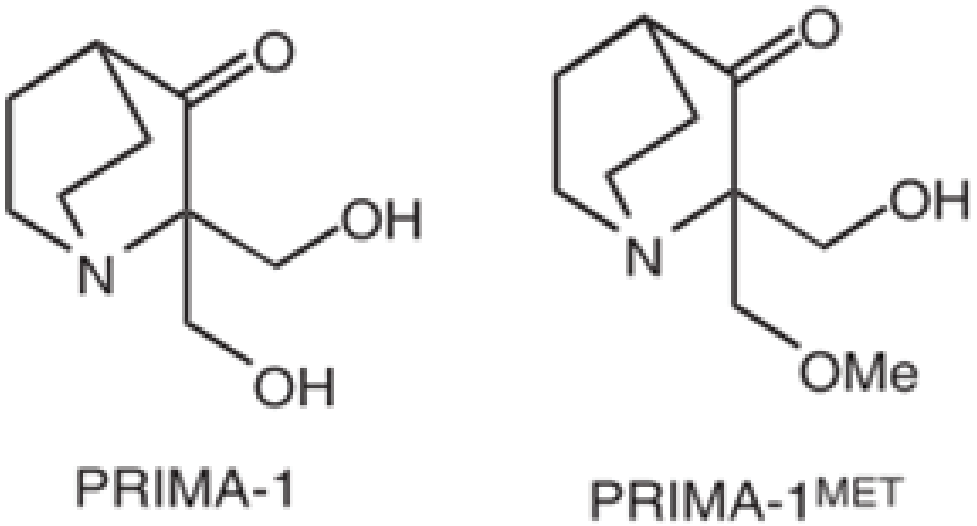

Figure 17 Structures of PRIMA-1 and PRIMA-1^{MET} The structures of PRIMA-1 and PRIMA-1^{MET} are shown (adapted from [88]).

Protein expression of p53 and TP53 mutation status in ovarian cancer cell lines

First, we evaluated levels of p53 protein expression in EOC cell lines by western immunoblot analysis. The mutational status of the cell lines are also shown in Table 3. Not only the mutant p53 harbouring cell lines, but also wild-type p53 harbouring cell lines; A2780 and NOS2 displayed basal expression of p53 to some extent. This result demonstrates that EOC cells bearing mutant p53 do not always express a higher level of p53 than those bearing wild-type p53.

PRIMA-1^{MET} treatment results in reduced cell viability and morphological change in EOC cells

To assess the anti-tumour activity of PRIMA-1^{MET} ,the anti-proliferative effects with various concentrations of PRIMA-1^{MET} (approximately 0-100 μM) were determined on

total 13 EOC cell lines; TOV21G, A2780, NOS2, ES-2, OV-90, OVCAR-3, CAOV-3, SKOV-3, NOS3, NOS2CR, NOS2TR, NOS3CR, and NOS3TR. Figure 18A shows the cell viability of wild-type p53 cell lines (TOV21G, A2780, and NOS2) and mutant p53 cell lines (ES-2, OV-90, OVCAR-3, CAOV-3, SKOV-3, NOS3) treated with PRIMA-1^{MET} for 48 h. PRIMA-1^{MET} reduced cell survival after 48 h in all EOC cell lines in a dose-dependent manner. The IC50 value of EOC cells were ranging from 2.6-20.1 μM. However, the sensitivities of PRIMA-1^{MET} were independent of p53 mutation status (Figure 18b). Furthermore, PRIMA-1^{MET} treatment induced morphological changes within 24 h (Figure 19). These results suggest that PRIMA-1^{MET} induces cell death effectively and rapidly.

Cancer cell lines	p53 status	p53 protein expression
TOV21G	wt	-
A2780	wt	+
NOS2	wt	+
ES-2	S241F	+++
OV-90	S215R	+
OVCAR-3	R248Q	+
CaOV-3	Q136Term	+
NOS3	L257P	++
SKOV-3	null	-

Table 3 Mutation status and protein expression of p53 in EOC cells.

Genomic DNA was extracted from cultured cells and the exons and flanking introns of *TP53* were

amplified by polymerase chain reaction (PCR). The exons and flanking introns of TP53 were amplified by polymerase chain reaction (PCR). The primers we used are shown in Table 2. 5 μL of PCR products were purified with QIAquick PCR Purification Kit (QIAGEN). Sequencing reaction was performed with BigDye Terminator**,** followed by sequencing.

Figure 18

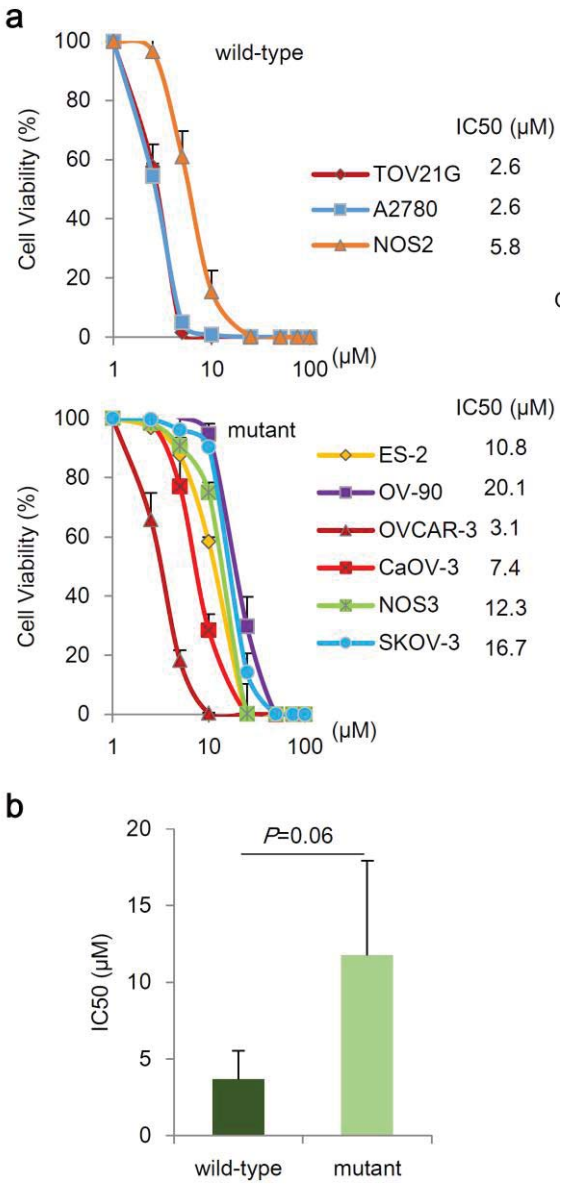

Figure 18 **The effects of PRIMA-1^{MET} on tumour cell growth in ovarian cancer cells.**

a: PRIMA-1^{MET}-induced growth suppressive dose response curves of EOC cells following 48 h of PRIMA-1^{MET} treatment. The IC50 value of PRIMA-1^{MET} were determined on total 9 EOC cell lines by cell viability assay. Data represents mean + standard deviation (STDEV) from triplicate reactions **b**: Correlation between PRIMA-1^{MET} 48 h IC50 values and TP53 status. EOC cell lines with wild-type p53 were slightly more sensitive than those with mutant p53 (not significant).

Figure 19

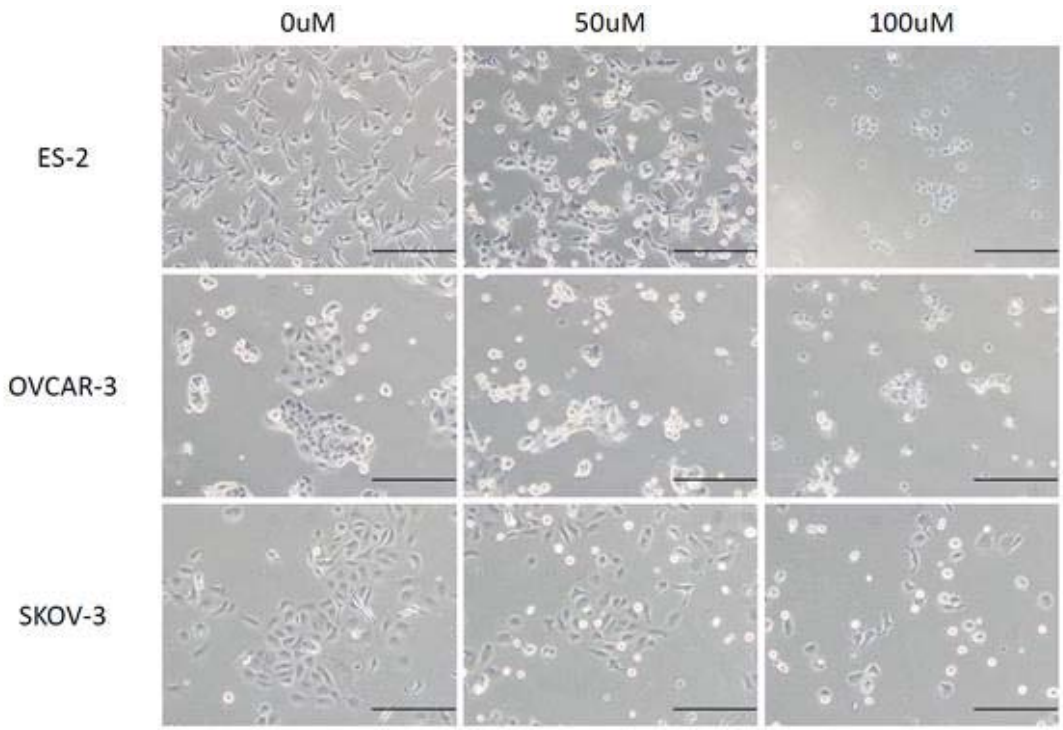

Figure 19 PRIMA-1^{MET} induces morphological changes in ovarian cancer cells within 24 h.

PRIMA-1^{MET}-induced morphological changes in EOC cells. ES-2, OVCAR-3, and SKOV-3 cells were cultured in 6-well plate, and then treated with 0, 50, 100 μM PRIMA-1^{MET} for 24 h. PRIMA-1^{MET}-induced morphological changes were observed with a microscopy (Scale bar =200 μm).

PRIMA-1^{MET} efficiently suppressed growth of chemo-resistant EOC cells

We next investigated whether PRIMA-1^{MET} treatment could display sufficient effects on cisplatin and paclitaxel-resistant cell lines, which were previously developed from the parental NOS2 and NOS3 cells (NOS2CR, NOS2TR, NOS3CR, and NO3TR)[94]. Dose responsive cell viability assays with PRIMA-1^{MET} were performed to evaluate the sensitivities of chemo-resistant cells. As shown in Figure 20, PRIMA-1^{MET} displayed anti-proliferative effects on both parental and chemo-resistant cells. The IC_{50} values of NOS2, NOS2CR, and NOS2TR were 6.5, 7.4, and 8.8 μM, respectively. The IC50 value of NOS3CR was slightly higher than those of NOS3 and NOS3TR. Thus, PRIMA-1^{MET} displayed sufficient growth suppressing effects on chemo-resistant cell lines.

PRIMA-1^{MET} induced apoptosis in a dose-dependent manner in EOC cells

We performed annexin V-FITC PI staining assay to investigate whether PRIMA-1^{MET} actually could induce apoptotic cell death in EOC cells. Indeed, treatment with PRIMA-1^{MET} for 16 h against EOC cells, TOV21G and A2780, increased the fraction of early and late apoptosis (Figure 21). In TOV21G cells, the fraction of early and late apoptotic cells was significantly increased from 1.1% and 4.3% at control vehicle treatment to 3.3% and 54.5% at 20 μM of PRIMA-1^{MET} treatment. In A2780 cells, the proportion of late apoptotic cells was significantly elevated from 5.3% at control vehicle treatment to 17.6% at 20 μM treatment.

Figure 20

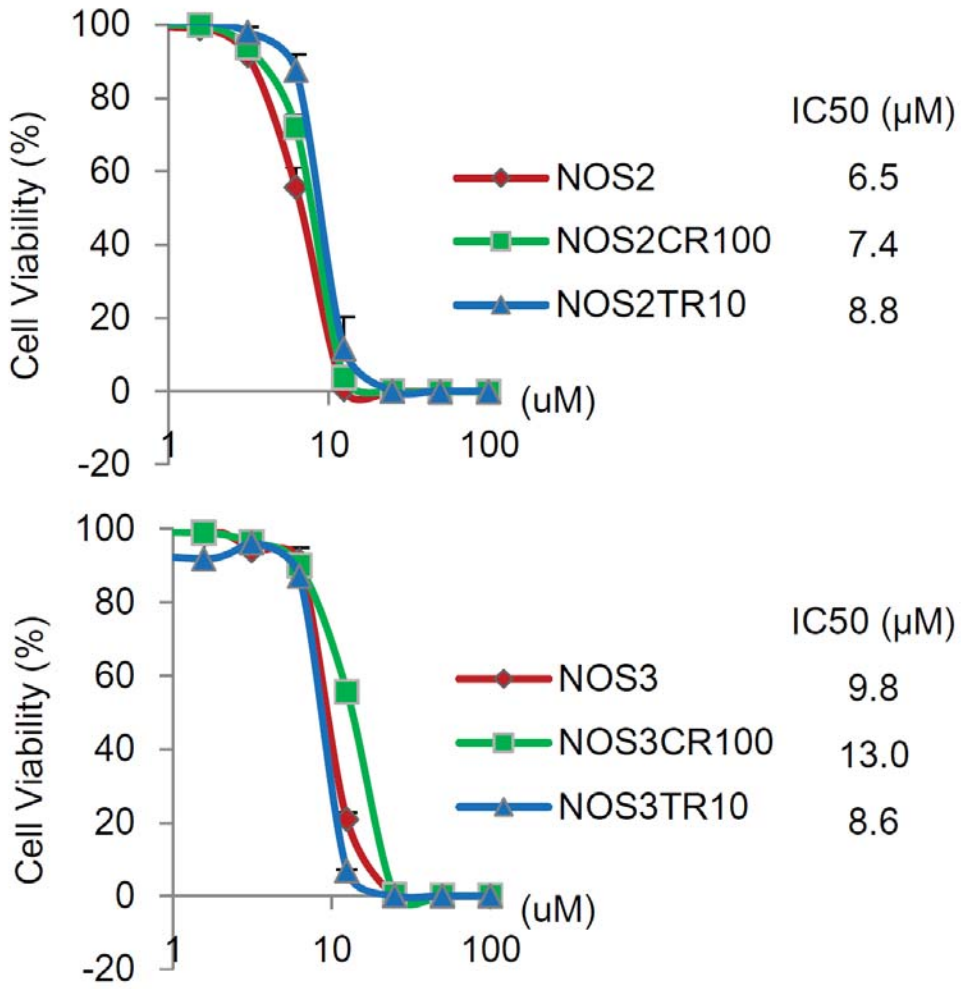

Figure 20 PRIMA-1^{MET} efficiently suppresses growth of chemoresistant cell lines.

PRIMA-1^{MET}-induced growth suppressive dose response curves of NOS2, NOS3, and their chemo-resistant cells. The IC50 values of 48 h PRIMA-1^{MET} were determined by cell viability assay. Data displays mean + standard deviation (STDEV) from triplicate reactions

Figure 21

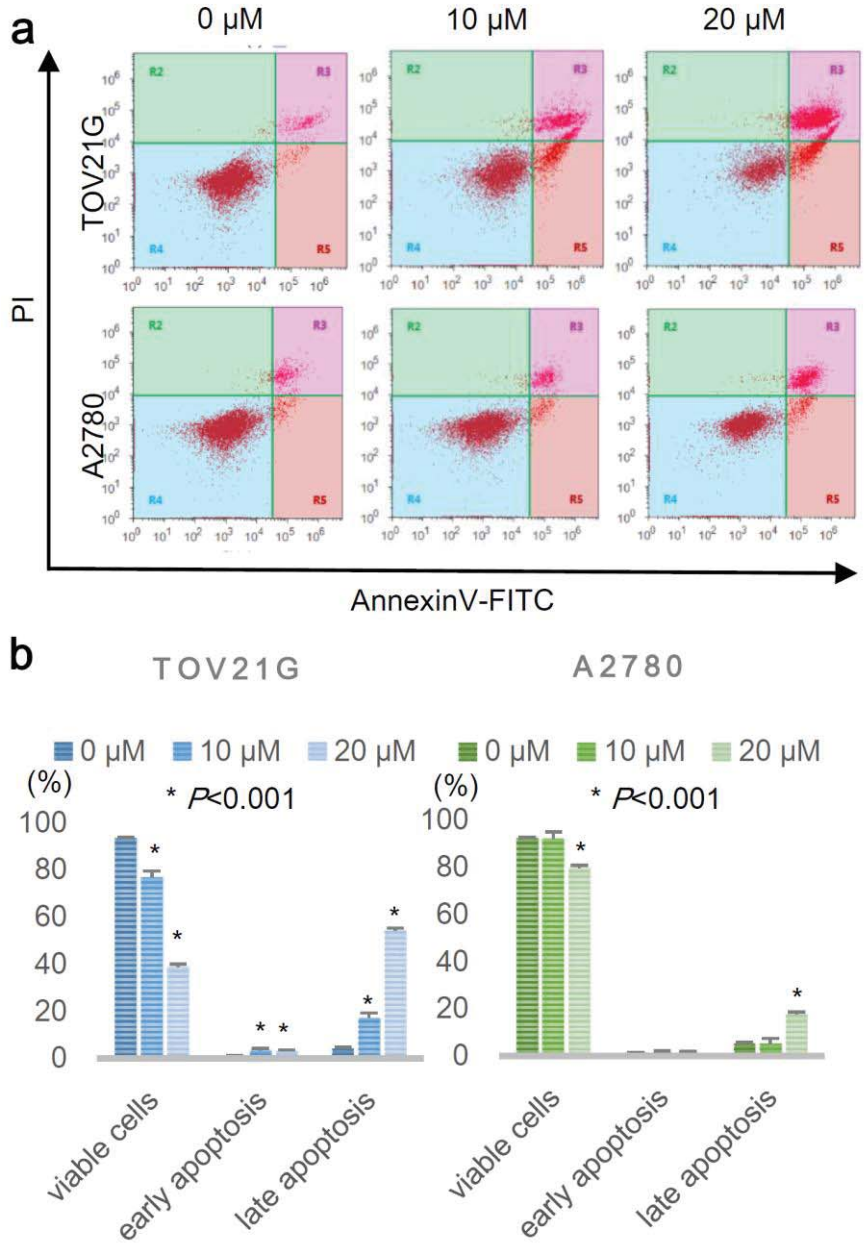

Figure 21 PRIMA-1^{MET} induces apoptosis in dose-dependent manner in ovarian cancer cell lines.

A: TOV21G and A2780 cells were treated with 0, 10, 20 μM of PRIMA-1^{MET} for 16 h, and then stained with annexin V and PI. The annexin-positive and PI-negative cells were defined as early apoptosis, and the annexin-positive and PI-positive cells were defined as late apoptosis. B: Percentage of apoptotic cells was analysed.

PRIMA-1^{MET} displayed sufficient cytotoxic effects on chemo-resistant EOC cells

To determine whether PRIMA-1^{MET} could induce apoptosis in chemo-resistant EOC cells, we assessed cell apoptosis in another way using fluorescence microscopy. The cells after 24 h treatment with PRIMA-1^{MET} were fixed with 4% paraformaldehyde, stained with Hoechst 33342, and then identified morphologic changes. The cells which had fragmented or condensed nuclei were defined as apoptosis and counted manually under fluorescence microscopy [95]. Figure 22 - 24 show that PRIMA-1^{MET} treatment increase apoptotic cells with fragmented or condensed nuclei in a dose-dependent manner.

Figure 22

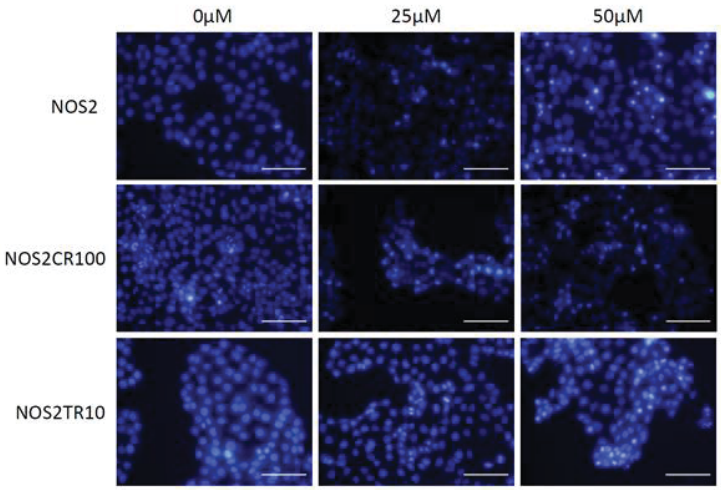

Figure 22 Representative images of Hoechst 33342 staining of NOS2 and its chemo-resistant ovarian cancer cells.

Apoptotic cells were defined by their condensed and fragmented nuclei with a fluorescence microscopy (Scale bar = 200 μM).

Figure 23

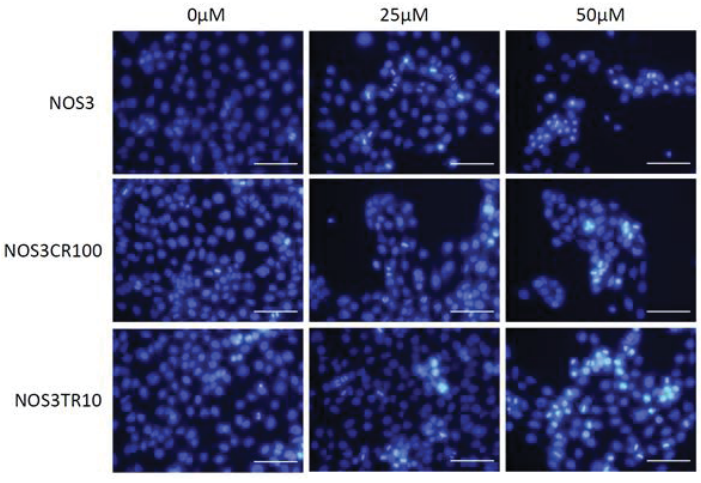

Figure 23 Representative images of Hoechst 33342 staining of n NOS3 and its chemo-resistant ovarian cancer cells

Figure 24

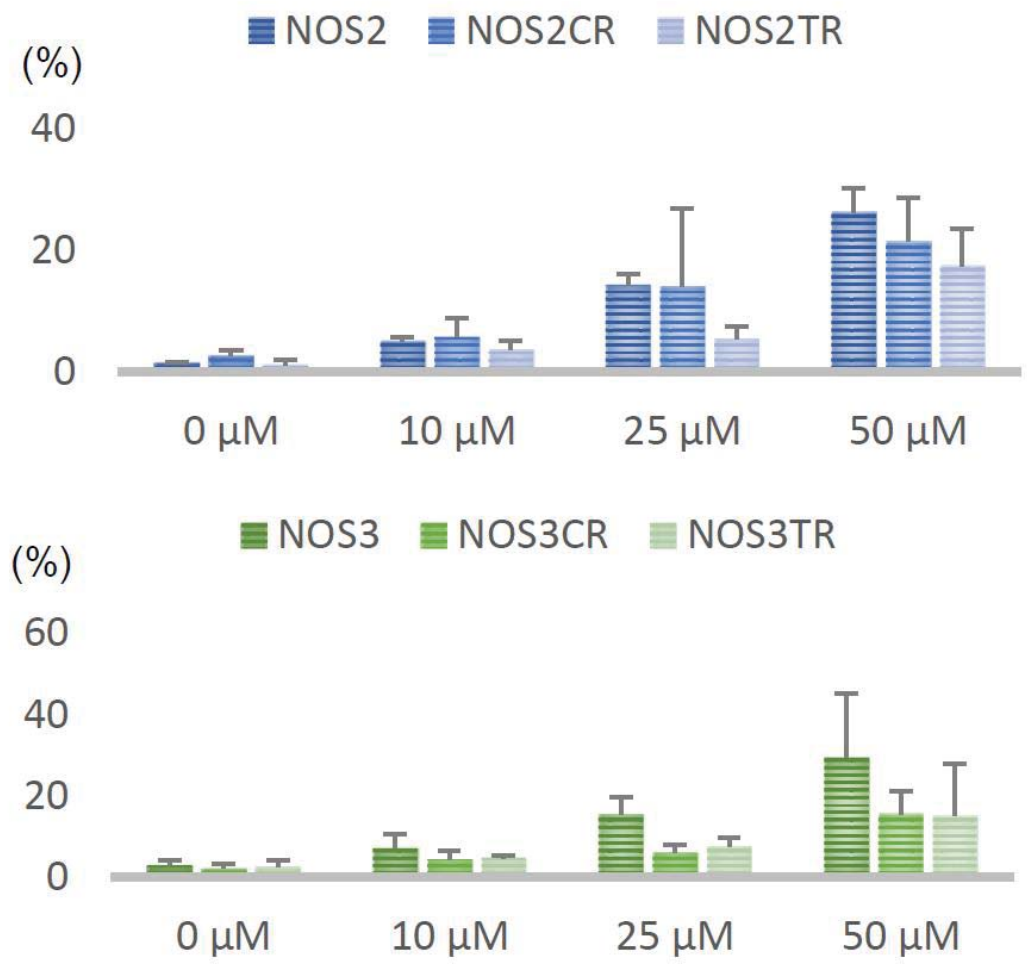

Figure 24 Apoptosis levels of NOS2, NOS3, and their chemo-resistant cells after 0, 10, 25, 50 µM 20 h PRIMA-1^{MET} treatment.

Bars represent the percentages of apoptotic nuclei counted in each treatment group and are expressed as the mean + STDEV. This experiments was performed for each sample in triplicate.

PRIMA-1^{MET} activates PARP cleavage

To identify the mechanism of PRIMA-1^{MET}-induced cell death, we assessed the effects of PRIMA-1^{MET} on EOC cells by western blot analysis. Immunoblotting analysis elucidated that PRIMA-1^{MET} induced dose-dependent PARP cleavage in NOS2, NOS3, and their chemo-resistant cells (Figure 25). This result shows that PRIMA-1^{MET} activates apoptosis through PARP cleavage.

PRIMA-1^{MET} increased intracellular ROS

Because it was reported that PRIMA-1^{MET} induced intracellular ROS accumulation, we investigated intracellular ROS accumulation by using 5-6-chloromethyl-2'7'-dichlorodihydroflorescein diacetate, acetyl ester (CM-H_2DCFDA; Molecular Probes Invitrogen, Calsbad, Ca) [48, 96]. The results revealed that PRIMA-1^{MET} treatment promoted Intracellular ROS accumulation in NOS2, NOS3, and their chemo-resistant cells (Figure 26, 27). To quantify the proportion of fluorescence-positive cells in TOV21G cells after treatment with PRIMA-1^{MET}, fluorescence activated cell sorting (FACS) was performed. The proportion of fluorescence-positive cells was increased in TOV21G cells treated with PRIMA-1^{MET} in a dose-dependent manner, and the increase was significant (Figure 28). These results demonstrate that PRIMA-1^{MET} effectively induces apoptotic cell death in chemo-resistant EOC cells.

Figure 25

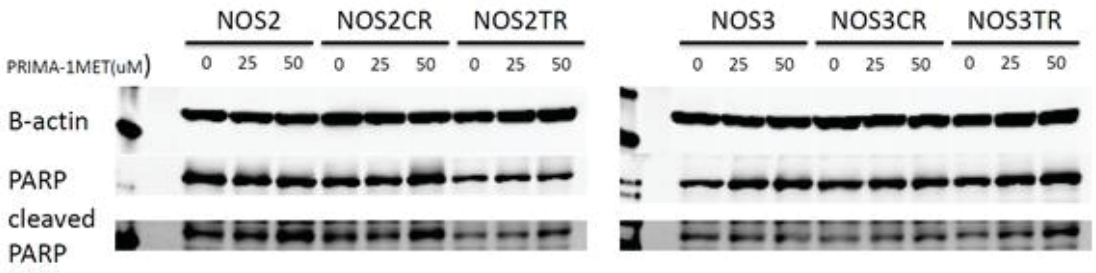

Figure 25 PRIMA-1^{MET} induces PARP cleavage in EOC cells.

NOS2, NOS3, and their chemo-resistant cells were treated with 0, 25, 50 μM PRIMA-1^{MET} for 24 h, and then lysed with lysis buffer. Cell lysates were subjected to Western blot analysis. β-actin was used as a loading control.

Figure 26

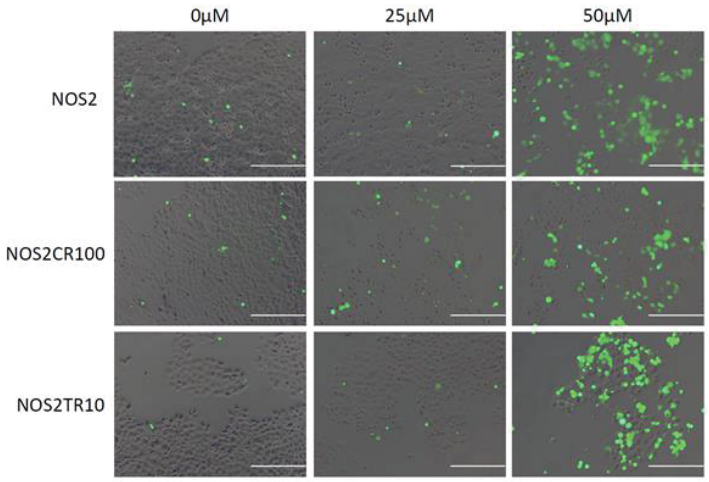

Figure 26 Intracellular ROS generation after treatment with PRIMA-1^{MET} in NOS2 and its chemo-resistant cells.

Intracellular ROS accumulation after 16 h PRIMA-1^{MET} treatment in NOS2, NOS3, and their chemo-resistant cells. Intracellular ROS levels were detected by CM-H_2DCFDA, resulting in fluorescence-positive under fluorescence microscopy.

Figure 27

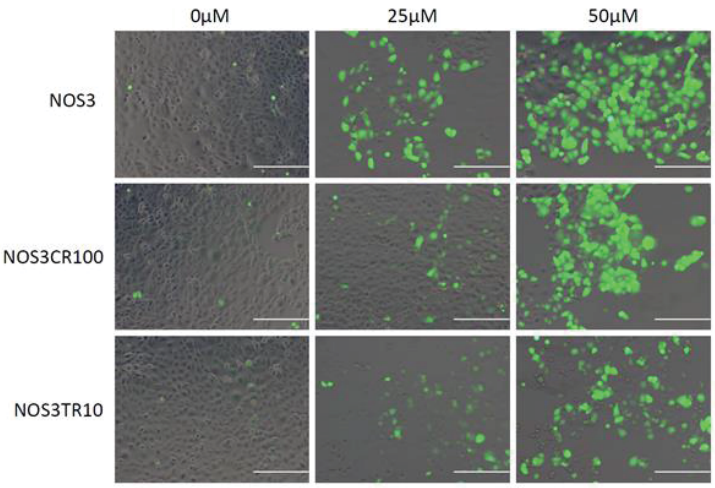

Figure 27 Intracellular ROS generation after treatment with PRIMA-1^{MET} in NOS3 and its chemo-resistant cells.

Figure 28

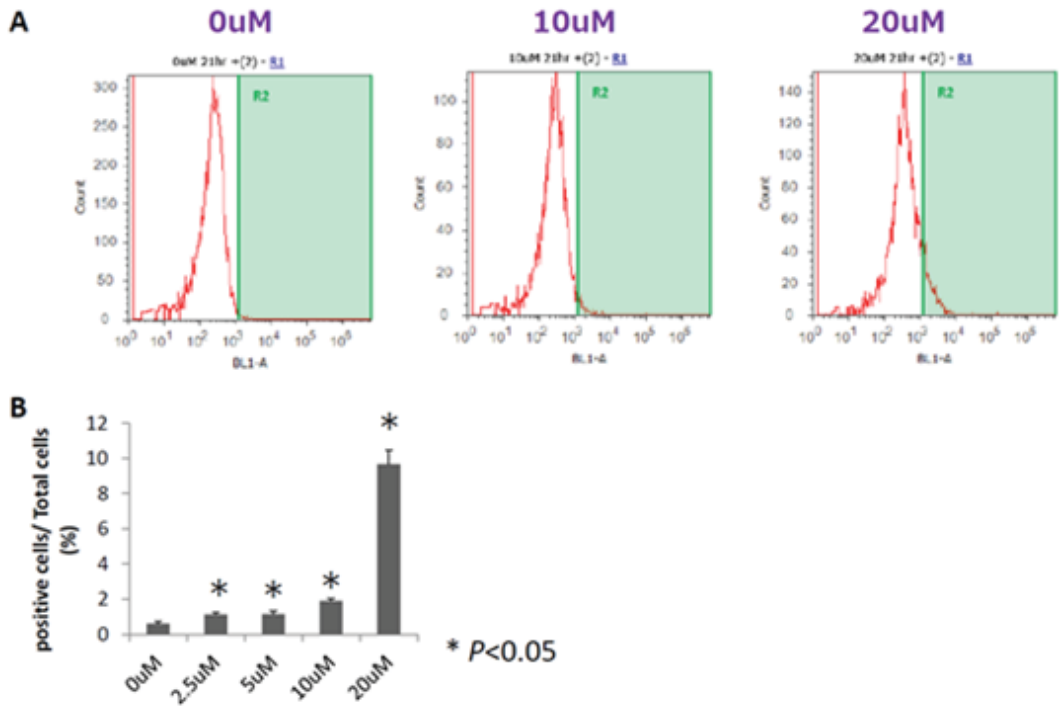

Figure 28 Significant increase of intracellular ROS generation after treatment with PRIMA-1^{MET}.

A: TOV21G cells were maintained in medium with indicated concentrations of PRIMA-1^{MET}, labelled with

5 μM CM-H_2DCFDA, and then subjected to flow cytometry. The percentage of cells with fluorescence intensity above the level of 1,000 FL was measured. **B**: Bars represent the mean percentage of fluorescence-positive cells. Error bars represent standard deviations.

ROS scavenger rescued apoptosis induced by PRIMA-1^{MET}

To determine whether intracellular ROS accumulation by treatment with PRIMA-1^{MET} actually could induce apoptosis, we used the ROS scavenger, N-acetyl cysteine (NAC). The compound NAC was supplemented to cultured cells with 20 μM PRIM-1^{MET} medium at a final concentration of 10 mM. Sixteen hours after co-treatment with PRIMA-1^{MET} and NAC, the apoptotic cells were assessed by annexin V-FITC PI staining. Indeed, the addition of NAC inhibited apoptosis and growth suppressing effect induced by PRIMA-1^{MET} treatment (Figure 29a, b). Our results suggest that anti-tumour effects of PRIMA-1^{MET} are mediated by intracellular ROS accumulation.

PRIMA-1^{MET} inhibited antioxidant enzymes, PRX3 and GPX1

To examine the effect of PRIMA-1^{MET} on the expression of antioxidant enzymes, PRX3 and GPx-1, we treated TOV21G and A2780 cells with PRIMA-1^{MET} for 6 h and thereafter evaluated their mRNA levels by real-time RT-PCR. The levels of PRX3 and GPx-1 were significantly decreased after 20 hr of treatment with PRIMA-1^{MET} in a dose-dependent manner (Figure 29c). This result suggests that the intracellular ROS accumulation and the cytotoxic effect by PRIMA-1^{MET} may be due to downregulation of PRX3 and GPx-1.

Figure 29

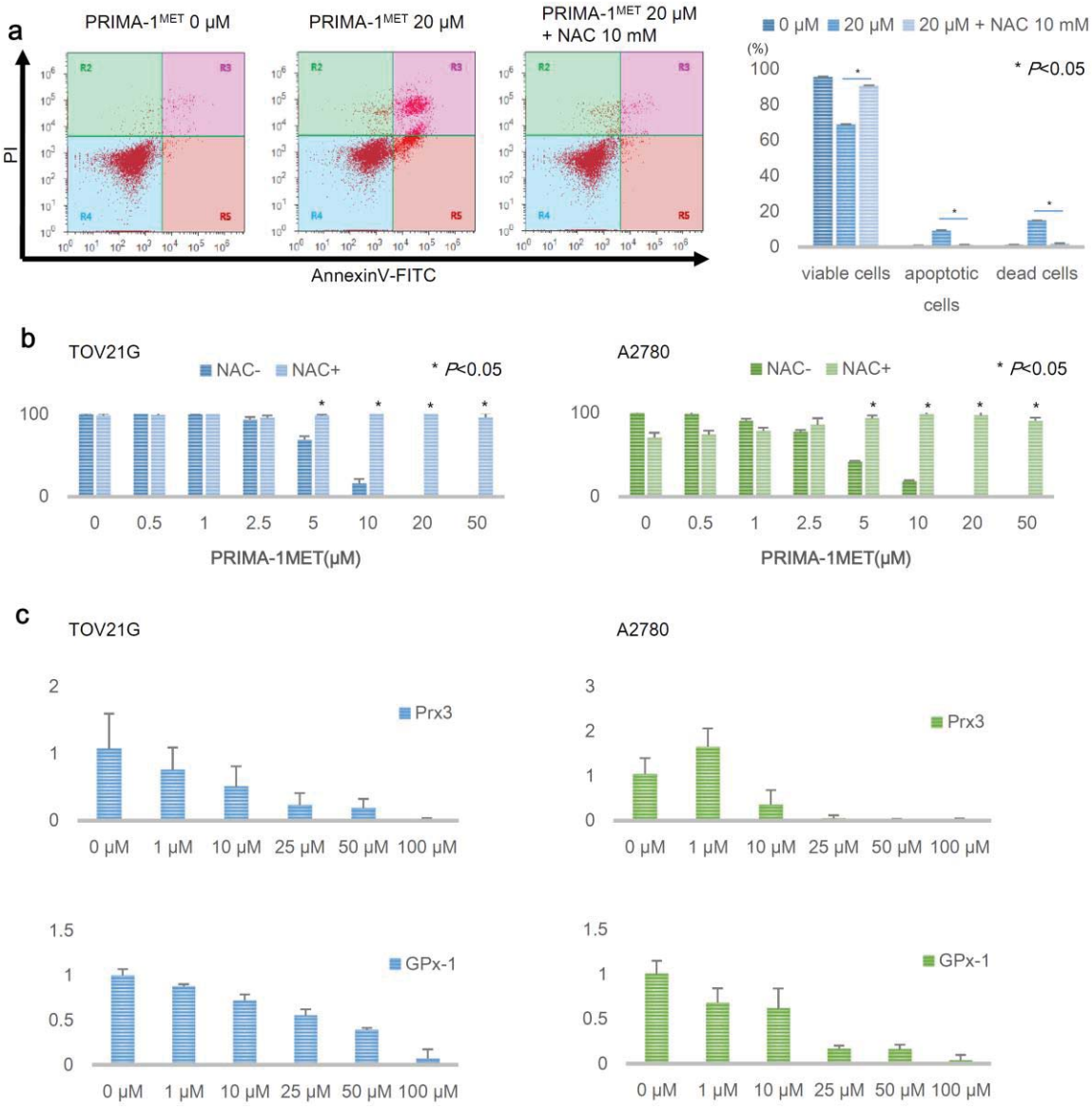

Figure 29 NAC inhibits the biological effect of PRIMA-1^{MET}.

a) NAC completely blocked the cytotoxic effect of 16 h PRIMA-1^{MET} treatment in TOV21G cells, as shown by Annexin V-FITC PI staining analysis. After 20 μM PRIMA-1^{MET} treatment with or without 10 mM NAC for 16 h, the fraction of viable, early apoptotic, and late apoptotic cells were examined Bars represents the mean percentages. Error bars represent standard deviations. Asterisk indicates statistical significance (P<0.05). b) Treatment with NAC prevented the PRIMA-1^{MET}-induced growth suppressive

effect in TOV21G and A2780 cells according to the cell viability assay. After several concentrations of PRIMA-1^{MET} treatment with or without 10 mM NAC, viable cells were evaluated. Bars represents the mean percentages of viable cells. Error bars represent standard deviations. Asterisk indicates statistical significance (P<0.05). d) Inhibition of antioxidant enzymes by PRIMA-1^{MET}. TOV21G and A2780 cells were treated with PRIMA-1^{MET} for 6 h and thereafter evaluated their mRNA levels by real-time RT-PCR. Data represents mean + STDEV from triplicate reactions.

Discussion

Most of the EOC patients finally experience recurrent disease, despite of high rate of complete clinical remission. Although recurrent EOC patients will frequently receive chemotherapy, they are basically incurable due to acquisition of chemo-resistance. Resistance to cytotoxic agents is a major obstacle to complete cure, and a number of attempts to overcome the chemo-resistance have been made in EOC [94, 97]. While much effort has been made to restore chemo-sensitivity to resistant cells, no fabulous molecules to overcome the chemo-resistance have been identified. Thus, there is an imperious need to develop novel therapeutics for the treatment of EOC. Despite the fact that PRIMA-1^{MET} has been confirmed to exhibit tumour-suppressing effects on various cancer cells, there has been a few reports on the effect of PRIMA-1^{MET} on chemo-resistant cells in EOC [98-100]. Thus, in our current study, we attempted to verify whether PRIMA-1^{MET} could have anti-tumour effects on chemo-resistant EOC.

PRIMA-1^{MET} is a prodrug converted to methylene quinuclidinone (MQ) with potential to bind to cysteine residues and change the conformation of the core domain of mutant p53 [48]. In addition, PRIMA-1/PRIMA-1^{MET} has been reported to synergize with cytotoxic agents to induce apoptotic cell death [98, 101, 102]. Recently, Mohell et al. reported that combined treatment with APR-246 and platinum or other drugs could give

rise to improved strategy for recurrent high-grade serous ovarian cancer [102]. In this study, chemo-resistant cells incubated with PRIMA-1^{MET} underwent apoptosis induction, which is characterized by morphological features, such as chromosomal DNA condensation and fragmentation. Furthermore, the efficacy of PRIMA-1^{MET} on cell viability of chemo-resistant cells was similar to that of parental cells. Interestingly, the cell lines we used include both wild-type p53 cell lines and mutant p53 cell lines, thus our results showed that PRIMA-1^{MET} was highly effective on both wild type and mutant p53 cell lines. The results suggest that PRIMA-1^{MET} may have the possibility to be utilized for cancer patients bearing not only mutant p53 but also wild-type p53.

In our current study, we investigated the efficacy of PRIMA-1^{MET} in growth suppression and apoptosis induction in ovarian cancer cell lines (n=9) in vitro. We demonstrated that PRIMA-1^{MET} suppressed cell viability and induced massive apoptosis, regardless of *TP53* mutational status. Furthermore, ovarian cancer cell lines carrying wild-type p53 were slightly more sensitive than those carrying mutant p53 (not significant). Until now, previous reports showed that PRIMA-1/PRIMA-1^{MET} were more effective on pancreatic and small cell lung cancer cells expressing mutant p53 than on those expressing wild-type p53 or null [87, 91]. Interestingly, despite the fact that there are a number of evidences that PRIMA-1^{MET} restores wild-type p53 functions to mutant p53, recent several studies showed that PRIMA-1^{MET} displayed cytotoxic effects on Ewing sarcoma cells, acute myeloid leukemia cells, and human myeloma cells irrespective of *TP53* mutational status [89, 103, 104]. This inconsistency may be because PRIMA-1^{MET} not only restores wild-type p53 functions to mutant p53, but also induces apoptosis mediated through other pathways, such as intracellular ROS accumulation or

endoplasmic reticulum (ER) stress [48, 105]. Indeed, in this study, we demonstrated that incubation with PRIMA-1^{MET} resulted in an anti-tumour effect with intracellular ROS accumulation on ovarian cancer cells, and co-treatment with PRIMA-1^{MET} and ROS scavenger, NAC, blocked the cytotoxic effects, suggesting that the effects of PRIMA-1^{MET} are due to ROS increase in ovarian cancer cells. Our results were consistent with previous reports, and supported that anti-tumour effects of PRIMA-1^{MET} are universal irrespective of *TP53* mutational status. These reports suggest that PRIMA-1^{MET} induces apoptosis through binding covalently to cysteine residues in mutant p53 and glutathione, and may have unknown target genes to modulate cell viability and induce cell death. This diverse mechanism of PRIMA-1^{MET} may provide a convincing strategy for overcoming chemo-resistance in not only EOC but also other cancers.

ROS can generate oxidative stress against cells that induce DNA damage, protein degradation, peroxidation of lipids, and finally cell death at high concentration (30). It is well known that cancer cells are normally more tolerant to high levels of oxidative stress than normal cells. One of the underlying mechanisms of cancer cells to survive under high oxidative condition is overexpression of antioxidant enzymes to scavenge ROS. Indeed, an inhibitor of glutathione synthesis, buthionine sulfoximine (BSO) was attempted to be used in clinical situation [106]. In this study, we demonstrated that PRIMA-1^{MET} induced intracellular accumulation and also efficiently suppressed antioxidant enzymes, PRX3 and GPX1 in ovarian cancer cells. PRX3 is one of the 2-Cys peroxiredoxin family (PRX 1-4) and operates as the reductase to metabolize ROS [107]. Cunniff et al. reported that knockdown of PRX3 increased oxidative stress and

mitochondrial dysfunction in malignant mesothelioma cells, suggesting that PRX3 plays a critical role in cell cycle progression and sustaining mitochondrial structure [108]. Furthermore, the recent report by Song et al. showed that PRX3 was highly upregulated in colon cancer stem cells and knockdown of PRX3 led to decreased cellular viability [109]. In addition, a number of studies have already shown that GPX1 could protect cancer cells from exposing to severe oxidative stress [110, 111]. According to our findings, PRIMA-1^{MET} suppressed the expression of both PRX3 and GPX1, suggesting that PRIMA-1^{MET} might induce intracellular ROS increase mediated by downregulation of PRX3 and GPX1.

In conclusion, we demonstrated that PRIMA-1^{MET} had anti-tumour effects on chemo-resistant cells through intracellular ROS accumulation and repressed antioxidant enzymes. To utilize PRIMA-1^{MET} for recurrent EOC, we need to investigate the further mechanism how PRIMA-1^{MET} suppresses PRX3 and GPX1 (direct target or not? transcriptional control?). PRIMA-1^{MET} is a promising compound for further development as a potential cytotoxic agent for EOC.

Chapter 2

PRRX1 regulates cell invasion and anchorage-independent cell growth in EOC cells

Introduction

Epithelia-to-Mesenchymal Transition

Epithelial-to-mesenchymal Transition (EMT) is a complicated process that happens during embryonic development, tumour metastasis, or tissue fibrosis [112]. Epithelial cells tend to lose their epithelial features and acquire mesenchymal phenotypes during EMT. Not only morphological changes but also drastic changes in gene expression are often recognized in a process of EMT. The suppression of E-cadherin is the hall mark of EMT and the loss of expression of E-cadherin promotes a number of pathways that are associated with invasion and metastasis. Comprehensive studies have revealed that a number of regulatory networks govern EMT, induced by extracellular stimuli, such as soluble factors and extracellular matrix. These factors induce changes in cell-cell junctions and cytoskeletal organization through activation of multiple signaling pathways. In addition to activation of signaling pathways, some transcription factors, namely Twist, Snail, Slug, and Zeb1, have been reported to be related to EMT [113]. These four transcription factors have been extensively studied and shown to promote EMT-related phenotypes as described above and be associated with tumour-promoting functions. Not only these four transcription factors but also other EMT-related transcription factors, such as the FOX family and SIX1 have also been reported to play crucial roles in the promotion of EMT phenotypes in various types of cancers [114, 115]. Furthermore, the expression of EMT-related transcription factors has been reported to be related to poor cancer patient prognosis. The discovery of additional transcription factors will provide further insights into the mechanisms how EMT is modulated. We previously performed a siRNA screen, and identified that Aristaless-like homeobox 1 (ALX1) plays an important role in the induction of EMT in ovarian cancer cells [116].

In our current study, we investigated the function of paired-related homeobox 1 (*PRRX1*), which was recently reported as a novel EMT inducer [117]. Although the two major isoforms of the paired-related homeodomain transcription factor 1, *PRRX1a* and *PRRX1b*, are reported to be involved in pancreatic development, pancreatitis, and carcinogenesis, the biological role in ovarian cancer has not been investigated. *PRRX1* was reported to induce EMT in glioma cells and colorectal cancer cells. In addition, high level of *PRRX1* expression was dominantly related to poor prognosis in colorectal cancer, although the opposite result was observed in breast cancer [118]. Therefore, the clinical implication of *PRRX1* is still controversial. It is largely unknown whether *PRRX1* could induce EMT in ovarian cancer cells.

In this study, we investigated whether *PRRX1* over-expression confers EOC cells to gain malignant properties and to identify the functional roles of *PRRX1* in EOC.

Materials and methods

Cell culture

EOC cells; ES-2, SKOV-3, OVCAR-3, OVCAR-3, and OV-90 were maintained at 37℃ with 5% CO2 in RPMI-1640 medium (Sigma) supplemented with 10% FBS, streptomycin (100μg/mL), and penicillin (100U/mL). Cells were incubated in a 37℃ humidified incubator with 5% CO_2. Replacement of growth media was performed every 2-3 days.

Quantitative real-time RT-PCR

Total RNA was isolated using RNeasy Mini Kit (QIAGEN, Venlo, Netherlands) according to the manufacturer's instructions. cDNA was generated using PrimeScript RT Master Mix (TAKARA, Tokyo, Japan). Quantitative real-time RT-PCR was performed using specific primers for each gene. The primers we used are shown in Table 4.

	Forward primer	Reverse primer	size (bp)
Fibronectin	GTCAGTCAAAGCAAGCCCGG	CAGTCCCAGATCATGGAGTC	237
E-cadherin	CGGGAATGCAGTTGGGATC	AGGATGGTGTAAGCGATGGC	201
SNAI1	CGCGCTCTTTCCTCGTCAG	TCCCAGATGAGCATTGGCAG	181
Slug	GAGCATTTGCAGACAGGTCA	ACAGCAGCCAGATTCCTCAT	137
Twist1	CGGGAGTCCGCAGTCTTA	TGAATCTTGCTCAGCTTGTC	130
ZEB1	AGCAGTGAAAGAGAAGGGAATGC	GGTCCTCTTCAGGTGCCTCAG	226
TGFB1	CAGCAATTCCTGGCGATA	AAGGCGAAAGCCCTCAATTT	136
VEGFA	GGCCTCCGAAACCATGAACT	CTGGGACCACTTGGCATGG	88
IGF1	CCCTGGGTTGCTGTAAGGGT	GGAGCATTCAATTCACCAATCTC	112
IGF2	CTGTTCGGTTTGCGACACG	AGAAGGTGAGAAGCACCAGCA	86
MMP2	CACCCTGGAGCGAGGGTAC	CTGATTAGCTGTAGAGCTGAAGGC	465
MMP9	CATTTCGACGATGACGAGTTGT	CGGGTGTAGAGTCTCTCGC	229

Table 4 Specific primers for each gene.

Generation of stable knockdown cell lines

pSIREN-RetroQ-puro vector (Clontech) designed to express a small hairpin RNA (shRNA) using human U6 promoter was used for retroviral infection to establish stable *PRRX1* knockdown cells. To obtain ES-2 cells that expressed shRNAs, oligonucleotides encoding shRNA specific for human *PRRX1* were ligated into pSIREN-RetroQ-puro vector. 293T cells were transfected with the pSIREN-RetroQ-puro vector and the packaging vectors (Stratagene, Tokyo, Japan). The culture supernatant was aspirated 2 days later and added to ES-2 cell cultures with 2 μg/mL of polybrene (Sigma). Cells were cultured for 24 h, and then an appropriate concentration of puromycin (1ug/mL) was added to select for transduced cells.

Immunohistochemistry

EOC cells cultured on glass coverslips for 24 h were fixed in 4% paraformaldehyde for 1 h, washed with PBS 3 times, permeabilized with 0.1% Triton X-100, and blocked with 1% BSA for 1 h at room temperature. Alexa Fluor 546 Phalloidin and Hoechst 33342 were used to visualize morphology and nuclei.

Soft agar assay

1 x 10^4 cells were suspended in 0.36% agarose (2x RPMI 1640 medium plus 0.72% agarose, and then spread onto a 0.72% agarose (2x RPMI 1640 medium plus 1.44% agarose) plate. 2-3 weeks later, colonies were counted after staining with crystal violet under microscopy. Colonies >100 um diameter were counted, and the number and size of colonies were recorded.

Migration and Invasion assay

To identify cell migratory and invasive ability, the Boyden apparatus assay was performed [116]. We used 24-well Transwell^{TM} chambers with a 8-um polycarbonate filter (Corning). The filter was pre-coated with Matrigel for the invasion assay. The shControl and sh*PRRX1* cells were used for the migration and invasion assay. A total 1.0 x 10^5 ES-2 cells in 200 μL of serum free medium were added into the upper chamber. In addition, 700 μL of medium with 10% serum was added to the lower wells. After 16 h of incubation, the remaining cells on the top surface of the filters were removed by wiping with cotton swabs, and the cells that migrated or invaded to the lower surface were stained with May-Grunwald Giemsa. The number of cells on the filter were counted manually using a microscope.

Results

PRRX1 expression is associated with survival of EOC patients

To determine whether *PRRX1* expression is related to survival of EOC patients, we analyzed the association between the *PRRX1* expression level and survival data from the TCGA database, which is available on line [5]. *PRRX1* mRNA expression of 316 EOC tissues were investigated by quantitative RT-PCR [5]. Cases were divided into two groups according to the median score of *PRRX1* expression. The *PRRX1* higher expression group exhibited a significantly poorer prognosis than the *PRRX1* lower expression group (Figure 30).

The relative expression of PRRX1 mRNA normalized to GAPDH mRNA in EOC cells

Previous studies reported that *PRRX1* promoted EMT and was related to poor prognosis in gastric cancer and colorectal cancer [118, 119]. On the other hand, *PRRX1* was reported to be associated with favorable prognosis in breast cancer and hepatocellular carcinoma [117, 120]. Taken into consideration of this discrepancy, the molecular mechanism of *PRRX1* is complex and may be dependent on the type of cancer. To our knowledge, the functional roles of *PRRX1* in EOC have not been explored. To obtain insight into the function of *PRRX1* in EOC, we evaluated the basal expression of both isoforms of *PRRX1, PRRX1a* and *PRRX1b,* mRNA in a panel of EOC cell lines. Relatively high expression of *PRRX1* was observed in ES-2, A2780, and SKOV-3 (Figure 31). These three cell lines exhibited spiky cell morphology typical of mesenchymal cells and also expressed the mRNAs for Vimentin, Twist1, Slug, and Zeb1 at comparably high level. These results suggest that *PRRX1* could have regulates EMT-related molecules or is regulated by EMT-related transcription factors.

Figure 30

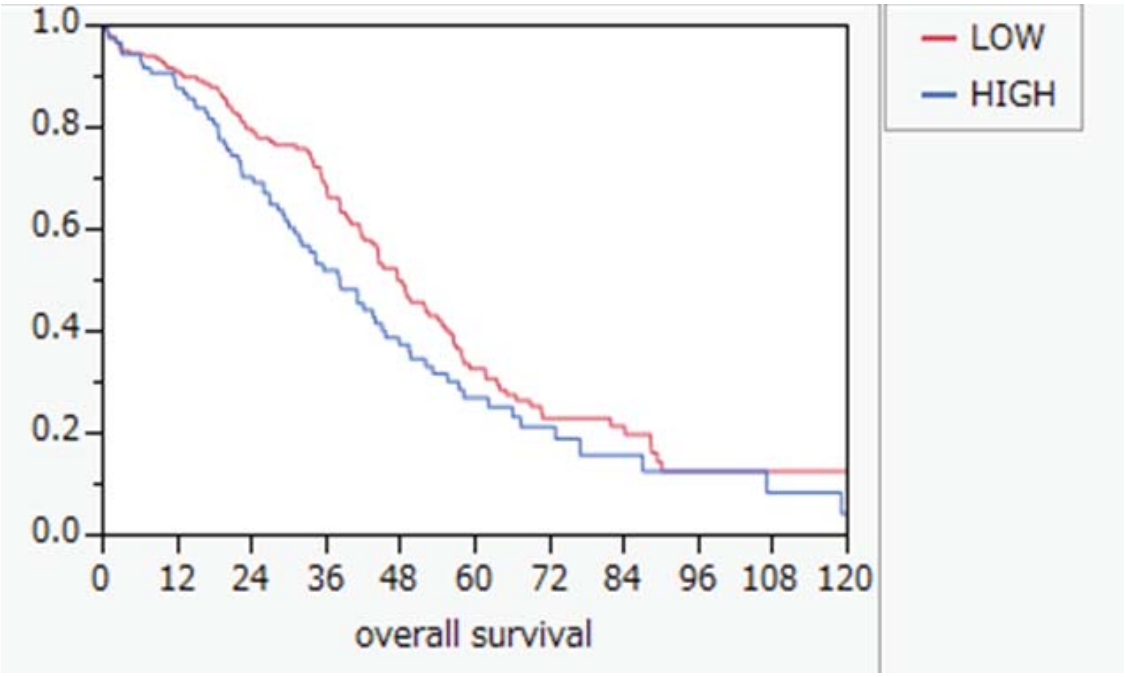

Figure 30 Kaplan-Meier-estimated overall survival of 316 EOC patients with lower or higher expression of *PRRX1*.

We retrospectively analysed the TCGA database recruiting 316 HGSOC patients. The TCGA study consists of various comprehensive analyses of messenger RNA expression, microRNA expression, promoter methylation and DNA copy number in HGSOC. The patients were divided into two groups according to the mRNA expression levels of PRRX1 at the median. Log-rank analysis revealed that patients with higher expression of *PRRX1* exhibited significantly poorer prognosis than those with lower expression of *PRRX1* ($P<0.05$)

Figure 31

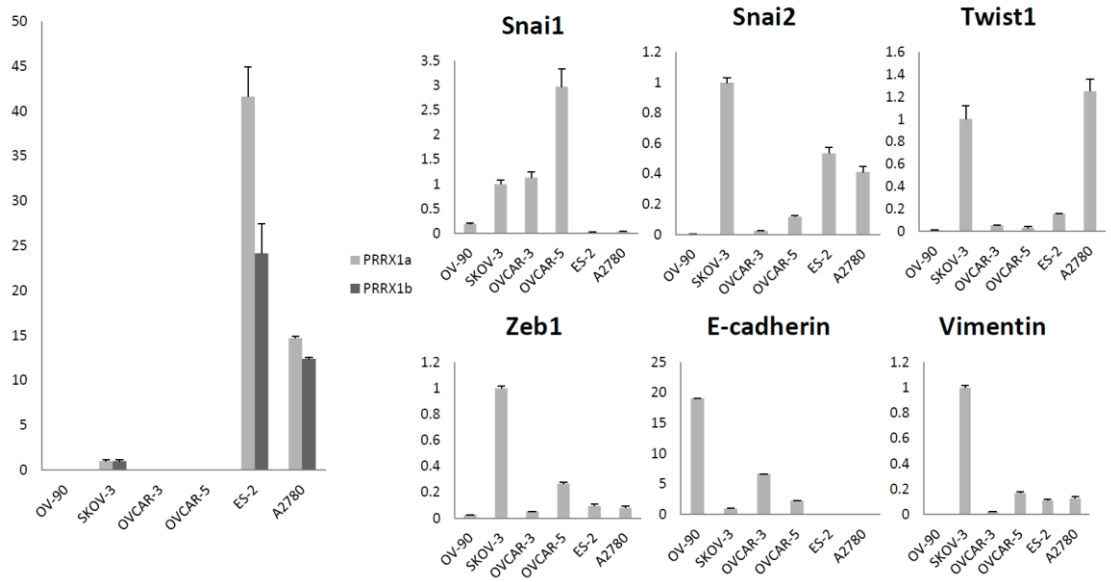

Figure 31 Real-time RT-PCR for EMT-related molecules in EOC cell lines.

To evaluate the association between *PRRX1* and EMT-related molecules, changes in the mRNA expression were evaluated using real-time RT-PCR. The relative mRNA expression of EMT-related molecules normalized to glyceraldehyde-3 (GAPDH) mRNA was examined. Three independent experiments were performed, and the data are shown as the mean ± SD.

Depletion of PRRX1 induced round-shape morphological changes in EOC cells

To identify the role of *PRRX1* in EOC cells, we next knocked-down *PRRX1* expression by shRNA, in ES-2 and A2780 cells, which are *PRRX1* high expression cell lines. The control shRNA (shCont or shScramble) and *PRRX1* shRNA (sh*PRRX1*-1 and sh*PRRX1*-2) cells were established by retroviral infection. Real-time RT-PCR revealed that *PRRX1* shRNA efficiently suppressed the mRNA expressions of *PRRX1* in both ES-2 and A2780 cells (Figure 32). Immunostaining analysis revealed that knocking down the *PRRX1* expression induced drastic epithelial-like changes in ES-2 cells (Figure 33). These results suggested that the elimination of *PRRX1* expressions induced a mesenchymal-to-epithelial transition (MET). This was further investigated by determining if *PRRX1* knockdown resulted in changes in the expression of EMT-related transcription factors.

Figure 32

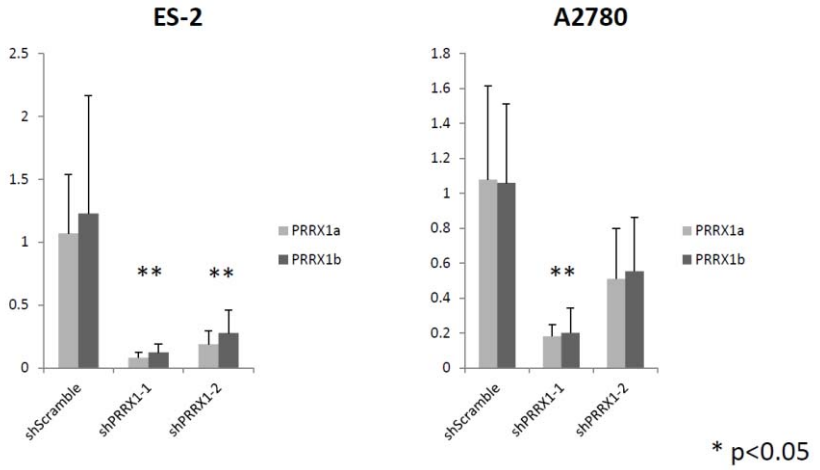

Figure 32 Effect of short hairpin RNA (shRNA) transfection on endogenous *PRRX1* mRNA levels in ES-2 and A2780 cells.

ES-2 and A2780 cells were transfected with shRNA plasmid targeting *PRRX1* by retroviral infection. The relative expression of *PRRX1* mRNA normalized to glyceraldehyde-3 (GAPDH) mRNA was examined by real-time RT-PCR. Three independent experiments were performed, and the data are shown as the mean ± SD.

Figure 33

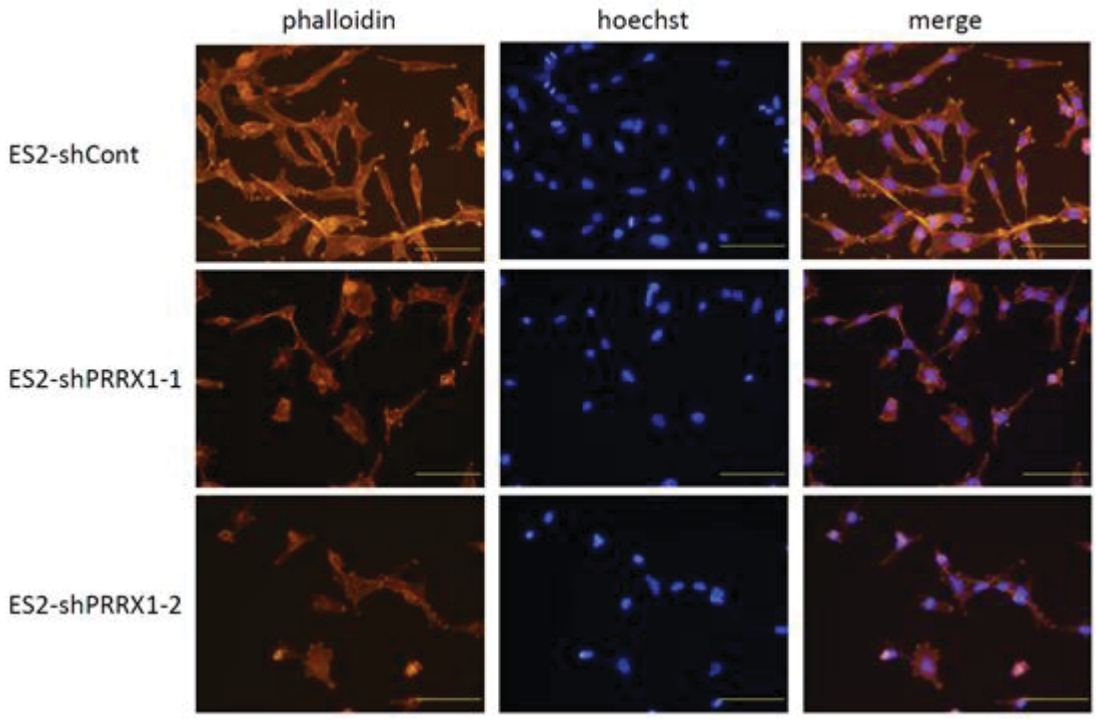

Figure 33 Immunofluorescence images of ES-2 cells transfected with shCont, sh*PRRX1*-1, or sh*PRRX1*-2.

Cells were fixed with 4% paraformaldehyde in PBS, and then stained with phalloidin and Hoechst 33432. Elimination of *PRRX1* expressions in ES-2 induced round-shape morphological changes.

Depletion of PRRX1 did not affect the expression of EMT-related molecules in EOC cells

To confirm whether changes in *PRRX1* expression was reflected in changes in the expression of EMT-related molecules, the expression levels of EMT-related transcription factors were examined by real-time RT-PCR. Although the mRNA expressions of *PRRX1* were repressed greater than 50% by either shRNAs (Figure 32), no significant changes in the mRNA expression levels of the EMT-related molecules were detected (Figure 34). The depletion of *PRRX1* causes EMT cell type changes. However, changes in *PRRX1* expression does not influence the expression of various EMT-related transcription factors. This suggests *PRRX1* is not upstream in the molecular pathways of these transcription factors.

Figure 34

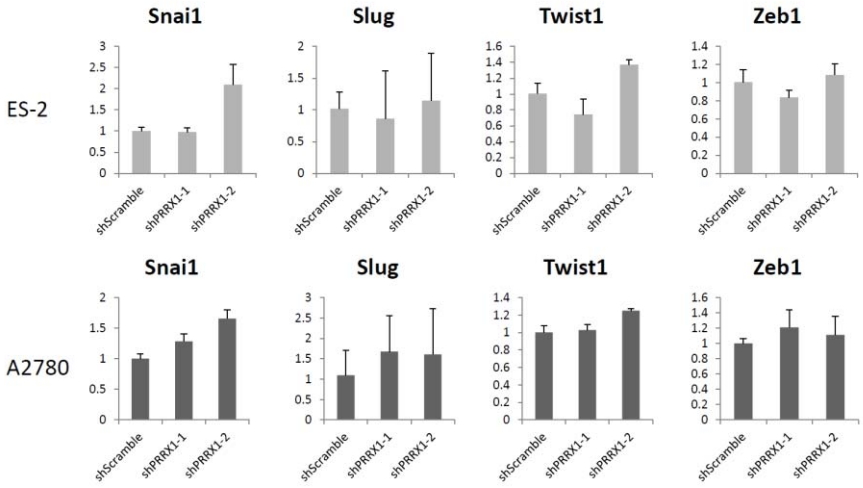

Figure 34 Depletion of *PRRX1* induces no apparent changes of the mRNA levels of EMT-related transcription factors in ES-2 cell.

The relative expression of *PRRX1* mRNA normalized to glyceraldehyde-3 (GAPDH) mRNA was examined by real-time RT-PCR. Three independent experiments were performed, and the data are shown as the mean ± SD.

PRRX1 regulates cell invasion and anchorage-independent cell growth in EOC cells

Round-shaped morphology represented by EMT is frequently related to malignant phenotypes, such as anchorage-independent growth and invasive properties [121]. To evaluate invasive properties, we performed an invasion assay using Matrigel-coated Boyden chambers. The invasion of ES-2 cells was significantly repressed when *PRRX1* was depleted by shRNAs (Figure 35). We next assessed anchorage-independent cell growth in the *PRRX1*-depleted cells. As shown in Figure 36, the depletion of *PRRX1* expression suppressed both the number and the size of colonies in soft agar. These results suggest that *PRRX1* plays an essential role for the invasive and anchorage-independent cell growth abilities in EOC cells.

Figure 35

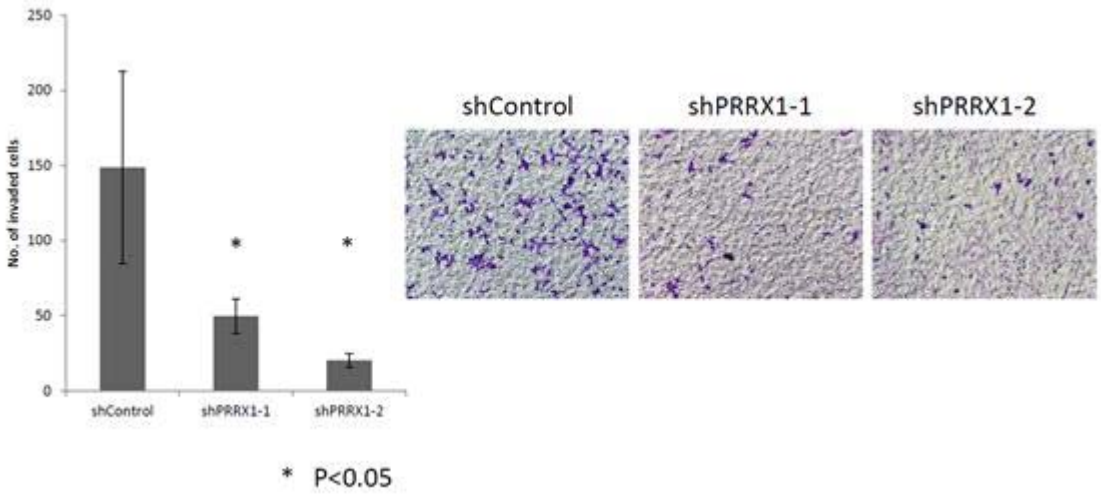

Figure 35 *PRRX1* is required for cell invasion in ES-2 cells.

Cells transfected with shControl, sh*PRRX1*-1, or sh*PRRX1*-2 were subjected to in vitro invasion assay. Representative images are shown on right. The graph indicates the average number of invaded cells per field. Three independent experiments were performed, and the data are shown as the mean ± SD.

Figure 36

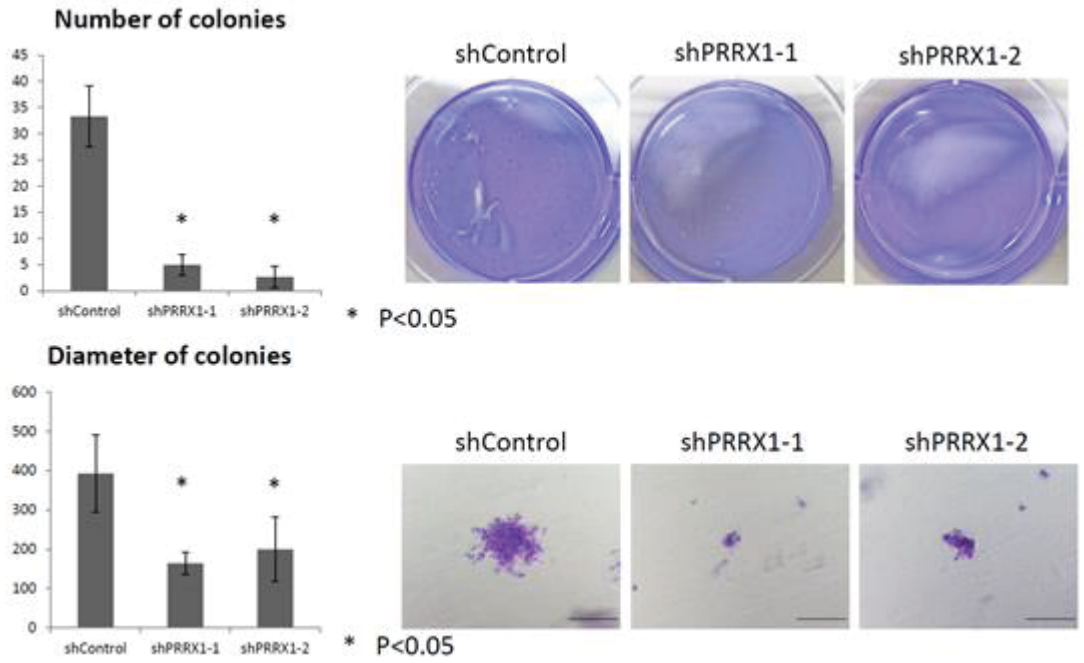

Figure 36 *PRRX1* is required for anchorage-independent cell growth in ES-2 cells.

Cells transfected with shControl, sh*PRRX1*-1, or sh*PRRX1*-2 were subjected to soft agar assay. Representative images are shown on right. The graph indicates the average number of colonies (>100 um) per field. Three independent experiments were performed, and the data are shown as the mean ± SD.

PRRX1 expression is regulated by Twist 1 in EOC cells

Although the transcription factor Twist1 was not altered following *PRRX1* knockdown, it is possible that this transcription factor may be an upstream regulator. This was investigated by establishing stable Twist1 knockdown in ES-2 and A2780 cells, which was then confirmed by the subsequently observed suppression of Twist1 expression by real-time RT-PCR (Figure 37). In both ES-2 and A2780 cells, the mRNA expression of *PRRX1* was also decreased by the knockdown of Twist1 (54% and 38% respectively). This result indicates that Twist 1 regulates *PRRX1* expression in EOC cells.

Figure 37

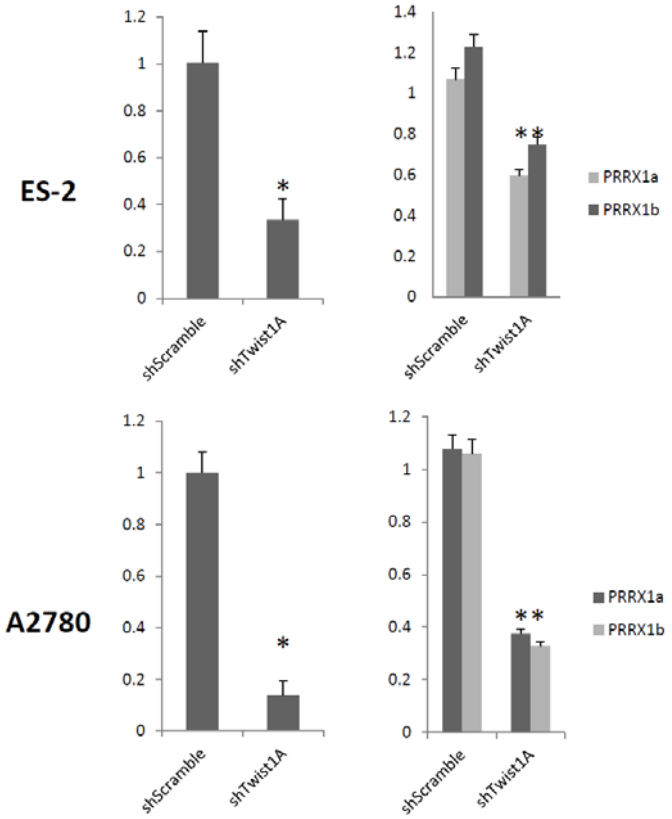

Figure 37 Depletion of Twist 1 decreased the expression of *PRRX1*.

The relative expression of *PRRX1* and Twist 1 mRNA normalized to glyceraldehyde-3 (GAPDH) mRNA was examined by real-time RT-PCR. Three independent experiments were performed, and the data are shown as the mean ± SD.

Discussion

Evidence demonstrates that EMT-related transcription factors are related to cancer cell malignant phenotypes, of metastasis, invasion, and chemo-resistance [116]. PRRX1 is a transcription coactivator, which promotes the DNA-binding activity of serum response factor. PRRX1 has been reported to regulate the differentiation of mesenchymal precursors. It has also been reported that PRRX1 induces EMT by regulating the expression of E-cadherin, N-cadherin and vimentin[120]. In our current study, we demonstrated that the depletion of *PRRX1* in ES-2 cells significantly reduced cell invasion and anchorage-independent cell growth. These results suggest that *PRRX1* expression induces cell invasion and anchorage-independent cell growth. Moreover, this is consistent with our clinical data that revealed high expression of *PRRX1* was associated with poor prognosis in EOC patients. We found that the depletion of *PRRX1* induced morphological changes in ES-2 cells consistent with EMT but did not change any major EMT-related transcription factors. Previous reports showed that *PRRX1* plays an important role in EMT processes in several types of cancer, but we could not find any observable correlation between major EMT-related markers and *PRRX1* [117, 118]. Malignant properties of cancer cells are caused by not only EMT processes, but also integrin/FAK/ERK signaling pathway, Hippo signaling pathway, and Wnt/β-Catenin signaling pathway [122, 123]. Although we could not reach a significant target gene and pathway regulated by *PRRX1*, comprehensive investigation may reveal further insight into the association between *PRRX1* and the well-known major pathways.

We also found that *PRRX1* expression was positively regulated by Twist 1. Knockdown of Twist 1 has been reported to inhibit EMT and cell invasion in EOC cells [124-126]. Furthermore, earlier studies demonstrated that Twist 1 promotes malignant phenotypes

in various cancer cells through regulation of miR-199a/214, TGFβ2, and AKT2 [126, 127]. Our findings suggests that *PRRX1* can be a candidate which assumes a partial role in promoting EMT process by Twist 1. Unfortunately there was insufficient time to complete the full analysis of the *PRRX1* knockouts in EOC cells. Considering the clinical significance of our clinical data concerning *PRRX1*, comprehensive studies may provide a further insight into oncologic roles of *PRRX1* in EOC.

In summary, we have identified that depletion of *PRRX1* induced morphological changes and suppressed malignant phenotypes in ES-2 cells. In addition, the suppression of Twist 1 expression decreased *PRRX1* expression. The elucidation of the mechanism how endogenous *PRRX1* confers invasiveness and anchorage-independent cell growth ability will provide further information of the regulatory systems governing malignant phenotypes.

Chapter 3

Investigation of tumour-promoting role of peritoneal mesothelial cells in EOC

Introduction

Unlike other types of cancers, EOC does not mainly metastasize through hematogenous dissemination. EOC cells are detached from the primary tumour, and then directly circulate throughout the peritoneal cavity. EOC patients are frequently complicated with peritoneal carcinomatosis characterized by massive ascites and bowel obstruction. The microenvironment of EOC is constituted by several types of cells, such as macrophages, adipocytes, and mesothelial cells. Therefore, investigating the mechanisms how EOC cells interact with the intraperitoneal microenvironment is helpful for understanding the characteristics of EOC and exploring novel therapeutic strategies.

EOC cells are likely to disseminate into intraperitoneal sites, such as omentum and uterus. This trend is driven by the components of the microenvironment, such as mesenchymal stem cells, immune cells or mesothelial cells that can produce the extracellular matrix (ECM), or by secreted molecules that attract EOC cells to these sites [128, 129]. In particular, mesothelial cells are specifically located in the peritoneal cavity. Therefore, we focused on investigating the relationship between EOC cells and mesothelial cells.

The peritoneal cavity is covered by mesothelial cells, which prevent adhesions of intraperitoneal organs. In addition, mesothelial cells have been reported to express various ECM factors, such as hyaluronan and fibronectin, which promotes cancer cell adhesion and migration [130, 131]. In contrast, mesothelial cells also have ability to prevent cancer cells from adhesion and invasion, and act like a barrier to protect the intraperitoneal tissue from cancer cells [132]. Moreover, mesothelial cells are able to produce several secreted proteins, such as IL-6 and VEGF, which enhance migration, invasion, and proliferation [133, 134]. Therefore, mesothelial cells not only play a

protective role under a normal condition, but also are manipulated by cancer cells in a cell-cell contact fashion.

Transforming Growth Factor-β1, one of the secreted proteins from EOC cells, has been reported to be related to invasive phenotypes and poor prognosis [135]. We speculated that EOC cells secrete TGF-β1, triggering tumour-supporting changes of mesothelial cells in the EOC microenvironment. To identify a key molecule secreted by mesothelial cells following TGF-β1 stimulation from EOC cells, the transcriptional profiles of the control and TGFβ1-stimulated mesothelial cells were investigated by RNA expression analyses.

Materials and Methods

Cell culture and Preparation of Serum Free Conditioned Media

Human peritoneal mesothelial cells (HPMCs) were isolated from human omentum as described previously [136]. Briefly, a few pieces of omentum were excised surgically under aseptic conditions and were trypsinized at 37℃ for 15-30 min. The cell suspension was centrifuged at 2,000 rpm for 5min. The isolated cells were re-suspended in RPMI 1640 supplemented with 10% fetal bovine serum (FBS) and were plated onto collagen-coated plates. To induce HPMCs by secreted proteins from EOC cells, we prepared serum free conditioned medium (SFCM). ES-2 or SKOV-3 cells were grown to subconfluence in 10 cm dishes and then washed once with sterilized PBS. The washed cells were cultured in 5 mL of serum free medium for 24 h at 37℃ and then the medium was collected. When we collected the SFCM from HPMC stimulated by TGF-β1, cultured HPMCs were treated with 10 μg/mL of TGF-β1 for 24 h, were washed twice with sterilized PBS, and were cultured in 5 mL of serum-free medium for 24 h.

RNA extraction

RNA extraction from the cells was undertaken by using Qiagen RNeasy Mini Kit according to the manufacturer's protocols. The cells were lysed in 250μL of buffer RLT and filtered through the filtration spin column. The samples were applied to RNeasy Mini spin column. Total RNA binded to the membrane and contaminants were washed consequitively with buffers RW1 and RPE. RNA was eluted in RNase free water.

Extracted RNA was immediately stored in -80℃. RNA concentration was determined by NanoDrop 1000 Spectrophotometer.

Reverse Transcription

To obtain complementary DNA (cDNA), 1μg of RNA and 0.2μg of random primer (Promega, Madison, USA) was used. After incubation at 72℃ for 4 minutes, mixture of RNA and random primer was placed on ice for 4 minutes. M-MLV RT 1x Reaction Buffer, M-MLV Reverse Transcriptase RNase Minus, and 10mM dNTP (Promega, Madison, USA) was added to the mixture and then incubated at 42℃ for 90 minutes followed by 70℃ for 15 minutes. cDNA was stored in -20℃.

Quantitative Real Time PCR (qRT-PCR)

Quantitative RT-PCR (qRT-PCR) was performed on a MyiQ instrument using the SYBR Green detection system (Bio-Rad). Cycler conditions consisted of a 3 minutes hot start at 95℃, followed by 40 cycles of denaturation at 95℃ for 10 seconds, annealing at 58-60℃ for 10 seconds, and extension at 72℃ for 10 seconds, then a final inactivation at 95℃ for 10 seconds. Dissociation curve analyses were done at the end of cycling to confirm one specific product is measured in each reaction. Relative quantification was performed by using ΔΔCT method. Expression normalization was done by expression of GAPDH, a housekeeping gene shown to have stable expression in cancer cell lines. All experiments were performed in triplicate.

In vitro migration assay

To exam the effects of conditioned media from HPMCs on cell migratory and invasive ability of EOC cells, Boyden apparatus assay was performed. We used 24-well Transwell^{TM} chambers with 8-um polycarbonate filter (Corning). The filter was pre-coated with Matrigel for invasion assay. ES2 cells were applied for the migration and invasion assay. A total 1.0 x 10^5 ES-2 cells in 200 μL of serum free medium were added into the upper chamber. While 700 μL of SFCM from control or TGF-β1-treated HPMCs was added to the lower wells. After 16 h of incubation, the remaining cells on the top surface of the filters were removed by wiping with cotton swabs. The cells that migrated or invaded to the lower surface of the filter were stained with May-Grunwald Giemsa, and counted under a microscope.

Results

TGF-β1 induces morphological changes in HPMCs

We first isolated HPMCs from surgically resected omentum of EOC patients. The majority of HPMCs exhibited a cobblestone-appearance, while some HPMCs displayed a spindle-like appearance. Then, we investigated morphological changes in normal HPMCs after treatment with TGF-β1 for 72 h (Figure 38). The normal HPMCs displayed a spindle-like morphological change following treatment with TGF-β1. These results suggest that HPMCs stimulated by TGF-β1 have the capability for acquiring a novel function during morphological changes.

EOC cells affects the morphology of HPMCs in a cell-to-cell fashion

We next investigated whether contact between EOC and HPMCs cells could induce morphological changes in the HPMCs. To distinguish EOC cells from HPMCs, we established fluorescence-labeled ES-2 cells (ES-2 ZsGreen) by retroviral infection of the pQCXIP-ZsGreen vector. In addition, we used immortalized HPMCs (HOmMC) previously established in our institution. HOmMC cells were seeded subconfluently on a collagen coated 6-well plate, and then ES-2 ZsGreen cells embedded in 1% collagen gel were added onto the HOmMC cells. As shown in Figure 39, ES-2 ZsGreen cells migrated from the collagen gel into the monolayer of HOmMC cells. Both ES-2 ZsGreen and HOmMC cells close to the gel interface displayed a spindle-like morphology. This result indicates that ES-2 ZsGreen cells induced spindle-like morphological changes in HOmMC cells.

Figure 38

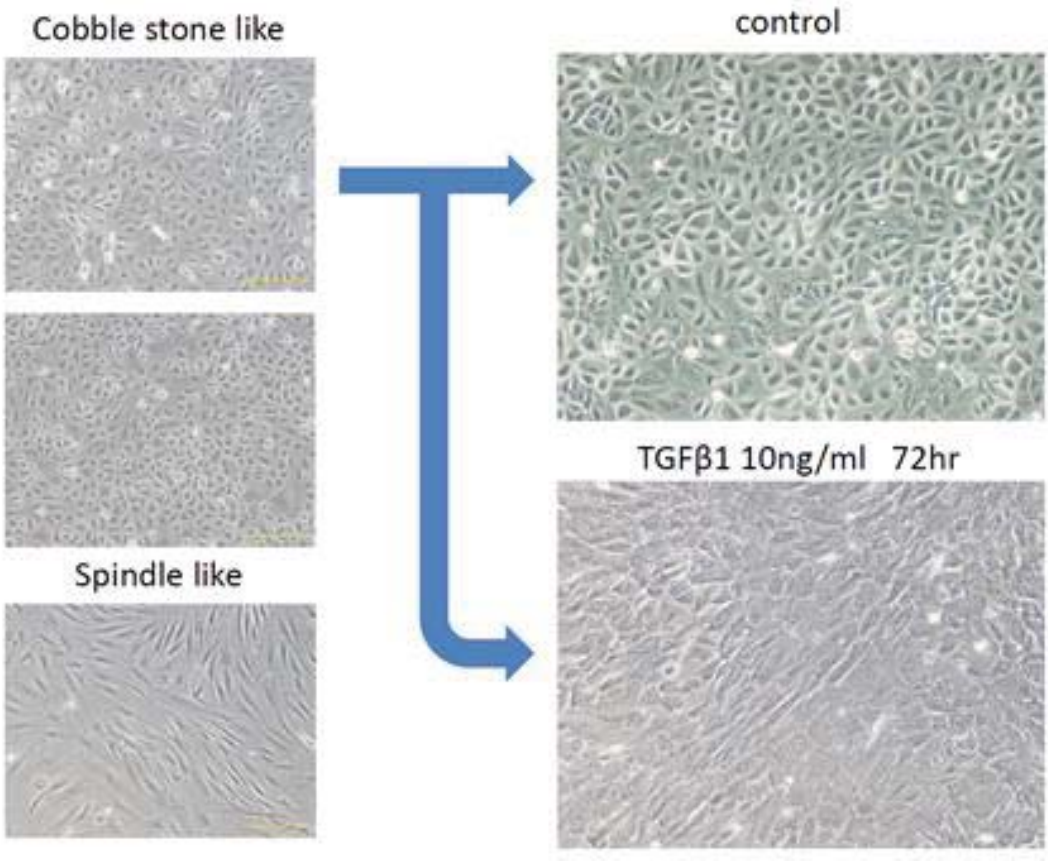

Figure 38 Morphological changes induced by TGF-β1 in cultured HPMCs.

To obtain HPMCs from EOC patients, a few pieces of omentum were excised surgically under aseptic conditions and were trypsinized at 37℃ for 15-30 min. The cell suspension was centrifuged at 2,000 rpm for 5 min. The isolated cells were re-suspended in RPMI 1640 supplemented with 10% fetal bovine serum (FBS) and were plated onto collagen-coated plates. HPMCs were grown in a 6-well plate. Before the cells became subconfluent, the medium was changed to RPMI 1640 supplemented with 10% FBS with or without 10 ng/ml TGF-β1. After a 72 h incubation, the cell morphology was observed under light microscopy at ×100 magnification.

Figure 39

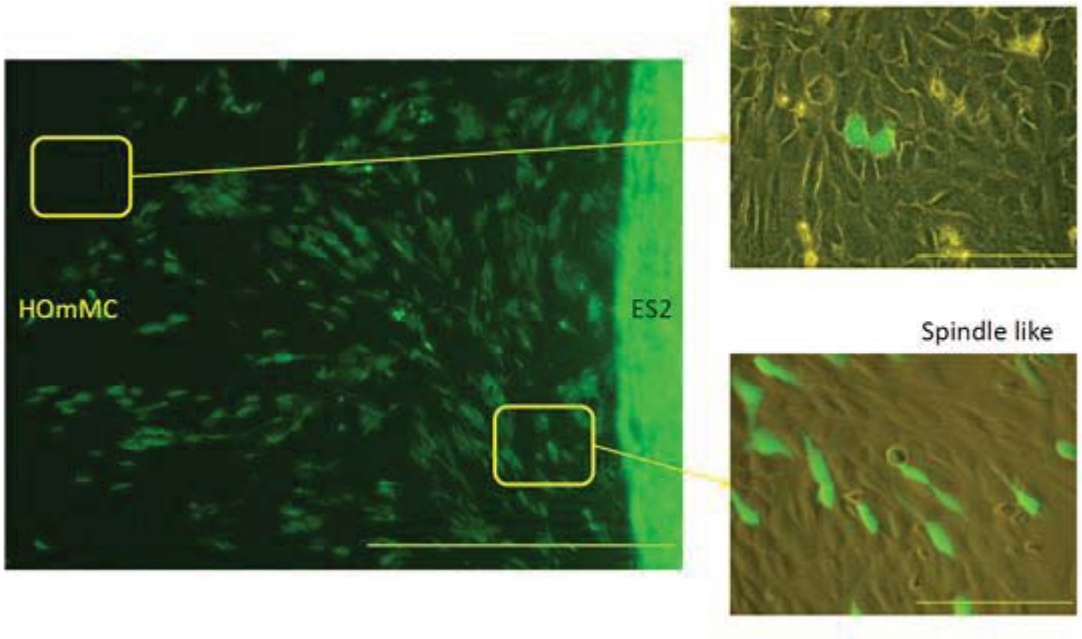

Figure 39 EOC cells induces spindle-like morphology of HOmMC.

To distinguish EOC cells from mesothelial cells, we established fluorescence-labeled ES-2 cells (ES-2 ZsGreen) by retroviral infection of pQCXIP-ZsGreen vector. In this assay, we used the immortalized HPMCs (HOmMC) previously established in our institution. HOmMC cells were cultured subconfluently on a collagen coated 6-well plate, and then ES-2 ZsGreen cells embedded in 1% collagen gel were put on the HOmMC cells. ES-2 ZsGreen cells detached from the collagen gel onto the monolayer of HOmMC cells. Both ES-2 ZsGreen and HOmMC cells nearby the gel displayed a spindle-like morphology.

TGF-β1 induces EMT-related markers of HPMCs in a dose-dependent manner

To examine the effect of TGF-β1 on the expression of EMT-related markers of HPMCs during morphological change, we performed real-time PCR. Real-time PCR revealed that TGF-β1 stimulation increased mesenchymal markers, such as Fibronectin and αSMA and EMT-promoting transcription factors including SNAI1 and ZEB1 in a dose-dependent manner (Figure 40). Moreover, the expression of E-cadherin was decreased by TGF-β1. TGF-β1 treatment also increased the expression of the mRNA expression of VEGFA. This indicates that TGF-β1 induces spindle-like morphological changes in HPMCs through induction of EMT.

TGF-β1 increases the expression of secreted proteins in HPMCs in a time-dependent manner

On the next step, we examined the mRNA expression of secreted proteins, such as matrix metalloprotease (MMP), vascular endothelial growth factor A (VEGFA), insulin-like growth factor (IGF) in order to identify a supportive role of HPMCs in EOC microenvironment. As shown in Figure 41, TGF-β1 upregulated the mRNA expression of secreted proteins of HPMCs in a time-dependent manner.

Figure 40

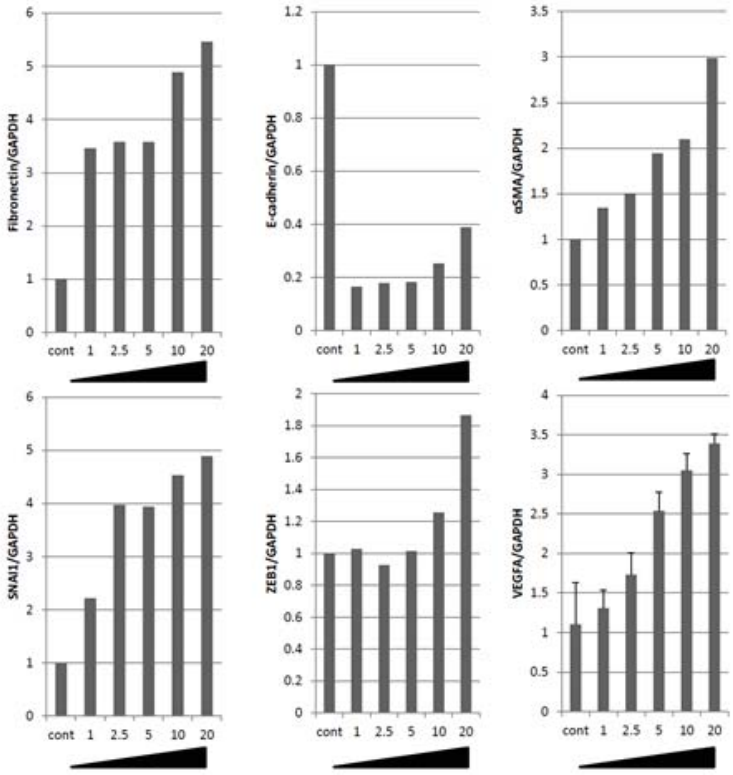

Figure 40 Dose-dependent upregulation of EMT-related proteins by treatment with TGF-β1

To evaluate the effect of TGF-β1 on the expression of EMT-related markers of HPMCs during morphological change, we performed real-time PCR. Real-time PCR revealed that TGF-β1 stimulation increased mesenchymal markers, such as Fibronectin and αSMA and EMT-promoting transcription factors including SNAI1 and ZEB1 in a dose-dependent manner.

Figure 41

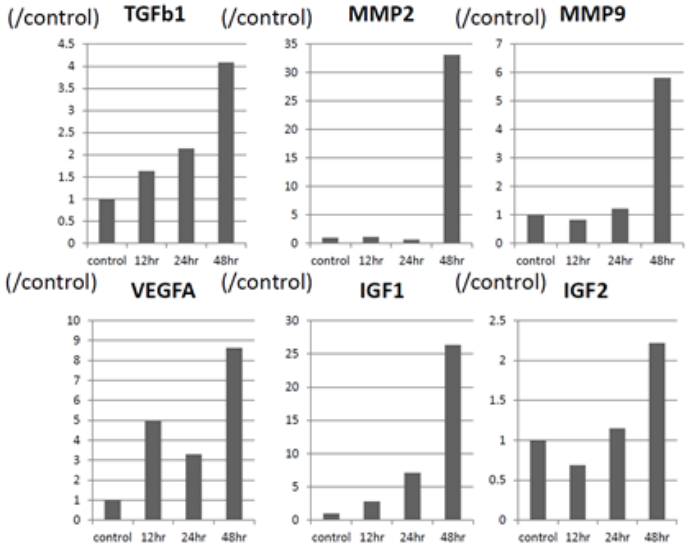

Figure 41 TGF-β1 increases the expression of secreted proteins in HPMCs in a time-dependent manner

Real-time PCR revealed that TGF-β1 stimulation increased mesenchymal markers, such as Fibronectin and αSMA and EMT-promoting transcription factors including SNAI1 and ZEB1 in a time-dependent manner.

SB-431542, a specific inhibitor of TGFβR1, partially neutralized the effects of SFCM from EOC cells against HPMCs.

To determine whether EOC cells might induce morphological changes of HPMCs with TGF-β1 the key molecule involved in this induction, we conducted a series of in vitro experiments. Serum-free media or SFCM from ES-2 cells were added to the confluent HPMCs, and the RNA of the HPMCs extracted 24 h later. Similar to the treatment with TGF-β1, the mRNA level of mesenchymal markers and EMT-promoting transcription factors were elevated by treatment with SFCM from ES-2 cells. The observed increase of VEGFA expression after treatment with the SFCM was similar to that observed following treatment of TGF-β1. In addition, SB-431542, a specific inhibitor of TGFβR1,

largely neutralized the effects of SFCM from ES-2 cells on the expression of EMT-related proteins of HPMCs (Figure 42). These results suggest that SFCM from ES-2 cells, can induce morphological changes and EMT-like changes in a paracrine manner, and this is largely driven by secreted-TGF-β1.

HPMCs stimulated by TGF-β1 conferred migratory and invasive ability to EOC cells

To examine the ability of HPMCs stimulated by TGF-β1 to confer invasive properties to EOC cells, we conducted migration and invasion assay using SFCM from HPMC treated with or without TGF-β1. SFCM from HPMCs treated with TGF-β1 significantly conferred migratory and invasive abilities to ES-2 cells compared with SFCM from control HPMCs. Addition of the inhibitor SB-431542 resulted in attenuation of the effects of SFCM from stimulated HPMCs on EOC cells (Figure 43). These results indicate that HPMCs are consistant with an ability to generate and support a tumour microenvironment in a paracrine manner.

Figure 42

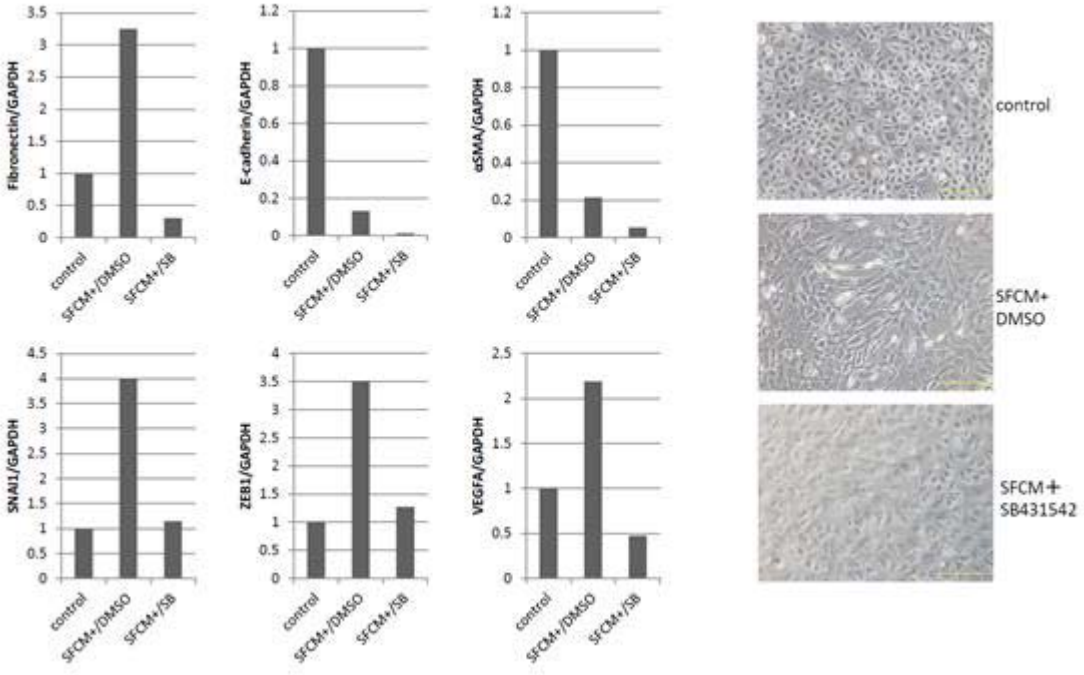

Figure 42 SB-431542, a specific inhibitor of TGFβR1, partially neutralized the effects of SFCM from EOC cells against HPMCs.

SB-431542, a specific inhibitor of TGFβR1, largely neutralized the effects of SFCM from ES-2 cells on the expression of EMT-related proteins of HPMCs

Figure 43

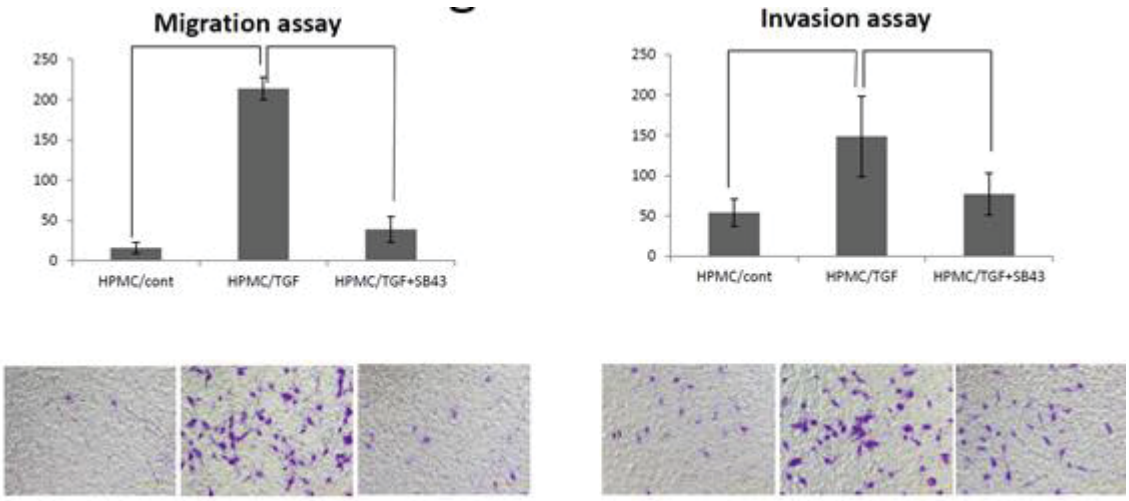

Figure 43 Activated HPMCs by TGF-β1 provided migratory and invasive properties for EOC cells.

Addition of the inhibitor SB-431542 resulted in attenuation of the effects of SFCM from stimulated HPMCs on EOC cells

Discussion

TGF-β1 is a member of the transforming growth factor family of proteins and a number of studies implicate TGF-β1 in tumour progression and malignant phenotypes [137, 138]. Intriguingly, TGF-β1 has been reported to relate to malignancy and poor prognosis in various types of cancer, but is also known as a tumour-repressor gene in other cancers especially at the early stages of cancer development [139-144]. Overexpression of TGF-β1 is found in breast cancer [145, 146], colorectal cancer [141], gastric cancer [147], and cervical cancer [148]. Although TGF-β1 has been shown to be a major inducer of EMT in EOC [149], the role of HPMCs as a component of the EOC microenvironment remains unknown.

In our current study, we observed that HPMCs exhibited spindle-like morphology similar to myofibroblasts after TGF-β1 treatment. Moreover, the epithelial marker E-cadherin was decreased, and the mesenchymal marker αSMA was increased in a time- and dose-dependent manner, when HPMCs were treated with TGF-β1. The increase of mesenchymal markers and the decrease of epithelial markers are fundamental for the EMT process [150]. Therefore, our results indicated that TGF-β1 had the ability to induce EMT in HPMCs.

In this study, the findings that SFCM from EOC cells induced the EMT process and that SB-431542, a specific inhibitor of TGFβR1, attenuated the induction of EMT process by SFCM have led to the hypothesis that TGF-β1 from EOC cells may be a major mediator during the EMT process of HPMCs. Recent studies have revealed that stromal cells and T-cells are manipulated by the TGF-β1 produced by cancer cells, resulting in the creation and maintenance of a cancer microenvironment [151-153].

Taken together, our findings suggested that the EMT process of HPMCs largely depended on the presence of TGF-β1 produced in a paracrine manner.

We found that SFCM from TGF-β1-induced HPMCs promoted their migratory and invasive ability, and that TGF-β1 upregulated the expression of various secreted proteins. Lv et al. previously reported that peritoneal fibrosis activated the attachment of gastric cancer cell to HPMCs [154]. Our groups also revealed that SDF-1α enhanced the migratory potential of TGF-β1-induced HPMCs [136]. Our findings suggested that HPMCs may have the ability to promote tumour progression through upregulation of secreted proteins in a paracrine manner.

In conclusion, our current study demonstrated that HPMCs were potent cellular components manipulated by cancer cells, which results in the promotion of migration and invasion of EOC cells. These findings provide a biological rationale for further examination to explore novel therapeutic approaches targeting the EOC microenvironment.

Chapter 4

General discussion and Future direction

Currently, there are a number of treatment modalities for patients with EOC and the developments in chemotherapy have resulted in patients having a better quality of life with less adverse effects of these agents. However, overall there has been little change in the prognosis of EOC patients. This is due to in part their presentation with relatively advance disease since there is no current approach that enables early detection of EOC [70]. In addition, the current standard chemotherapy treatments are associated with high recurrence rate due to the inevitable development of resistance. Advanced and recurrent EOCs frequently consist of a diffuse peritoneal dissemination, resulting in incurable disease. Peritoneal dissemination is associated with a bowel obstruction and a massive ascites, resulting in a serious erosion of a patient's quality of life. The clinical management of peritoneal dissemination would be a major contributor to improve EOC patients' prognosis and quality of life. Therefore, there is a critical need to explore and develop novel therapeutics for the treatment of recurrent EOC.

TP53 mutation is a hallmark of EOC, especially high-grade serous ovarian carcinoma [5]. In addition to the critical roles of p53 as a tumour suppressor, *TP53* mutation provides cancer cells with aggressive phenotypes, termed gain-of-function. Most of the conventional chemotherapies induce apoptosis via activation of the p53 signaling pathway, and therefore, *TP53* mutation is related to resistance by which EOC cells avoid apoptosis induced by such chemotherapies. A novel approach is to use molecules which restore wild-type p53 functions to mutant p53. These would be expected to induce apoptosis in the p53 mutant cancer cells but have no adverse effects to normal cells. As a result, therapies designed to target mutant p53 have the potential to be effective against various types of cancers with mutant p53.

One appealing anticancer strategy for cancers with mutant p53 is a gene

correction of mutant p53 into wild-type p53 in cancer cells. Recent developments of a novel gene editing technology, CRISPR-Cas, have the potential to modify any genomic DNA sequences into a desired sequence *in vitro* and *in vivo* and thus have the potential to be used to edit tumour cells *in vivo* [60]. Another potential approach is a small molecule which induces apoptosis via reactivation of wild-type p53 functions, such as PRIMA-1/PRIMA-1^{MET} and RITA. Both strategies have not been well investigated in EOC cells.

The first aim of this project was to explore the possibility of the CRISPR-Cas system to modify a *TP53* genomic sequence in EOC cells. In this study, we achieved a high frequency of mutations of p53 by the CRISPR-Cas system, resulting in elimination of p53 protein expression. This suggested that the CRISPR-Cas system have potential to be used as a gene-knockout system like siRNA. Unfortunately within the time available we could not complete the full analysis of the mutant p53 knockouts in the EOC cell lines. These cell lines will provide a further insight into p53 functions with genetically identical backgrounds. The second aim of this study was to identify the efficacy of PRIMA-1^{MET} on EOC cells. The experiments shown in this thesis, demonstrated that PRIMA-1^{MET} treatment resulted in activity leading to suppressed viability and increased apoptosis of EOC cells regardless of the mutation status of the p53 and chemo-sensitivity of the cell lines. Our experiments also identified that PRIMA-1^{MET}-induced apoptosis was largely mediated by intracellular ROS accumulation, caused by elimination of antioxidant enzymes, PRX3 and GPX1. Although these results did not support a role for PRIMA-1^{MET} in activating mutant p53, these results did indicate a potential mechanism of PRIMA-1^{MET}-induced apoptosis in EOC cells and provides an opportunity for further investigation including clinical trials

in EOC.

EMT is a key process in the tumour invasion and metastasis which enables cancer cells to acquire malignant properties [155]. In EOC, various EMT-related transcription factors, such as Twist1 and Zeb1, have been reported to be associated with poor patient prognosis and invasive phenotypes in cancers [156, 157]. Although *PRRX1* is one of the EMT-related transcription factors and is associated with cancer patient prognosis, the expression and biological function of *PRRX1* in EOC remains unknown. The third aim of this study was to identify whether *PRRX1* over-expression confers malignant properties to EOC cells and to identify the functional roles of *PRRX1* in EOC. In our current study, we identified that *PRR1* over-expression was related to invasive and anchorage-independent cell growth of EOC cells *in vitro* and was associated with poor patient prognosis. Our results suggest that *PRRX1* may serve as an EMT-promoting transcription factor in EOC. Further investigation may provide a further insight into the association between *PRRX1* and the major pathways contributing to poor prognosis of EOC patients.

Peritoneal dissemination of EOC cells is normally driven by the components of the microenvironment, including mesothelial cells that produce the ECM and soluble factors that attract EOC cells. Normally, peritoneal mesothelial cells serves as a barrier to prevent adhesions of intraperitoneal organs. However, in the presence of cancer cells, mesothelial cells are reprogrammed by TGF-β1, one of the secreted proteins from cancer cells. The fourth aim of this study was to identify a key molecule secreted by mesothelial cells following exposure to TGF-β1. We identified that HPMCs, following TGF-β1 treatment, displayed spindle-like morphology similar to myofibroblasts, resulting in increased expression of mesenchymal markers and various soluble factors,

such as VEGFA and MMPs. This suggests that HPMCs have the potential to promote migration and invasion of EOC cells in a paracrine manner. These findings provide a biological rationale for further investigation to identify novel therapeutic approaches targeting the EOC microenvironment.

Bibliography

1. Sankaranarayanan, R. and J. Ferlay, *Worldwide burden of gynaecological cancer: the size of the problem.* Best Pract Res Clin Obstet Gynaecol, 2006. **20**(2): p. 207-25.
2. Chan, J.K., et al., *Prognostic factors for high-risk early-stage epithelial ovarian cancer: a Gynecologic Oncology Group study.* Cancer, 2008. **112**(10): p. 2202-10.
3. Chan, J.K., et al., *Do clear cell ovarian carcinomas have poorer prognosis compared to other epithelial cell types? A study of 1411 clear cell ovarian cancers.* Gynecol Oncol, 2008. **109**(3): p. 370-6.
4. Jemal, A., et al., *Cancer statistics, 2009.* CA Cancer J Clin, 2009. **59**(4): p. 225-49.
5. Cancer Genome Atlas Research, N., *Integrated genomic analyses of ovarian carcinoma.* Nature, 2011. **474**(7353): p. 609-15.
6. Havrilesky, L., et al., *Prognostic significance of p53 mutation and p53 overexpression in advanced epithelial ovarian cancer: a Gynecologic Oncology Group Study.* J Clin Oncol, 2003. **21**(20): p. 3814-25.
7. Risch, H.A., et al., *Population BRCA1 and BRCA2 mutation frequencies and cancer penetrances: a kin-cohort study in Ontario, Canada.* J Natl Cancer Inst, 2006. **98**(23): p. 1694-706.
8. Kang, H.J., et al., *Clinical relevance of gain-of-function mutations of p53 in high-grade serous ovarian carcinoma.* PLoS One, 2013. **8**(8): p. e72609.
9. Carlson, J.W., et al., *Serous tubal intraepithelial carcinoma: its potential role in primary peritoneal serous carcinoma and serous cancer prevention.* J Clin Oncol, 2008. **26**(25): p. 4160-5.
10. Giaccia, A.J. and M.B. Kastan, *The complexity of p53 modulation: emerging patterns from divergent signals.* Genes Dev, 1998. **12**(19): p. 2973-83.
11. Jacks, T., et al., *Tumor spectrum analysis in p53-mutant mice.* Curr Biol, 1994. **4**(1): p. 1-7.
12. Brosh, R. and V. Rotter, *When mutants gain new powers: news from the mutant p53 field.* Nat Rev Cancer, 2009. **9**(10): p. 701-13.
13. Joerger, A.C. and A.R. Fersht, *The tumor suppressor p53: from structures to drug discovery.* Cold Spring Harb Perspect Biol, 2010. **2**(6): p. a000919.
14. Bullock, A.N. and A.R. Fersht, *Rescuing the function of mutant p53.* Nat Rev Cancer, 2001. **1**(1): p. 68-76.
15. Alsner, J., et al., *A comparison between p53 accumulation determined by immunohistochemistry and TP53 mutations as prognostic variables in tumours from breast cancer patients.* Acta Oncol, 2008. **47**(4): p. 600-7.
16. Bartek, J., et al., *Genetic and immunochemical analysis of mutant p53 in human breast cancer cell lines.* Oncogene, 1990. **5**(6): p. 893-9.
17. Oren, M. and V. Rotter, *Mutant p53 gain-of-function in cancer.* Cold Spring Harb Perspect Biol, 2010. **2**(2): p. a001107.
18. Gualberto, A., et al., *An oncogenic form of p53 confers a dominant, gain-of-function phenotype that disrupts spindle checkpoint control.* Proc Natl Acad Sci U S A, 1998. **95**(9): p. 5166-71.
19. Murphy, K.L., A.P. Dennis, and J.M. Rosen, *A gain of function p53 mutant promotes both genomic instability and cell survival in a novel p53-null mammary epithelial cell model.* FASEB J, 2000. **14**(14): p. 2291-302.
20. Tarapore, P., et al., *Direct regulation of the centrosome duplication cycle by the p53-p21Waf1/Cip1 pathway.* Oncogene, 2001. **20**(25): p. 3173-84.
21. Hingorani, S.R., et al., *Trp53R172H and KrasG12D cooperate to promote chromosomal instability and widely metastatic pancreatic ductal adenocarcinoma in mice.* Cancer Cell, 2005. **7**(5): p. 469-83.
22. Adorno, M., et al., *A Mutant-p53/Smad complex opposes p63 to empower TGFbeta-induced metastasis.* Cell, 2009. **137**(1): p. 87-98.
23. Neilsen, P.M., et al., *Mutant p53 drives invasion in breast tumors through up-regulation of miR-155.* Oncogene, 2013. **32**(24): p. 2992-3000.
24. Muller, P.A., et al., *Mutant p53 regulates Dicer through p63-dependent and*

-independent mechanisms to promote an invasive phenotype. J Biol Chem, 2014. **289**(1): p. 122-32.
25. Said, R., et al., *P53 mutations in advanced cancers: clinical characteristics, outcomes, and correlation between progression-free survival and bevacizumab-containing therapy.* Oncotarget, 2013. **4**(5): p. 705-14.
26. Muller, P.A. and K.H. Vousden, *Mutant p53 in cancer: new functions and therapeutic opportunities.* Cancer Cell, 2014. **25**(3): p. 304-17.
27. Blandino, G., A.J. Levine, and M. Oren, *Mutant p53 gain of function: differential effects of different p53 mutants on resistance of cultured cells to chemotherapy.* Oncogene, 1999. **18**(2): p. 477-85.
28. Masciarelli, S., et al., *Gain-of-function mutant p53 downregulates miR-223 contributing to chemoresistance of cultured tumor cells.* Oncogene, 2014. **33**(12): p. 1601-8.
29. Stefancikova, L., et al., *Prognostic impact of p53 aberrations for R-CHOP-treated patients with diffuse large B-cell lymphoma.* Int J Oncol, 2011. **39**(6): p. 1413-20.
30. Wong, K.K., et al., *Poor survival with wild-type TP53 ovarian cancer?* Gynecol Oncol, 2013. **130**(3): p. 565-9.
31. Zhang, C.C., et al., *The role of MAP4 expression in the sensitivity to paclitaxel and resistance to vinca alkaloids in p53 mutant cells.* Oncogene, 1998. **16**(12): p. 1617-24.
32. Freed-Pastor, W.A., et al., *Mutant p53 disrupts mammary tissue architecture via the mevalonate pathway.* Cell, 2012. **148**(1-2): p. 244-58.
33. Clendening, J.W., et al., *Dysregulation of the mevalonate pathway promotes transformation.* Proc Natl Acad Sci U S A, 2010. **107**(34): p. 15051-6.
34. Koyuturk, M., M. Ersoz, and N. Altiok, *Simvastatin induces apoptosis in human breast cancer cells: p53 and estrogen receptor independent pathway requiring signalling through JNK.* Cancer Lett, 2007. **250**(2): p. 220-8.
35. Goel, A., S.P. Mathupala, and P.L. Pedersen, *Glucose metabolism in cancer. Evidence that demethylation events play a role in activating type II hexokinase gene expression.* J Biol Chem, 2003. **278**(17): p. 15333-40.
36. Kress, M., et al., *Simian virus 40-transformed cells express new species of proteins precipitable by anti-simian virus 40 tumor serum.* J Virol, 1979. **31**(2): p. 472-83.
37. Takeba, Y., et al., *Irinotecan activates p53 with its active metabolite, resulting in human hepatocellular carcinoma apoptosis.* J Pharmacol Sci, 2007. **104**(3): p. 232-42.
38. Birrell, G.W. and J.R. Ramsay, *Induction of p53 protein by gamma radiation in lymphocyte lines from breast cancer and ataxia telangiectasia patients.* Br J Cancer, 1995. **72**(5): p. 1096-101.
39. Lowe, S.W., et al., *p53 status and the efficacy of cancer therapy in vivo.* Science, 1994. **266**(5186): p. 807-10.
40. Gadducci, A., et al., *P53 gene status in patients with advanced serous epithelial ovarian cancer in relation to response to paclitaxel- plus platinum-based chemotherapy and long-term clinical outcome.* Anticancer Res, 2006. **26**(1B): p. 687-93.
41. Issaeva, N., et al., *Small molecule RITA binds to p53, blocks p53-HDM-2 interaction and activates p53 function in tumors.* Nat Med, 2004. **10**(12): p. 1321-8.
42. Wang, Z. and Y. Sun, *Targeting p53 for Novel Anticancer Therapy.* Transl Oncol, 2010. **3**(1): p. 1-12.
43. Ahmed, A.A., et al., *Driver mutations in TP53 are ubiquitous in high grade serous carcinoma of the ovary.* J Pathol, 2010. **221**(1): p. 49-56.
44. Issaeva, N., et al., *Rescue of mutants of the tumor suppressor p53 in cancer cells by a designed peptide.* Proc Natl Acad Sci U S A, 2003. **100**(23): p. 13303-7.
45. Foster, B.A., et al., *Pharmacological rescue of mutant p53 conformation and function.* Science, 1999. **286**(5449): p. 2507-10.
46. Rippin, T.M., et al., *Characterization of the p53-rescue drug CP-31398 in vitro and in living cells.* Oncogene, 2002. **21**(14): p. 2119-29.

47. Bykov, V.J., et al., *Restoration of the tumor suppressor function to mutant p53 by a low-molecular-weight compound.* Nat Med, 2002. **8**(3): p. 282-8.
48. Lambert, J.M., et al., *PRIMA-1 reactivates mutant p53 by covalent binding to the core domain.* Cancer Cell, 2009. **15**(5): p. 376-88.
49. Kobayashi, N., et al., *PRIMA-1 increases cisplatin sensitivity in chemoresistant ovarian cancer cells with p53 mutation: a requirement for Akt down-regulation.* J Ovarian Res, 2013. **6**(1): p. 7.
50. Weinmann, L., et al., *A novel p53 rescue compound induces p53-dependent growth arrest and sensitises glioma cells to Apo2L/TRAIL-induced apoptosis.* Cell Death Differ, 2008. **15**(4): p. 718-29.
51. Haupt, Y., et al., *Mdm2 promotes the rapid degradation of p53.* Nature, 1997. **387**(6630): p. 296-9.
52. Wang, Z., et al., *Cardiac glycosides inhibit p53 synthesis by a mechanism relieved by Src or MAPK inhibition.* Cancer Res, 2009. **69**(16): p. 6556-64.
53. Suh, Y.A., et al., *Multiple stress signals activate mutant p53 in vivo.* Cancer Res, 2011. **71**(23): p. 7168-75.
54. Lukashchuk, N. and K.H. Vousden, *Ubiquitination and degradation of mutant p53.* Mol Cell Biol, 2007. **27**(23): p. 8284-95.
55. Li, D., N.D. Marchenko, and U.M. Moll, *SAHA shows preferential cytotoxicity in mutant p53 cancer cells by destabilizing mutant p53 through inhibition of the HDAC6-Hsp90 chaperone axis.* Cell Death Differ, 2011. **18**(12): p. 1904-13.
56. Braicu, C., et al., *p53siRNA therapy reduces cell proliferation, migration and induces apoptosis in triple negative breast cancer cells.* Mol Cell Biochem, 2013. **381**(1-2): p. 61-8.
57. Zhu, H.B., et al., *Silencing of mutant p53 by siRNA induces cell cycle arrest and apoptosis in human bladder cancer cells.* World J Surg Oncol, 2013. **11**: p. 22.
58. Cong, L., et al., *Multiplex genome engineering using CRISPR/Cas systems.* Science, 2013. **339**(6121): p. 819-23.
59. Wang, H., et al., *One-step generation of mice carrying mutations in multiple genes by CRISPR/Cas-mediated genome engineering.* Cell, 2013. **153**(4): p. 910-8.
60. Schwank, G., et al., *Functional Repair of CFTR by CRISPR/Cas9 in Intestinal Stem Cell Organoids of Cystic Fibrosis Patients.* Cell Stem Cell, 2013. **13**(6): p. 653-8.
61. Wu, Y., et al., *Correction of a genetic disease in mouse via use of CRISPR-Cas9.* Cell Stem Cell, 2013. **13**(6): p. 659-62.
62. Yin, H., et al., *Genome editing with Cas9 in adult mice corrects a disease mutation and phenotype.* Nat Biotechnol, 2014.
63. Wiedenheft, B., S.H. Sternberg, and J.A. Doudna, *RNA-guided genetic silencing systems in bacteria and archaea.* Nature, 2012. **482**(7385): p. 331-8.
64. Chang, N., et al., *Genome editing with RNA-guided Cas9 nuclease in zebrafish embryos.* Cell Res, 2013. **23**(4): p. 465-72.
65. Cho, S.W., et al., *Targeted genome engineering in human cells with the Cas9 RNA-guided endonuclease.* Nat Biotechnol, 2013. **31**(3): p. 230-2.
66. Sander, J.D. and J.K. Joung, *CRISPR-Cas systems for editing, regulating and targeting genomes.* Nat Biotechnol, 2014.
67. Zimmermann, M., et al., *53BP1 regulates DSB repair using Rif1 to control 5' end resection.* Science, 2013. **339**(6120): p. 700-4.
68. Bunting, S.F., et al., *53BP1 inhibits homologous recombination in Brca1-deficient cells by blocking resection of DNA breaks.* Cell, 2010. **141**(2): p. 243-54.
69. Sugiyama, T., et al., *Clinical characteristics of clear cell carcinoma of the ovary: a distinct histologic type with poor prognosis and resistance to platinum-based chemotherapy.* Cancer, 2000. **88**(11): p. 2584-9.
70. Vaughan, S., et al., *Rethinking ovarian cancer: recommendations for improving outcomes.* Nat Rev Cancer, 2011. **11**(10): p. 719-25.
71. Hogdall, E.V., et al., *P53 mutations in tissue from Danish ovarian cancer patients:*

from the Danish "MALOVA" ovarian cancer study. Gynecol Oncol, 2006. **100**(1): p. 76-82.
72. Concin, N., et al., *Clinical relevance of dominant-negative p73 isoforms for responsiveness to chemotherapy and survival in ovarian cancer: evidence for a crucial p53-p73 cross-talk in vivo.* Clin Cancer Res, 2005. **11**(23): p. 8372-83.
73. Wang, Y., et al., *TP53 mutations in early-stage ovarian carcinoma, relation to long-term survival.* Br J Cancer, 2004. **90**(3): p. 678-85.
74. Ueno, Y., et al., *Prognostic significance of p53 mutation in suboptimally resected advanced ovarian carcinoma treated with the combination chemotherapy of paclitaxel and carboplatin.* Cancer Lett, 2006. **241**(2): p. 289-300.
75. Bartel, F., et al., *Both germ line and somatic genetics of the p53 pathway affect ovarian cancer incidence and survival.* Clin Cancer Res, 2008. **14**(1): p. 89-96.
76. Do, S.I., et al., *Aberrant DNA methylation of integrin alpha4 in human breast cancer.* Tumour Biol, 2014. **35**(7): p. 7079-84.
77. Sonego, M., et al., *Stathmin regulates mutant p53 stability and transcriptional activity in ovarian cancer.* EMBO Mol Med, 2013. **5**(5): p. 707-22.
78. Sun, X.X., K.B. Challagundla, and M.S. Dai, *Positive regulation of p53 stability and activity by the deubiquitinating enzyme Otubain 1.* EMBO J, 2012. **31**(3): p. 576-92.
79. Di Agostino, S., et al., *Gain of function of mutant p53: the mutant p53/NF-Y protein complex reveals an aberrant transcriptional mechanism of cell cycle regulation.* Cancer Cell, 2006. **10**(3): p. 191-202.
80. Lehmann, S., et al., *Targeting p53 in vivo: a first-in-human study with p53-targeting compound APR-246 in refractory hematologic malignancies and prostate cancer.* J Clin Oncol, 2012. **30**(29): p. 3633-9.
81. Misawa, T., et al., *Establishment and characterization of acquired resistance to platinum anticancer drugs in human ovarian carcinoma cells.* Jpn J Cancer Res, 1995. **86**(1): p. 88-94.
82. Kajiyama, H., et al., *Chemoresistance to paclitaxel induces epithelial-mesenchymal transition and enhances metastatic potential for epithelial ovarian carcinoma cells.* Int J Oncol, 2007. **31**(2): p. 277-83.
83. Kapitanovic, S., et al., *Effect of indomethacin on E-cadherin and beta-catenin expression in HT-29 colon cancer cells.* Exp Mol Pathol, 2006. **80**(1): p. 91-6.
84. Zhao, J., N. Araki, and S.K. Nishimoto, *Quantitation of matrix Gla protein mRNA by competitive polymerase chain reaction using glyceraldehyde-3-phosphate dehydrogenase as an internal control.* Gene, 1995. **155**(2): p. 159-65.
85. Dong, P., et al., *Mutant p53 gain-of-function induces epithelial-mesenchymal transition through modulation of the miR-130b-ZEB1 axis.* Oncogene, 2013. **32**(27): p. 3286-95.
86. Muller, P.A., K.H. Vousden, and J.C. Norman, *p53 and its mutants in tumor cell migration and invasion.* J Cell Biol, 2011. **192**(2): p. 209-18.
87. Izetti, P., et al., *PRIMA-1, a mutant p53 reactivator, induces apoptosis and enhances chemotherapeutic cytotoxicity in pancreatic cancer cell lines.* Invest New Drugs, 2014. **32**(5): p. 783-94.
88. Saha, M.N., et al., *PRIMA-1Met/APR-246 displays high antitumor activity in multiple myeloma by induction of p73 and Noxa.* Mol Cancer Ther, 2013. **12**(11): p. 2331-41.
89. Russo, D., et al., *PRIMA-1 induces autophagy in cancer cells carrying mutant or wild type p53.* Biochim Biophys Acta, 2013. **1833**(8): p. 1904-13.
90. Kobayashi, N., et al., *PRIMA-1 increases cisplatin sensitivity in chemoresistant ovarian cancer cells with p53 mutation: a requirement for Akt down-regulation.* J Ovarian Res, 2013. **6**: p. 7.
91. Zandi, R., et al., *PRIMA-1Met/APR-246 induces apoptosis and tumor growth delay in small cell lung cancer expressing mutant p53.* Clin Cancer Res, 2011. **17**(9): p. 2830-41.

92. Russo, D., et al., *PRIMA-1 cytotoxicity correlates with nucleolar localization and degradation of mutant p53 in breast cancer cells.* Biochem Biophys Res Commun, 2010. **402**(2): p. 345-50.
93. Rokaeus, N., et al., *PRIMA-1(MET)/APR-246 targets mutant forms of p53 family members p63 and p73.* Oncogene, 2010. **29**(49): p. 6442-51.
94. Utsumi, F., et al., *Effect of indirect nonequilibrium atmospheric pressure plasma on anti-proliferative activity against chronic chemo-resistant ovarian cancer cells in vitro and in vivo.* PLoS One, 2013. **8**(12): p. e81576.
95. Nakahara, T., et al., *Sphingosine-1-phosphate inhibits H2O2-induced granulosa cell apoptosis via the PI3K/Akt signaling pathway.* Fertil Steril, 2012. **98**(4): p. 1001-8 e1.
96. Peng, X., et al., *APR-246/PRIMA-1MET inhibits thioredoxin reductase 1 and converts the enzyme to a dedicated NADPH oxidase.* Cell Death Dis, 2013. **4**: p. e881.
97. Duan, Z., E. Choy, and F.J. Hornicek, *NSC23925, identified in a high-throughput cell-based screen, reverses multidrug resistance.* PLoS One, 2009. **4**(10): p. e7415.
98. Bykov, V.J., et al., *PRIMA-1(MET) synergizes with cisplatin to induce tumor cell apoptosis.* Oncogene, 2005. **24**(21): p. 3484-91.
99. Supiot, S., et al., *PRIMA-1(met) radiosensitizes prostate cancer cells independent of their MTp53-status.* Radiother Oncol, 2008. **86**(3): p. 407-11.
100. Ali, D., et al., *APR-246 exhibits anti-leukemic activity and synergism with conventional chemotherapeutic drugs in acute myeloid leukemia cells.* Eur J Haematol, 2011. **86**(3): p. 206-15.
101. Nahi, H., et al., *Effects of PRIMA-1 on chronic lymphocytic leukaemia cells with and without hemizygous p53 deletion.* Br J Haematol, 2004. **127**(3): p. 285-91.
102. Mohell, N., et al., *APR-246 overcomes resistance to cisplatin and doxorubicin in ovarian cancer cells.* Cell Death Dis, 2015. **6**: p. e1794.
103. Tessoulin, B., et al., *PRIMA-1Met induces myeloma cell death independent of p53 by impairing the GSH/ROS balance.* Blood, 2014. **124**(10): p. 1626-36.
104. Aryee, D.N., et al., *Variability in functional p53 reactivation by PRIMA-1(Met)/APR-246 in Ewing sarcoma.* Br J Cancer, 2013. **109**(10): p. 2696-704.
105. Lambert, J.M., et al., *Mutant p53 reactivation by PRIMA-1MET induces multiple signaling pathways converging on apoptosis.* Oncogene, 2010. **29**(9): p. 1329-38.
106. Bailey, H.H., et al., *Phase I clinical trial of intravenous L-buthionine sulfoximine and melphalan: an attempt at modulation of glutathione.* J Clin Oncol, 1994. **12**(1): p. 194-205.
107. Cox, A.G., et al., *Redox potential and peroxide reactivity of human peroxiredoxin 3.* Biochemistry, 2009. **48**(27): p. 6495-501.
108. Cunniff, B., et al., *Peroxiredoxin 3 levels regulate a mitochondrial redox setpoint in malignant mesothelioma cells.* Redox Biol, 2014. **3**: p. 79-87.
109. Song, I.S., et al., *FOXM1-induced PRX3 Regulates Stemness and Survival of Colon Cancer Cells via Maintenance of Mitochondrial Function.* Gastroenterology, 2015.
110. Huang, C., et al., *Decreased selenium-binding protein 1 enhances glutathione peroxidase 1 activity and downregulates HIF-1alpha to promote hepatocellular carcinoma invasiveness.* Clin Cancer Res, 2012. **18**(11): p. 3042-53.
111. Gan, X., et al., *High GPX1 expression promotes esophageal squamous cell carcinoma invasion, migration, proliferation and cisplatin-resistance but can be reduced by vitamin D.* Int J Clin Exp Med, 2014. **7**(9): p. 2530-40.
112. Yang, J. and R.A. Weinberg, *Epithelial-mesenchymal transition: at the crossroads of development and tumor metastasis.* Dev Cell, 2008. **14**(6): p. 818-29.
113. Peinado, H., D. Olmeda, and A. Cano, *Snail, Zeb and bHLH factors in tumour progression: an alliance against the epithelial phenotype?* Nat Rev Cancer, 2007. **7**(6): p. 415-28.
114. Micalizzi, D.S., et al., *The Six1 homeoprotein induces human mammary carcinoma*

cells to undergo epithelial-mesenchymal transition and metastasis in mice through increasing TGF-beta signaling. J Clin Invest, 2009. **119**(9): p. 2678-90.
115. Zhang, H., et al., *Forkhead transcription factor foxq1 promotes epithelial-mesenchymal transition and breast cancer metastasis.* Cancer Res, 2011. **71**(4): p. 1292-301.
116. Yuan, H., et al., *ALX1 induces snail expression to promote epithelial-to-mesenchymal transition and invasion of ovarian cancer cells.* Cancer Res, 2013. **73**(5): p. 1581-90.
117. Ocana, O.H., et al., *Metastatic colonization requires the repression of the epithelial-mesenchymal transition inducer Prrx1.* Cancer Cell, 2012. **22**(6): p. 709-24.
118. Takahashi, Y., et al., *Paired related homoeobox 1, a new EMT inducer, is involved in metastasis and poor prognosis in colorectal cancer.* Br J Cancer, 2013. **109**(2): p. 307-11.
119. Guo, J., et al., *PRRX1 promotes epithelial-mesenchymal transition through the Wnt/beta-catenin pathway in gastric cancer.* Med Oncol, 2015. **32**(1): p. 393.
120. Hirata, H., et al., *Downregulation of PRRX1 Confers Cancer Stem Cell-Like Properties and Predicts Poor Prognosis in Hepatocellular Carcinoma.* Ann Surg Oncol, 2014.
121. Schmalhofer, O., S. Brabletz, and T. Brabletz, *E-cadherin, beta-catenin, and ZEB1 in malignant progression of cancer.* Cancer Metastasis Rev, 2009. **28**(1-2): p. 151-66.
122. Yun, S.I., et al., *Ubiquitin specific protease 4 positively regulates the WNT/beta-catenin signaling in colorectal cancer.* Mol Oncol, 2015.
123. Palmer, T.D., et al., *Integrin-free tetraspanin CD151 can inhibit tumor cell motility upon clustering and is a clinical indicator of prostate cancer progression.* Cancer Res, 2014. **74**(1): p. 173-87.
124. Wang, W.S., et al., *Silencing of twist expression by RNA interference suppresses epithelial-mesenchymal transition, invasion, and metastasis of ovarian cancer.* Asian Pac J Cancer Prev, 2012. **13**(9): p. 4435-9.
125. Wang, W.S., et al., *Expression and significance of twist and E-cadherin in ovarian cancer tissues.* Asian Pac J Cancer Prev, 2013. **14**(2): p. 669-72.
126. Lee, Y.B., et al., *Twist-1 regulates the miR-199a/214 cluster during development.* Nucleic Acids Res, 2009. **37**(1): p. 123-8.
127. Cheng, G.Z., et al., *Twist transcriptionally up-regulates AKT2 in breast cancer cells leading to increased migration, invasion, and resistance to paclitaxel.* Cancer Res, 2007. **67**(5): p. 1979-87.
128. Touboul, C., et al., *Mesenchymal stem cells enhance ovarian cancer cell infiltration through IL6 secretion in an amniochorionic membrane based 3D model.* J Transl Med, 2013. **11**: p. 28.
129. Rieppi, M., et al., *Mesothelial cells induce the motility of human ovarian carcinoma cells.* Int J Cancer, 1999. **80**(2): p. 303-7.
130. Anttila, M.A., et al., *High levels of stromal hyaluronan predict poor disease outcome in epithelial ovarian cancer.* Cancer Res, 2000. **60**(1): p. 150-5.
131. Sugiyama, K., et al., *Expression of the miR200 family of microRNAs in mesothelial cells suppresses the dissemination of ovarian cancer cells.* Mol Cancer Ther, 2014. **13**(8): p. 2081-91.
132. Kenny, H.A., et al., *Use of a novel 3D culture model to elucidate the role of mesothelial cells, fibroblasts and extra-cellular matrices on adhesion and invasion of ovarian cancer cells to the omentum.* Int J Cancer, 2007. **121**(7): p. 1463-72.
133. Offner, F.A., et al., *IL-6 secretion by human peritoneal mesothelial and ovarian cancer cells.* Cytokine, 1995. **7**(6): p. 542-7.
134. Stadlmann, S., et al., *Ovarian carcinoma cells and IL-1beta-activated human peritoneal mesothelial cells are possible sources of vascular endothelial growth factor in inflammatory and malignant peritoneal effusions.* Gynecol Oncol, 2005.

97(3): p. 784-9.
135. Chou, J.L., et al., *Hypermethylation of the TGF-beta target, ABCA1 is associated with poor prognosis in ovarian cancer patients.* Clin Epigenetics, 2015. **7**(1): p. 1.
136. Kajiyama, H., et al., *Possible involvement of SDF-1alpha/CXCR4-DPPIV axis in TGF-beta1-induced enhancement of migratory potential in human peritoneal mesothelial cells.* Cell Tissue Res, 2007. **330**(2): p. 221-9.
137. Kenny, H.A., et al., *Mesothelial cells promote early ovarian cancer metastasis through fibronectin secretion.* J Clin Invest, 2014. **124**(10): p. 4614-28.
138. Miao, Z.F., et al., *Lung cancer cells induce senescence and apoptosis of pleural mesothelial cells via transforming growth factor-beta1.* Tumour Biol, 2015. **36**(4): p. 2657-65.
139. Gore, A.J., et al., *Pancreatic cancer-associated retinoblastoma 1 dysfunction enables TGF-beta to promote proliferation.* J Clin Invest, 2014. **124**(1): p. 338-52.
140. Munoz, N.M., J.Y. Baek, and W.M. Grady, *TGF-beta has paradoxical and context dependent effects on proliferation and anoikis in human colorectal cancer cell lines.* Growth Factors, 2008. **26**(5): p. 254-62.
141. Kim, Y.H., et al., *TWIST1 and SNAI1 as markers of poor prognosis in human colorectal cancer are associated with the expression of ALDH1 and TGF-beta1.* Oncol Rep, 2014. **31**(3): p. 1380-8.
142. Javle, M., et al., *Biomarkers of TGF-beta signaling pathway and prognosis of pancreatic cancer.* PLoS One, 2014. **9**(1): p. e85942.
143. Davies, M., et al., *Overexpression of autocrine TGF-beta 1 suppresses the growth of spindle epithelial cells in vitro and in vivo in the rat 4NQO model of oral carcinogenesis.* Int J Cancer, 1997. **73**(1): p. 68-74.
144. Taylor, M.A., et al., *TGF-beta upregulates miR-181a expression to promote breast cancer metastasis.* J Clin Invest, 2013. **123**(1): p. 150-63.
145. Christeli, E., et al., *TGF-beta 1 overexpression in breast cancer.* Oncol Rep, 1996. **3**(6): p. 1115-8.
146. Kim, S., et al., *Elevated TGF-beta1 and -beta2 expression accelerates the epithelial to mesenchymal transition in triple-negative breast cancer cells.* Cytokine, 2015.
147. Ma, H., et al., *TGF-beta1-induced expression of Id-1 is associated with tumor progression in gastric cancer.* Med Oncol, 2014. **31**(7): p. 19.
148. Lin, H., et al., *High immunohistochemical expression of TGF-beta1 predicts a poor prognosis in cervical cancer patients who harbor enriched endoglin microvessel density.* Int J Gynecol Pathol, 2012. **31**(5): p. 482-9.
149. Gao, J., et al., *TGF-beta isoforms induce EMT independent migration of ovarian cancer cells.* Cancer Cell Int, 2014. **14**(1): p. 72.
150. Neilson, E.G., *Mechanisms of disease: Fibroblasts--a new look at an old problem.* Nat Clin Pract Nephrol, 2006. **2**(2): p. 101-8.
151. Shukla, A., et al., *CLIC4 regulates TGF-beta-dependent myofibroblast differentiation to produce a cancer stroma.* Oncogene, 2014. **33**(7): p. 842-50.
152. Gupta, D.K., N. Singh, and D.K. Sahu, *TGF-beta Mediated Crosstalk Between Malignant Hepatocyte and Tumor Microenvironment in Hepatocellular Carcinoma.* Cancer Growth Metastasis, 2014. **7**: p. 1-8.
153. Winkler, I., et al., *Regulatory T lymphocytes and transforming growth factor beta in epithelial ovarian tumors-prognostic significance.* J Ovarian Res, 2015. **8**(1): p. 39.
154. Lv, Z.D., et al., *Induction of gastric cancer cell adhesion through transforming growth factor-beta1-mediated peritoneal fibrosis.* J Exp Clin Cancer Res, 2010. **29**: p. 139.
155. Turley, E.A., et al., *Mechanisms of disease: epithelial-mesenchymal transition--does cellular plasticity fuel neoplastic progression?* Nat Clin Pract Oncol, 2008. **5**(5): p. 280-90.
156. Terauchi, M., et al., *Possible involvement of TWIST in enhanced peritoneal metastasis of epithelial ovarian carcinoma.* Clin Exp Metastasis, 2007. **24**(5): p.

329-39.
157. Chen, D., et al., *Effect of down-regulated transcriptional repressor ZEB1 on the epithelial-mesenchymal transition of ovarian cancer cells.* Int J Gynecol Cancer, 2013. **23**(8): p. 1357-66.